PEOPLE'S DEMOCRATIC REPUBLIC OF ALGERIA
MINISTRY OF HIGHER EDUCATION AND SCIENTIFIC RESEARCH
ECOLE NATIONALE POLYTECHNIQUE

Control Engineering Department
Laboratoire de Commandes des Processus

King Abdullah University of Science and Technology

Final Project Thesis

Thesis submitted for the obtaining of the
State Engineering Degree in Control Engineering

Non asymptotic estimation methods: a focus on the Volterra and modulating functions approaches

Presented by :
Rania TAFAT
Defended publicly on 02/07/2020.

Jury members:

President	Mr. D. BOUDANA	Lecturer	ENP
Examiner	Mr. M. TADJINE	Professor	ENP
Promoter	Mr. M. CHAKIR	Lecturer	ENP
Co-promoter	Mrs. T-M. LALEG-KIRATI	Professor	KAUST

ENP 2020

PEOPLE'S DEMOCRATIC REPUBLIC OF ALGERIA
MINISTRY OF HIGHER EDUCATION AND SCIENTIFIC RESEARCH
ECOLE NATIONALE POLYTECHNIQUE

Control Engineering Department
Laboratoire de Commandes des Processus

King Abdullah University of Science and Technology

Final Project Thesis

Thesis submitted for the obtaining of the
State Engineering Degree in Control Engineering

Non asymptotic estimation methods: a focus on the Volterra and modulating functions approaches

Presented by :
Rania TAFAT
Defended publicly on 02/07/2020.

Jury members:

President	Mr. D. BOUDANA	Lecturer	ENP
Examiner	Mr. M. TADJINE	Professor	ENP
Promoter	Mr. M. CHAKIR	Lecturer	ENP
Co-promoter	Mrs. T-M. LALEG-KIRATI	Professor	KAUST

ENP 2020

ملخص:

في هذه الاطروحة، نقدم طريقتين للقياس و التقدير تعتمدان مبدئيا على تحويل التكامل الغير المقارب: تقنية فولتيرا و تقنية تعديل الدوال. نهتم و نشرح طريقة تصميم وإعادة إنتاج كل من مقياس فولتيرا القوي لالدالات الجيبية المنحازة و طريقة مقياس فولتيرا التفاضلي. نساهم في مقياس فولتيرا التفاضلي من خلال بناء عائلة جديدة من الدوال المتغيرة النواة لشمل الحالات الخالية من التشويش و الحصول على نتائج واعدة. نقترح أيضًا نوعًا جديدًا من الدوال المعدلة العشوائية و تخفيف الشرط التفاضلي واختبارها على قياس و تقدير معادلات تفاضلية عادية و بسيطة في كل من الحالات الخالية من التشويش و الحالات المشوشة، حيث تحصلنا على خطأ أقصى قدره 5 بالمئة. أخيرًا ، نستخدم الطريقة القائمة على تعديل الدوال تقديرلقياس تدفق الدم الشرياني و طريقة ويند كيسل أولاً بضغط الدم المولد تحليليًا ثم باستخدام قاعدة بيانات التي نستنتج من خلالها حساسية بيانات .

كلمات دالة :مقياس فولتيرا, مقياس غير تقاربي, طريقة الدالة المعدلة.

Résumé:

Dans ce travail, nous présentons deux méthodes non-asymptotiques d'estimation basées sur les transformations intégrales: les approches Volterra et les fonctions modulatrices. Nous expliquons la conception et reproduisons à la fois l'observateur Volterra robuste d'un signal sinusoïdal biaisé et le différenciateur Volterra. Nous construisons une nouvelle famille de fonctions de noyaux bivariées et l'adaptons au différenciateur Volterra, afin d'étendre l'approche au scénario avec bruit et d'obtenir des résultats prometteurs. Nous proposons également un nouveau type de fonctions pseudo-modulatrices qui prennent des valeurs aléatoires, éliminant ainsi la condition de dérivabilité, et nous les testons sur une simple estimation d'un paramètre d'une ODE. Nous obtenons une erreur maximale de 5% indépendamment de la présence de bruits. . Enfin, à titre d'application des techniques étudiées, nous utilisons les fonctions modulatrice pour estimer le débit sanguin artériel et le paramètre Windkessel à deux éléments, d'abord en se basant sur la pression artérielle obtenue analytiquement, puis celle issue d'une base de données, ce qui permet de souligner la grande sensibilité de la méthode aux données utilisées.

Mots clés: *Estimateurs non-asymptotiques, Observateur de Volterra, Estimation via les fonctions modulatrices.*

Abstract:

In this work, we present two non-asymptotic integration transform based estimation methods: the Volterra and modulating functions approaches. We explain the design and reproduce both of the robust Volterra observer of a biased sinusoidal signal and Volterra differentiator. We contribute to the Volterra differentiator by constructing a novel bivariate kernel functions family in order to extend the approach to the noisy scenario and obtain promising results. We also propose a novel type of pseudo-modulating functions that are randomized, relax the differentiability condition and test them on a simple ODE parameter estimation in both noise-free and noisy cases where we obtain a maximum error of 5%. At last, we use the modulating functions based method to estimate the arterial blood flow and Windkessel 2-Element parameter first with analytically generated blood pressure and then using a database and conclude by underlying the data-sensitivity of the method.

Key words: *Non-asymptotic estimators, Volterra observers, Modulating functions based method.*

Acknowledgements

I would like to express my deep and sincere gratitude for both of my supervisors Dr. Messaoud CHAKIR and Pr. Taous-Meriem LALEG-KIRATI for their understanding, help and patience.

I would like to thank Dr. Messaoud CHAKIR for his guidance throughout this past three years, for his precious advice and for sharing with me his experience as a teacher and supervisor. I would also like to thank Pr. Taous-Meriem LALEG-KIRATI, for giving me the opportunity to work on such an interesting topic, for always finding time to meet with me and for being the most inspiring mentor I have ever had.

I want to express my utmost gratitude to all members of the Estimation, Modeling and Analysis KAUST research group for warmly welcoming me amongst them and for the great amount of scientific knowledge that I have learned from them. Especially, Mohamed A. BAHLOUL, Lilia GHAFFOUR and Evangelos PILIOURAS for all the long Zoom meetings where they kindly offered me their help and shared their experience with modulating functions with me.

I am also, of course, grateful to all my teachers and comrades of the Control Engineering department thanks to whom I developed a real passion about control theory.

Lastly, I wish also to thank my father, mother and sister without whom I could have never achieved any of this.

Contents

List of Figures

General introduction

Motivation

Accurate knowlegde of the parameters of a system's model and its states is crucial to solve many control theory problems. However, in practice it is often difficult to measure these parameters and states. This can be due to the inexistence of sensors, the lack of their liability or simply because such a direct observation would cost too much. Fortunately, there exists methods to get these information indirectly via mathematical estimation techniques and state observers.

By definition, a state observer is meant to be a replica of the system with one or two additional terms that are precisely chosen in order to make the state estimation dynamics converge. The first observer was introduced by Kalman and Bucy [30],[31], and the concept was generalized by Luenberger for deterministic linear systems. [40] From this point, observers and estimators were widely developed and studied. The concept was generalized on different class of non-linear systems and many applications have seen the light ever since. Today, observers and estimators are considered numerical sensors and are used in different fields.

The first estimators were designed in order to give asymptotical convergence only. This means that theoretically, it would take an infinite amount of time for the difference between the real parameter and the estimated one to vanish, which is sufficient for many applications. However, the evolution of technology has shown the limits of such an asymptotical convergence in several applications, where finite time convergence is needed. [49], [66], [13]

In this thesis, we will introduce in details the concept of finite time convergence, adapt it

to estimation theory and explore examples of finite time observers and estimators. Our main focus will be the Volterra approach and the method based on modulating functions.

Aims and Objectives

The first goal of this thesis is to have a better understanding of finite time convergence in general and finite time estimation techniques in particular. We will go through the details of such estimators by explaining the theory behind their concepts and giving clear steps for their design. We will also highlight their drawbacks and advantages. Our main focus, however, will be finite time estimators that are induced by integral transforms such as the Volterra observer and modulating function estimation methods. While such methods are often praised for their fast convergence and robustness, we will see that such qualifications highly depend on tuning parameters that can sometimes be difficult to find.

Description of the work

In chapter 2, we will begin by introducing the concept of a finite time observer. We will do so, by recalling the basic Lyapunov definitions of asymptotic convergence and by defining the finite time convergence in a specific framework. We will compare both concepts in order to highlight the difference between them. We will, then, have a quick glance at existing finite time observers, their advantages and their drawbacks before focusing on the Volterra and modulating function based methods.

In chapter 3, we will present an observer that combines both second order sliding mode and Volterra integral approach [51]. It is the Volterra observer that estimates the amplitude, frequency and phase of a given biased sinusoidal signal. This first estimation method will enable us to present the main Volterra definitions and explain the concept behind this technique. We will also highlight the steps for designing such cascading observers and provide extensive numerical examples.

Then, and once acquainted with the Volterra concept, we will present the Volterra differentiator in chapter 4. This differentiator was first introduced in [35] around a specific *kernel function*. Our main contribution will be the generalization of this idea for any *ker-*

nel function that satisfies specific conditions. Taking these conditions into consideration, we will construct our own kernel function family and develop the differentiator around it. We will then make a comparison between both methods and highlight their main characteristics.

In chapter 5, we will introduce another similar approach for estimation which is based on monovariate modulating functions. We will first define a modulating function, present the existing types of modulating functions and explain the estimation approach. Once familiar with the technique, we propose to extend the definition of the modulating function by trying out a new type: *randomized pseudo-modulating functions*. This is to have a better understanding of the modulating functions effect and importance in an estimation problem. We will provide numerical simulations to illustrate this.

At last, and in order to illustrate the practical effectiveness of such methods, we propose to tackle a real life estimation problem, in chapter 6: the estimation of the arterial blood flow using the modulating function technique. We will briefly explain how the the cardiac cycle functions and how to model it using the Windkessel electric analogy. This simple, but effective example, will enable us to highlight the parameters' tuning issues that come with the modulating function estimation based method.

Chapter 1

Finite time convergence

1.1 Introduction

This chapter recalls the several definitions of stability in the sens of Lyapunov and introduces a definition of the finite time stability in a framework that tackles the non-uniqueness of the solutions problem as it was done in [8]. Our goal is to give a brief but clear understanding of the difference between standard asymptotical convergence and the non-asymptotical one, with the mathematical and practical implications of these two concepts. We will then give examples of finite time observers from the literature, highlighting their advantages, drawbacks and challenges.

1.2 Lyapunov stability

In [41], the concept of stability is first introduced as a motion problem. Indeed, the author considers a nominal motion $x^*(t, t_0, x_0)$ of a dynamic system and studies wether it is possible to choose initial values x_0 and t_0 in order for this motion to stay bounded by limits given in advance. Therefore, the author studies small perturbations around the initial conditions. If they imply small deviations of perturbed motions from $x^*(t, t_0, x_0)$ then the nominal motions are called stable [55].
Let us consider the following dynamic system:

$$\dot{x}(t) = f(x, t),\ t > 0, \tag{1.1}$$

where $x \in\ \subseteq \mathbb{R}^N$. and $f :\ \times \mathbb{R}_+ \to \mathbb{R}^N$ is continuous on an open neighborhood $\mathcal{D}$ of the origin and is locally Lipschitz on $\mathcal{D} - \{0\}$, $f(0, t) = 0\, \forall t$. Thus, $\forall x_0 \in \mathcal{D} - \{0\}$, the solution of (1.1) is unique and the origin is an equilibrium point.

Definition 1 (L-stability): [32] The origin of system (1.1) is said to be *L-stable* or *Lyapunov stable* if: $\forall \epsilon \in \mathbb{R}_+$, $\forall t_0 \in \mathbb{R}_+$, $\exists \delta = \delta(\epsilon, t_0) \in \mathbb{R}_+$ such that:

$$\|x\,(t_0)\| < \delta \Rightarrow \|x(t)\| < \varepsilon, \quad \forall t \geqslant t_0 \geqslant 0. \tag{1.2}$$

If the origin does not satisfy this condition then it is said *unstable*.

Definition 2 (Uniform L-stability): [32] The origin of system (1.1) is said to be *uniformly stable* if : $\forall \epsilon > 0$, $\exists \delta = \delta(\epsilon) > 0$, independant of t_0 such that (1.2) is satisfied.

Definition 3 (A-stability): [32] The origin of system (1.1) is said to be *locally A-stable* or *locally asymptotically stable* if it is L-stable and asymptotically attractive and there is a positive constant $c = c(t_0)$ such that $x(t) \to 0$ as $t \to \infty, \forall \|x(t_0)\| < c$.

Definition 4 (Uniform A-stability): [32] The origin of system (1.1) is said to be *uniformly A-stable* or *uniformly asymptotically stable* if it is uniformly stable and there is a positive constant c, independent of t_0, such that: $\forall \|x(t_0)\| < c$, $x(t) \to 0$ as $t \to \infty$, uniformly in t_0, for each $\eta > 0$, there is $T = T(\eta) > 0$ such that:

$$\|x(t)\| < \eta, \quad \forall t \geqslant t_0 + T(\eta), \forall \|x(t_0)\| < c \tag{1.3}$$

Definition 5 (E-stability): [32] [14] The origin of system (1.1) is said to be *exponentially stable* if: $\exists c, k$ and such that:

$$\|x(t)\| \leqslant k \|x(t_0)\| e^{-\lambda(t-t_0)}, \forall \|x(t_0)\| < c \tag{1.4}$$

.

In the previous definitions, for simplicity, we have only tackled the stability of the origin of the dynamic system (1.1) but these definitions remain correct for any stability problem for a non-trivial solution $x^*(t, t^*, x_0^*)$ and can be generalized by using the variable change $y = x - x^*$.

For most dynamic system, control and observation problems, E-stability of an equilibrium is difficult to prove and we consider A-stability as a sufficient condition.

1.3 Finite time stability

The first available technique for feedback stabilization and observation lead to closed loop systems with Lipschitzien dynamics that are, at best, asymptotically stable. This means that the solutions with initial conditions in the origin's neighborhood do not necessarily converge exactly to the origin in infinite time. Indeed, finite time convergence cannot be established in presence of a Lipschitz condition, thus compromising the assumption on the uniqueness of the solution. In [8], this problem is well addressed, where a definition of finite time stability of such dynamic systems that are continuous with non-Lipschitzian right hand sides is proposed.

Definition 6 (Finite time stability) [9] The origin of 1.1 is said to be a *finite time equilibrium* if there exists an open neighborhood $\mathcal{N} \subseteq \mathcal{D}$ of the origin and a function $T : \mathcal{N} \to [0, +\infty[$ called the *settling time*, such that:

1. $\lim_{x_0 \to 0} T(x_0) = 0$,
2. $\forall x_0 \in \mathcal{N} - \{0\}$, the solution $x(t, t_o, x_0)$ is uniquely defined on $[0,\ T(x_0)[$, $x(t, t_o, x_0) \neq 0$, $t \in [0,\ T(x_0)[$ and $\lim_{t \to T(x_0)} x(t, t_o, x_0) = 0$,
3. $\forall \epsilon > 0$ such that $\mathcal{B}(\epsilon) \in \mathcal{N}$, $\exists \delta > 0$ such that if $x_0 \in \mathcal{B}(\delta) - \{0\}$, then $x(t, t_o, x_0) \in \mathcal{B}(\epsilon)$, $t \in [0,\ T(x_0)[$.

Note that finite time stability is sometimes referred to as non-asymptotical stability [9].

Definition 7 (Fixed time stability) [54] The origin of system (1.1) is said to be a *fixed time equilibrium* if:

1. it is finite time stable,
2. $\exists M > 0$ such that $\forall x_0 \in \mathcal{N} - \{0\}$ we have $T(x_0) < M$.

If $\mathcal{N} = \mathbb{R}$, then the origin is said *globally* finite time stable (resp. fixed time stable).

Note that in this section our goal is only to recall and explain these definitions, extensive methods on how to prove this type of stability for dynamic systems can be found in [9] and [8].

1.4 Examples of finite time observers

1.4.1 Sliding mode observer

The concept of sliding mode was first introduced for control and stabilization of dynamic systems. The idea is to drive the trajectory of the system into a desired curve or a line in space that is called the *sliding surface* and let it remain thereafter. The advantages of sliding mode control include robustness, finite time convergence and reduced-order compensated dynamics [60]. In [15], the authors present a tutorial on how to extend this concept to solve observation problems.

We will here briefly introduce the main ideas behind the design of a sliding mode observer on a simple linear system, further details can be found in [15] and [60].

Let us consider the following linear dynamic time invariant system:

$$\begin{aligned} \dot{x}(t) &= Ax(t) + Bu(t), \\ y(t) &= Cx(t), \quad t > 0. \end{aligned} \tag{1.5}$$

The observer proposed is similar to the Luenberger one [40],[39] but the linear innovative term is replaced by a *sign* function that is discontinuous by definition:

$$\dot{\hat{x}}(t) = A\hat{x}(t) + Bu(t) + Lsign(y(t) - C\hat{x}(t)), \tag{1.6}$$

The sliding surface here is $y(t) - C\hat{x}(t) = 0$, and the gain matrix L here is the degree of freedom. It must be chosen such that system (1.5) remains on that manifold.

The sliding mode observer is designed step by step by dividing the system into many subsystems. In this case, by using linear transformation of state variables and then chosing the parameters of the matrix L by applying the method of equivalent control [15].

This algorithm with the same idea of applying the equivalent control method is also generalized for nonlinear systems. The difference is that the observer will depend on the control in the case of nonlinear systems [26].

Chattering phenomenon

The main problem that occurs with this observer is the chattering phenomenon. It is a zigzag motion along the manifold caused by the high frequency motion on the sliding surface. Chattering comes inherently with the discontinuity of the *sign* function and especially when the frequency of the switching mode is high. One way of dealing with the chattering problem is to introduce the equivalent innovative term by using a low pass filter that is designed such that it allows for the slow component of motion to pass but it eliminates the high frequency component caused by the presence of nonidealities [63].
But this filter cannot found for every system. Another way to deal with this problem is to smoothen the *sign* function and replace it by a *sigmoid*. [61] [65] However this may alter the finite time convergence property of this observer in presence of disturbances [60].

1.4.2 Super-Twisting observer

Directly inspired by the discountinous and finite time converging sliding mode observer, the authors in [18] designed an observer for a special class of nonlinear systems with unknown inputs and called it the *Super Twisting* observer.
Let us here discuss the SISO case. We consider the SISO nonlinear system in triangular observable form:

$$\begin{aligned} \dot{x}_1 &= x_2, \\ \dot{x}_2 &= x_3, \\ &\vdots \\ \dot{x}_{N-1} &= x_N, \\ \dot{x}_N &= \alpha(x) + \beta(x)\omega, \\ y &= x_1, \end{aligned} \tag{1.7}$$

where the state vector is $x = \begin{bmatrix} x_1 & x_2 & \cdots x_N \end{bmatrix}^\top \in \mathbb{R}^N$, y is the output vector, $\omega \in \mathbb{R}$ is an unknown input $\alpha(x)$ and $\beta(x)$ are bounded smooth scalar functions. Dependencies on the time variable t are omitted for simplicity.

Assumptions:

1. $\forall i \in \{1, ..., N\}, \exists d_i \in \mathbb{R}$ such that $|x_i(t)| < d_i \ \forall t > 0$,
2. $|\omega(t)| < K_1$, $|\dot{\omega}(t)| < K_1'$,
3. $|\alpha(t)| < K_2$, $|\dot{\alpha}(t)| < K_2'$,
4. $|\alpha(t)| < K_3$, $|\dot{\alpha}(t)| < K_3'$,

where K_j and K_j' are known positive scalars.

The observer proposed for this system is the following:

$$\begin{cases} \dot{\hat{x}}_1 = \tilde{x}_2 + \lambda_1 |e_1|^{1/2} \operatorname{sign}(e_1), \\ \dot{\tilde{x}}_2 = \alpha_1 \operatorname{sign}(e_1), \\ \dot{\hat{x}}_2 = E_1 \left[\tilde{x}_3 + \lambda_2 |e_2|^{1/2} \operatorname{sign}(e_2) \right], \\ \dot{\tilde{x}}_3 = E_1 \alpha_2 \operatorname{sign}(e_2), \\ \dot{\hat{x}}_3 = E_2 \left[\tilde{x}_4 + \lambda_3 |e_3|^{1/2} \operatorname{sign}(e_3) \right], \\ \vdots \\ \dot{\tilde{x}}_{n-1} = E_{n-3} \alpha_{n-2} \operatorname{sign}(e_{n-2}), \\ \dot{\hat{x}}_{n-1} = E_{n-2} \left[\tilde{x}_n + \lambda_{n-1} |e_{n-1}|^{1/2} \operatorname{sign}(e_{n-1}) \right], \\ \dot{\tilde{x}}_n = E_{n-2} \alpha_{n-1} \operatorname{sign}(e_{n-1}), \\ \dot{\hat{x}}_n = E_{n-1} \left[\tilde{\theta} + \lambda_n |e_n|^{1/2} \operatorname{sign}(e_n) \right], \\ \dot{\tilde{\theta}} = E_{n-1} \alpha_n \operatorname{sign}(e_n), \end{cases} \tag{1.8}$$

where $e_i = \tilde{x}_i - \hat{x}_i \ \forall i = \{1, \cdots N\}$, $\tilde{x}_1 = x_1$, the observer's output is the vector $[\tilde{x}_1, \cdots, \tilde{x}_N, \tilde{\theta}]$, α_i and λ_i are the observer's gains.

E_i are scalar functions such that $\forall i = \{1, \cdots N\}$:

$$E_i = 1 \text{ if } |e_j| \leqslant \epsilon, \forall j \leqslant i, \text{ otherwise } E_i = 0. \tag{1.9}$$

Which means that E_i are activation terms that only activate when the ith error dynamic converges. This leads to a step by step algorithm to design this observer ($N-1$ steps in total). At each step, the observers gains are carefully chosen, obeing to certain inequalities in order to achieve the finite time convergence.

At last the unknown input $\omega(t)$ can be easily approximated by inverting $\beta(x)$ in (1.7). More details on the behavior of the dynamics error, the conditions on the gains and the generalization to the MIMO case can be found in [18]. The first drawback of this observer is that it is restrained to the class of systems (1.7). This obsever is designed in such a way that the equivalent outputs are injected in a smooth and continuous way without using a low pass filter like it is done for a classical sliding mode observer. The authors of [18] claim that this observer is less exposed to the chattering phenomenon. However, as it is stated in [62], the structure of the super twisting algorithm implies two sources for the chattering phenomenon: one from the discontinuous function and another from the non-Lipschitzian function with infinite derivative at the origin. A comparative study and behavior analysis between the standard sliding mode observer and the supertwisting algorithm concludes that the chattering's amplitude for the supertwisting observer is actually higher than in the conventional sliding mode observer when the system is exposed to a disturbance.

1.4.3 Global finite-time high-gain observer

The observers seen previously all rely on discontinuous functions. The goal now is to obtain a smooth and continuous observer that converges in finite time. One observer that can satisfy these conditions is the High-gain observer (see [23]). A first approach was proposed in [58], where the authors proved the existence of a semi-global and finite time high gain observer for non linear systems with a single output that are uniformly observable and globally Lipschitzian. In [42], the authors extended this observer and obtained a global result. In this section, we will only discuss the results, all the proofs and theory behind this observer can be found in [42], [45] and [24].

Let us consider the following system:

$$\begin{aligned}
\dot{x}_1 &= x_2 + \sum_{j=1}^{m} g_{1,j}(x_1)u_j, \\
\dot{x}_2 &= x_3 + \sum_{j=1}^{m} g_{2,j}(x_1, x_2)u_j, \\
&\vdots \\
\dot{x}_{N-1} &= x_N + \sum_{j=1}^{m} g_{N-1,j}(x_1, \ldots, x_{N-1})u_j, \\
\dot{x}_N &= \varphi(x) + \sum_{j=1}^{m} g_{N,j}(x)u_j, \\
y &= x_1 = Cx,
\end{aligned} \tag{1.10}$$

where the state vector is $x = \begin{bmatrix} x_1 & x_2 & \cdots x_N \end{bmatrix}^\top \in \subseteq \mathbb{R}^N$, $y \in \mathbb{R}$ the measured output vector, $u = \begin{bmatrix} u_1 & \cdots & u_m \end{bmatrix} \in \mathbb{R}^m$, $C = \begin{bmatrix} 1 & 0 & \cdots & 0 \end{bmatrix}$, ϕ and $g_{i,j}\, i = \{1, \cdots N\}\ j == \{1, \cdots m\}$ are continuous globally Lipschitz (l-Lipschitz) functions with null initial conditions, i.e: $\phi(0) = 0$, $g_{i,j} = 0$ and we assume $\exists u_0 \in \mathbb{R}$ such that: $\|u\|_\infty \leqslant u_0$.

Theorem 1: [42] Considering the system (1.10): $\exists 0 < \theta^* < \infty$ and $\exists \epsilon > 0$ such that: $\forall \theta > \theta^*$ and $\forall \alpha \in]1-\epsilon, 1[$ the system (1.10) admits the following observer:

$$\begin{cases}
\dot{\hat{x}}_1 = \hat{x}_2 + k_1 \left(\lceil e_1 \rfloor^{\alpha_1} + \rho e_1 \right) + \sum_{j=1}^{m} g_{1,j}(\hat{x}_1)u_j, \\
\dot{\hat{x}}_2 = \hat{x}_3 + k_2 \left(\lceil e_1 \rfloor^{\alpha_2} + \rho e_1 \right) + \sum_{j=1}^{m} g_{2,j}(\hat{x}_1, \hat{x}_2)u_j, \\
\vdots \\
\dot{\hat{x}}_n = k_n \left(\lceil e_1 \rfloor^{\alpha_n} + \rho e_1 \right) + \varphi(\hat{x}) + \sum_{j=1}^{m} g_{n,j}(\hat{x})u_j,
\end{cases} \tag{1.11}$$

where $e_1 = x_1 - \hat{x}_1$, $\rho = \frac{1}{2}(n^2\theta^{2/3}S_1 + 1)$, and $S_1 = \max_{1 \leqslant i,j \leqslant n} |S_\infty(1)_{i,j}| \,.\, |S_\infty^{-1}(1)_{j,1}|$, the gains $K = [k_1, \ldots, k_n]^\top = S_\infty^{-1}(\theta)C^\top$ and the powers $alpha_i$ are given by: $\alpha_i = i\alpha - (i-1), \quad i = 1, \ldots, n, \quad \alpha \in \left]1 - \frac{1}{n}, 1\right[$.

This observer was also extended for a class of nonlinear systems with non-Lipschitz conditions by introducing a new gain update law [36].

1.4.4 Integral based estimation methods

Integral based estimation methods are another kind of estimators that have been widely investigated in the literature since the fifties, when the concept was first introduced in [59]. These methods transform the observation problems from a space to another, using specific functions that can be referred to as *kernels, method function, modulating functions...* etc. Since these methods generally imply integration, they are known for their robustness in presence of disturbances as the integration dampens the noise. They are also famous for giving fast and finite convergence.

In the next chapters, we will address these methods in details.

1.5 Conclusion

In general, finite fime convergence is prefered to the asymptotical one. However, the non-Lipschtizien condition of the nonasymptotic convergence highly restrains its use. A rigorous framework to tackle this kind of convergence was set in [8]. This has lead to an abundont work in the litterature to solve observation and estimation problems in a finite time. The most famous tool to do so is the sliding mode observer (see [63] and[15]) but the discountinuity of its output injections causes the chattering phenomenon [61]. Generalization of the sliding mode observer were made on different classes of systems, for example: the supertwisting observer that tackles a class of nonlinear system with unknown inputs [18]. The main problem with this last observer is that it amplifies the chattering phenomenon when the system is exposed to a disturbance [62]. The high gain observer, which is originally asymptotic, has also been improved to give a non-asymptotical convergences for certain class of systems (see [45], [42], [24], [58] and [36]). Another tool is the integral based estimation method that rely on kernels to transform the observation from a space to another. This precise type of methods will be widely investigated in the next chapters.

Chapter 2

Volterra estimation of a biased sinusoidal signal

2.1 Introduction

In this chapter, we will introduce the general Volterra approach through one particular problem: the estimation of the amplitude, frequency and phase (AFP) of a biased sinusoidal signal. This problem is well known and there exists an abundont work in the literature to solve it. However, most of the estimation or identification tools used are often only asymptotically stable, which is not enough for certain applications. We will first recall some prerequisite definitions needed, define and explain the Volterra approach in general. We will then focus on the AFP estimation problem, develop and explain the steps of the estimation method proposed in [51]. Finally, we will present numerical simulations with a sensitive analysis of this observer and discuss the results.

2.2 Definitions and prerequisites

Definition 1 (Hilbert Space): [22] A Hilbert Space is an *inner product* space that can be real or complex, and that is *complete* with respect to the inner product's norm.

To illustrate this definition one can consider the Euclidian space that is the most famous Hilbert Space. The Euclidian space is a three dimention real space $\mathbb{R}^3$ and its inner product is the dot product.

Definition 2 (Hilbert-Schmidt kernel): [22] A Hilbert-Schmidt ($\mathcal{HS}$) is a function $k : \Gamma \times \Gamma \to \mathbb{C}$ such that:

$$\int_\Omega \int_\Omega |k(x,y)|^2 \, dx \, dy < \infty \tag{2.1}$$

where Γ is an opend and connected set in a the $\mathbb{R}^n$ Euclidean space.

Definition 4 (Leibniz Integral Rule): [57] Let us consider the continuous and continuously differentiable function $f(x,t)$. $a(x)$ and $b(x)$ are differentiable functions of x,

we have:

$$\frac{d}{dx}\left(\int_{a(x)}^{b(x)} f(x,t)\,dt\right) = f\big(x,b(x)\big)\cdot\frac{d}{dx}b(x) - f\big(x,a(x)\big)\cdot\frac{d}{dx}a(x) + \int_{a(x)}^{b(x)}\frac{\partial}{\partial x}f(x,t)\,dt, \quad (2.2)$$

where $a(x) < \infty/, b(x) < \infty$. If $a(x)$ and $b(x)$ are constant functions, this formula becomes:

$$\frac{\mathrm{d}}{\mathrm{d}x}\int_a^b f(x,t)\mathrm{d}t = \int_a^b \frac{\partial}{\partial x}f(x,t)\mathrm{d}t \quad (2.3)$$

Definition 5 (Volterra Integral): [27] Let $u(t) \in \mathbb{R},\ \forall t > 0$, be an Nth-order differentiable signal. Given a Hilbert-Schmidt ($\mathcal{HS}$) kernel function $K(.,.)$, in two variables. The Volterra integral operator induced by the kernel function is

$$[V_K u](t) \triangleq \int_0^t K(t,\tau)u(\tau)d\tau, \qquad t \in \mathbb{R}_+. \quad (2.4)$$

Lemma 1: [52] For a given $i \in \mathbb{N}$, consider a signal $u(.) \in \mathcal{L}^2(\mathbb{R})$ (the Hilbert space of locally square integrable functions) that admits its derivative and a $\mathcal{HS}$ kernel function $K(.,.)$, admitting the ith derivative with respect to the second argument. Then, it holds that:

$$\begin{aligned}[V_K u^{(i)}](t) = &\sum_{j=0}^{i-1}(-1)^{i-j-1}u^{(j)}(t)K^{(i-j-1)}(t,t) + \sum_{j=0}^{i-1}(-1)^{i-j}u^{(j)}(0)K^{(i-j-1)}(t,0)\\ &+ (-1)^i[V_{K^{(i)}}u](t).\end{aligned} \quad (2.5)$$

Definition 6 (Ith order non-asymmptotic kernel): [52] A $\mathcal{HS}$ kernel $K(.,.)$ is called an ith order non-asymptotic kernel function if it is at least $(i-1)$th order differentiable with respect to the second argument, and it verifies the condition:

$$K^{(j)}(t,0) = 0,\ \forall j \in \{0,1,...,i-1\}. \quad (2.6)$$

Lemma 2 [52] For a given $i \in \mathbb{N}$, consider a signal $u(.) \in \mathcal{L}^2(\mathbb{R})$ that admits its derivative and a ith order non-asymptotic $\mathcal{HS}$ kernel function $K(.,.)$, admitting the ith derivative

with respect to the second argument. Then, it holds that:

$$[V_K u^{(i)}](t) = \sum_{j=0}^{i-1} (-1)^{i-j-1} u^{(j)}(t) K^{(i-j-1)}(t,t) + (-1)^i [V_{K^{(i)}} u](t). \tag{2.7}$$

2.3 The AFP Volterra observer

2.3.1 Position of the problem

Let us now consider the following biased sinusoidal signal:

$$y(t) = A_0 + A^* \sin(v(t)), \quad \dot{v}(t) = \omega^*, \quad v_0 = \phi, \quad t \geqslant 0, \tag{2.8}$$

where $A_0 \in \mathbb{R}_+$ is the unknown bias, $A^* \in \mathbb{R}_+$ is the unknown amplitude, ω^* is the angular frequency and ϕ is the initial phase shift.

The objective is to estimate the amplitude, frequency and phase of this signal with only measurements $y(t)$.

General construction of the Volterra observer

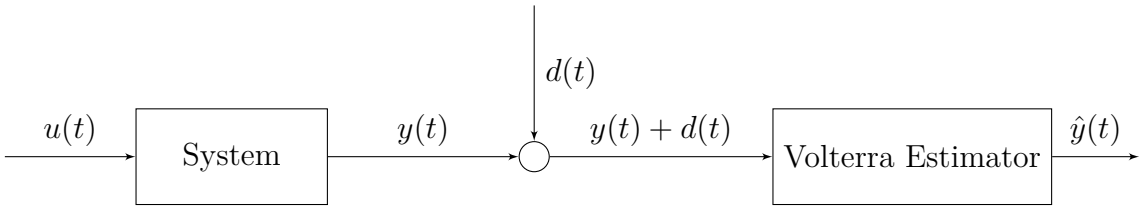

Figure 2.1: Block diagram of the Volterra observer

The observer works in an open loop and doesn't require feedback. Therefore, the system can be considered as a black box and the input are unknown. The only data needed is the output $y(t)$.

2.3.2 Frequency observer

Proposition: The frequency squared $\Omega(t) = \omega^2(t)$ can be observed using the following adaptation law:

$$\begin{aligned}
\hat{\Omega}(t) &= \begin{cases} \gamma_2(t)^{-1}\left(\eta_\Omega(t) + L_1\sqrt{|R_\Omega(t)|}\,\mathrm{sign}\left(R_\Omega(t)\right) - \widehat{\Omega}(t)\dot{\gamma}_2(t) + \dot{\gamma}_1(t)\right), & \text{if } \gamma_2(t) \geqslant \delta_\epsilon \\ 0, \quad \text{otherwise} \end{cases} \\
\dot{\eta}_\Omega(t) &= L_2\,\mathrm{sign}\left(R_\Omega(t)\right), \quad \eta_\Omega(0) = 0, \\
R_\Omega(t) &= \gamma_1(t) - \gamma_2(t)\widehat{\Omega}(t).
\end{aligned} \tag{2.9}$$

Where $\hat{\Omega}(0) > 0$ is chosen aribitrarly. The strictly postive gains L_1 and L_2 are set by the designer, and δ_ϵ is a strictly postive value that depends on the activation time set by the designer (see [51]) and the signals $\gamma_1(t)$ and $\gamma_2(t)$ are defined next.

Proof: It is noticeable that (2.8) is generated by a linear dynamical system modeled by the following ODE:

$$y^{(3)}(t) = -\Omega^* y^{(1)}(t), \quad \text{where } \Omega^* = \omega^{*2}, \quad t \geqslant 0. \tag{2.10}$$

Now, we introduce the Volterra integral operator. The linear property of this operator gives:

$$\left[V_K y^{(3)}\right](t) = -\Omega^* \left[V_K y^{(1)}\right](t). \tag{2.11}$$

Considering (2.7), for $i = 1$ we have:

$$\left[V_K y^{(1)}\right](t) = y(t)K(t,t) - \left[V_{K^{(1)}} y\right](t). \tag{2.12}$$

Let us now replace K with one of its derivatives with respect to the second argument $K^{(j)}$, and y by its ith derivative. (2.12) implies that:

$$\left[V_{K^{(j)}} y^{(i+1)}\right](t) = y^{(i)}(t)K^{(j)}(t,t) - \left[\mathcal{V}_{K^{(j+1)}} y^{(i)}\right](t). \tag{2.13}$$

Using this last result on both sides of (2.11) and after some algebra, we obtain:

$$\begin{aligned}&\left[V_{K^{(3)}}y\right](t) - K^{(2)}(t,t)y(t) + K^{(1)}(t,t)y^{(1)}(t) - K(t,t)y^{(2)}(t)\\&+\Omega^*\left(\left[V_{K^{(1)}}y\right](t) - K(t,t)y(t)\right) = 0.\end{aligned} \tag{2.14}$$

Let us remmember now that the kernel function K is a degree of freedom that we chose in this method, which means that this function and its derivatives can be computed. Ω^* is a parameter to be estimated and we suppose to have the measurement $y(t)$. Only the Volterra transformed signals and the signal's derivatives are unknown. Therefore, the idea is to estimate these signals. But first, we need to introduce the ith order non-asymptotical kernel function that we will use.

The authors in [51] proposed the following exponential bivariate kernel functions family:

$$F_h(t,\tau) = e^{-\omega_h(t-\tau)}(1-e^{-\bar{\omega}\tau})^N, \text{ where } \omega_h > 0\, \bar{\omega} > 0,\ N \in \mathbb{N}. \tag{2.15}$$

In this particular case, $N = 3$ and $h = \{1, 2, 3\}$.

Using this kernel function family, equation (2.14) becomes:

$$\begin{aligned}&\left[V_{F_h^{(3)}}y\right](t) - F_h^{(2)}(t,t)y(t) + F_h^{(1)}(t,t)y^{(1)}(t) - F_h(t,t)y^{(2)}(t)\\&+\Omega^*\left(\left[V_{F_h^{(1)}}y\right](t) - F_h(t,t)y(t)\right) = 0, \quad h = 1,2,3.\end{aligned} \tag{2.16}$$

The authors then proposed the introduction of the following auxiliary signals in order to simplify the writings:

$$\begin{aligned}&\kappa_{a,h}(t) \triangleq \left[V_{F_h^{(3)}}y\right](t) - F_h^{(2)}(t,t)y(t),\\&\kappa_{b,h}(t) \triangleq F_h^{(1)}(t,t), \quad \kappa_{c,h}(t) \triangleq -F_h(t,t),\\&\kappa_{d,h}(t) \triangleq \left[V_{F_h^{(1)}}y\right](t) - F_h(t,t)y(t), \quad \forall h = 1,2,3.\end{aligned} \tag{2.17}$$

Replacing the signals (2.17) in (2.16) we obtain a system of 3 equations. Exploiting the fact that $\kappa_{c,1}(t) = \kappa_{c,2}(t) = \kappa_{c,3}(t)$ and with some algebra we will obtain the following:

$$\begin{aligned}&\kappa_{a,1}\left(\kappa_{b,3} - \kappa_{b,2}\right) + \kappa_{a,2}\left(\kappa_{b,1} - \kappa_{b,3}\right) + \kappa_{a,3}\left(\kappa_{b,2} - \kappa_{b,1}\right)\\&+\Omega^*\left(\kappa_{d,1}\left(\kappa_{b,3} - \kappa_{b,2}\right) + \kappa_{d,2}\left(\kappa_{b,1} - \kappa_{b,3}\right) + \kappa_{d,3}\left(\kappa_{b,2} - \kappa_{b,1}\right)\right) = 0.\end{aligned} \tag{2.18}$$

This leads to the following system:

$$\kappa_1(t) = -\Omega^* \kappa_2(t), \tag{2.19}$$

where

$$\kappa_1(t) = \begin{bmatrix} \kappa_{a,1} & \kappa_{a,2} & \kappa_{a,3} \end{bmatrix} \begin{bmatrix} F_3^{(1)}(t,t) - F_2^{(1)}(t,t) \\ F_1^{(1)}(t,t) - F_3^{(1)}(t,t) \\ F_2^{(1)}(t,t) - F_1^{(1)}(t,t) \end{bmatrix}, \kappa_2(t) = \begin{bmatrix} \kappa_{d,1} & \kappa_{d,2} & \kappa_{d,3} \end{bmatrix} \begin{bmatrix} F_3^{(1)}(t,t) - F_2^{(1)}(t,t) \\ F_1^{(1)}(t,t) - F_3^{(1)}(t,t) \\ F_2^{(1)}(t,t) - F_1^{(1)}(t,t) \end{bmatrix}. \tag{2.20}$$

Let us consider the following $\xi_h(t) \triangleq [V_{F_h^{(i)}} y](t)$ where $i = \{1, 2, 3\}$. Applying the Leibniz integral rule (2.3) to the definition of the Volterra integral (2.4) we obtain:

$$\begin{aligned} \dot{\xi}_h(t) &= F_h^{(i)} y(t) + \int_0^t \frac{\partial}{\partial t} F_h(t,\tau) y(\tau) d\tau, \\ &= F_h^{(i)} y(t) - \bar{\omega} \int_0^t F_h(t,\tau) y(\tau) d\tau, \\ &= F_h^{(i)} y(t) - \bar{\omega} \xi_h(t), \ t \geqslant 0. \end{aligned} \tag{2.21}$$

Considering the state vector $\xi(t)$, we get the following time varying dynamic system:

$$\begin{aligned} \dot{\xi}(t) &= G\xi(t) + E(t) y(t), \ t \geqslant 0, \\ \xi(0) &= 0. \end{aligned} \tag{2.22}$$

where:

$$\xi(\mathrm{t})=\begin{bmatrix}[V_{F_1^{(1)}}y](t)\\ [V_{F_1^{(3)}}y](t)\\ [V_{F_2^{(1)}}y](t)\\ [V_{F_2^{(3)}}y](t)\\ [V_{F_3^{(1)}}y](t)\\ [V_{F_3^{(3)}}y](t)\end{bmatrix},\quad \mathrm{G}=\begin{bmatrix}-\omega_1 & 0 & 0 & 0 & 0 & 0\\ 0 & -\omega_1 & 0 & 0 & 0 & 0\\ 0 & 0 & -\omega_2 & 0 & 0 & 0\\ 0 & 0 & 0 & -\omega_2 & 0 & 0\\ 0 & 0 & 0 & 0 & -\omega_3 & 0\\ 0 & 0 & 0 & 0 & 0 & -\omega_3\end{bmatrix},\quad \mathrm{E(t)}=\begin{bmatrix}F_1^{(1)}(t,t)\\ F_1^{(3)}(t,t)\\ F_2^{(1)}(t,t)\\ F_2^{(3)}(t,t)\\ F_3^{(1)}(t,t)\\ F_3^{(3)}(t,t)\end{bmatrix}. \tag{2.23}$$

Since G is a Hurwitz matrix, the origin of this LTVI system converges.

Thus, $\kappa_{a,h}$, $\kappa_{d,h}$ can be deduced

$$\begin{aligned}\kappa_{a,h}(t) &= \xi_{2h}(t) - F_h^{(2)}(t,t)y(t),\\ \kappa_{d,h}(t) &= \xi_{2h-1}(t) - F_h(t,t)y(t),\ t \geqslant 0.\end{aligned} \tag{2.24}$$

where $h = \{1, 2, 3\}$.

Now that $\kappa_1(t)$ and $\kappa_2(t)$ can be estimated in (2.19), we can construct a second order sliding mode observer to estimate the frequency. To do so, we tranform the absolute value of (2.19) using another kernel function $K_g(t,\tau) = e^{-g(t-\tau)}$ where $g > 0$. We obtain:

$$\Omega^* \left[V_{K_g} |\kappa_2(t)|\right](t) = \left[V_{K_g} |\kappa_1(t)|\right](t) \tag{2.25}$$

Using the same reasoning as in (2.21), the authors define $\gamma_i(t) \triangleq \left[V_{K_g} |\kappa_i(t)|\right](t)$, $i = 1, 2$, and have:

$$\begin{aligned}\dot{\gamma}_1(t) &= |\kappa_1(t)| - g\gamma_1(t), \quad \gamma_1(0) = 0,\\ \dot{\gamma}_2(t) &= |\kappa_2(t)| - g\gamma_2(t), \quad \gamma_2(0) = 0.\end{aligned} \tag{2.26}$$

At last, we obtain the observer in (2.26).

2.3.3 Amplitude estimation

Proposition: The following second order sliding mode observer is proposed to estimate the amplitude:

$$\begin{aligned}\dot{\widehat{A}}(t) &= \begin{cases} \gamma_{A_2}(t)^{-1}\left(\eta_A(t) + L_3\sqrt{|R_A(t)|}\,\mathrm{sign}\left(R_A(t)\right) - \widehat{A}(t)\dot{\gamma}_{A_2}(t) + \dot{\gamma}_{A_1}(t)\right) & \forall t > t_\epsilon + \bar{T}_\Omega, \\ 0, \quad \text{otherwise}, \end{cases} \\ \dot{\eta}_A(t) &= L_4\,\mathrm{sign}\left(R_A(t)\right), \end{aligned} \tag{2.27}$$

where L_3 and L_4 are strictly positive real tuning gains that are set by the designer.

Proof: In order to estimate the amplitude, the authors propose another dynamic linear system to generate the signal (2.8), this is the novel ODE considered:

$$\Omega^* y^{(1)}(t)^2 + y^{(2)}(t)^2 = A^{*2}\Omega^{*2}. \tag{2.28}$$

We apply the Volterra operator to both sides with the kernel function $K_{g_a}(t,\tau) = e^{-g_a(t-\tau)},\ g_a \in \mathbb{R}_+$:

$$\left[V_{K_{g_a}}\sqrt{\Omega^* y^{(1)}(t)^2 + y^{(2)}(t)^2}\right](t) = A^*\left[K_{K_{g_a}}\Omega^*\right](t). \tag{2.29}$$

Based on this last equation, a time varyin residual signal is introduced:

$$\begin{aligned} R_A(t) \triangleq \left[V_{K_{g_a}}\sqrt{\widehat{\Omega}(t)(\widehat{y^{(1)}}(t))^2 + (\widehat{y^{(2)}}(t))^2}\right](t) - \widehat{A}(t)\left[V_{K_g}\widehat{\Omega}(t)\right](t) = \gamma_{A_1}(t) \\ -\widehat{A}(t)\gamma_{A_2}(t), \quad \forall t \geqslant t_\epsilon + \bar{T}_\Omega \end{aligned} \tag{2.30}$$

where T_Ω is the upper bound of the finite convergence time of the observer in (2.26) and t_ϵ is the activation time set by the designer.

Notice that the first and second derivatives of the signal's intervene in this residual. The authors in [51] proposed to estimate the derivatives by first defining the signal $\rho_h\left(\Omega^*, t\right) = \kappa_{a,h}(t) + \Omega^*\kappa_{d,h}(t), \quad h = 1,2,3$. From (2.16) we can estimate the derivatives through these identities:

$$\begin{cases} y^{(1)}(t) = \frac{F_1(t,t)\rho_h(\Omega^*,t) - F_h(t,t)\rho_1(\Omega^*,t)}{F_1^{(1)}(t,t)F_h(t,t) - F_1(t,t)F_h^{(1)}(t,t)}, \\ y^{(2)}(t) = \frac{F_1^{(1)}(t,t)\rho_h(\Omega^*,t) - F_h^{(1)}(t,t)\rho_1(\Omega^*,t)}{F_1^{(1)}(t,t)F_h(t,t) - F_1(t,t)F_h^{(1)}(t,t)}. \end{cases} \tag{2.31}$$

The well posness of these expressions for $h \neq 1$ is proved in [51].

Once the derivatives can be estimated, we introduce the following system:

$$\begin{aligned}\dot{\gamma}_{A_1}(t) &= \psi(t)\left(\sqrt{\widehat{\Omega}(\widehat{y^{(1)}}(t))^2 + (\widehat{y^{(2)}}(t))^2} - g_a\gamma_{A_1}(t)\right), \quad \gamma_{A_1}(0) = 0,\\ \dot{\gamma}_{A_2}(t) &= \psi(t)\left(\widehat{\Omega}(t) - g_a\gamma_{A_2}(t)\right), \quad \gamma_{A_2}(0) = 0,\end{aligned} \tag{2.32}$$

where $\psi(t)$ is a switching signal such that:

$$\psi(t) = \begin{cases} 1, & \text{if } t \geqslant t_\epsilon + T_\Omega,\\ 0, & \text{otherwise.}\end{cases} \tag{2.33}$$

2.3.4 Phase estimation

At last, the phase of the signal (2.8) is the argurment of a complex number and it can be deduced from:

$$\widehat{\vartheta}(t) = \angle[\widehat{\omega}(t)\widehat{y^{(1)}}(t) - j\widehat{y^{(2)}}(t)], \quad \forall t \geqslant t_\epsilon + \bar{T}_\Omega. \tag{2.34}$$

2.4 Numerical simulations

2.4.1 Constant amplitude and frequency:

Noise-free scenario:

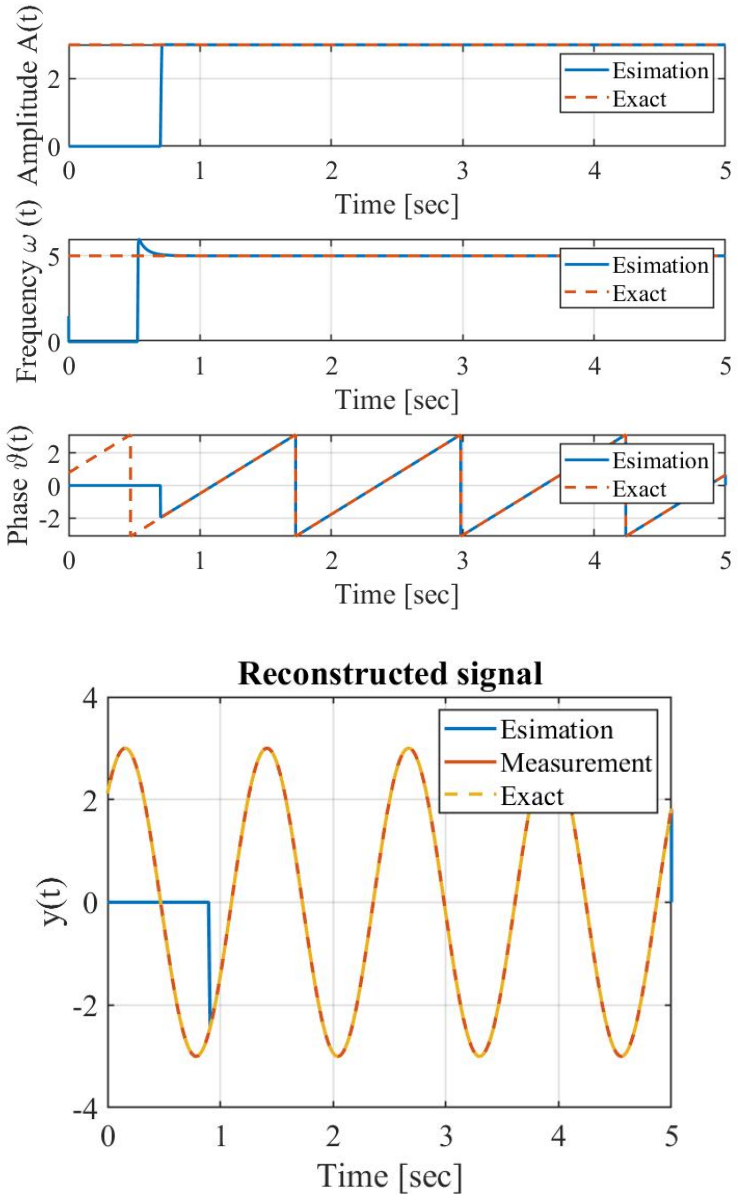

Figure 2.2: Amplitude, frequency and phase estimation of the unbiased signal $y_1(t)$

Let us begin with a simple introduction example where we consider the following unbiased sinusoidal signal: $y_1(t) = 3\sin(5t + \frac{\pi}{4})$, and propose to use the Volterra observer to estimate the amplitude, frequency and phase of this signal and reconstruct it.

As it has been stated in [51], Euler's discretization is sufficient to obtain accurate results

with a sampling time of $T_s = 10^{-4}s$. We first take $\bar{\omega} = 2.5$, $\omega = [1\ 2\ 3]$ and set the observers gains at $L_1 = 30$, $L_2 = 2$, $L_3 = 300$ and $L_5 = 5$. We also consider $g = g_a = 25$, and set the frequency's squared initial condition $\Omega(0) = \sqrt{5}$ and $\delta_\epsilon = 10^{-4}$ and $T_\Omega = 0,7s$.

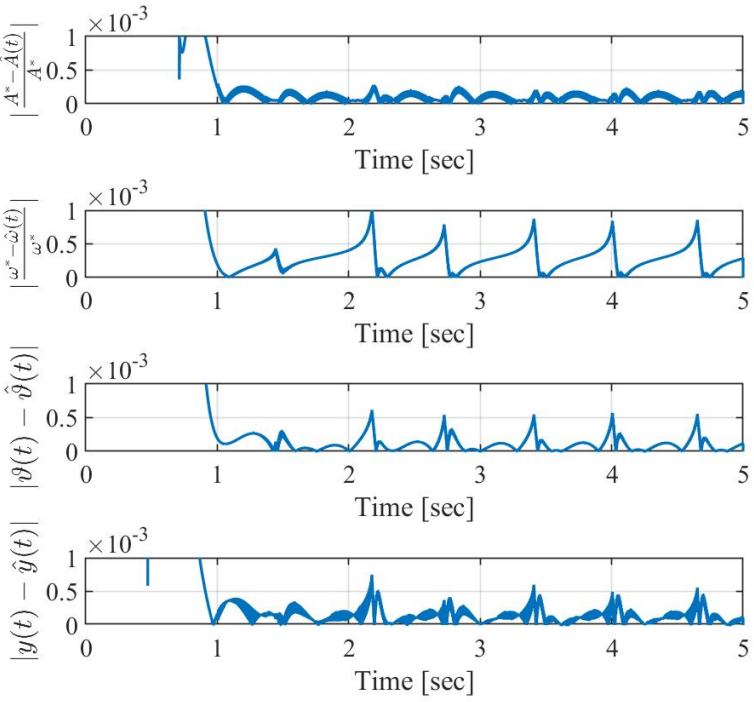

Figure 2.3: Estimation errors of $y_1(t)$

This exemple confirms the fast convergence and accuracy of the AFP Volterra observer as figure (2.2) shows. In order to illustrate this accuracy quantitavely, we computed the relative errors of the amplitude and frequency and absolute errors of the phase and signal. The two latter signals vanish periodically which will lead the relative error to tend to high values and this does not translate the estimation's accuracy, which is why the absolute error is preferred in this case. The results are shown in figure (2.3). All errors have the same magnitude of 10^{-3}. However, notice that : $\forall t \leqslant t_0$ where $t_0 = 1s$, the errors are higher and this translates to the transitional phase.

Noisy scenario:

Now let us consider the same signal as previously but with a bias such that the measurement is $y_{m1}(t) = y_1(t) + d_1(t)$, where $d_1(t)$ is an additive normally distributed signal in $[-0.25\ 0.25]$. We compute the estimation with the same parameters as in the noise-free scenario.

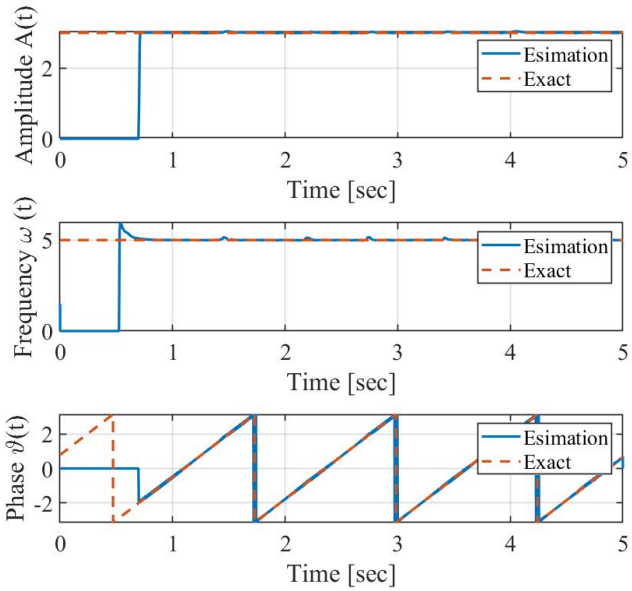

Figure 2.4: Amplitude, frequency and phase estimation of the biased signal $y_{m1}(t)$

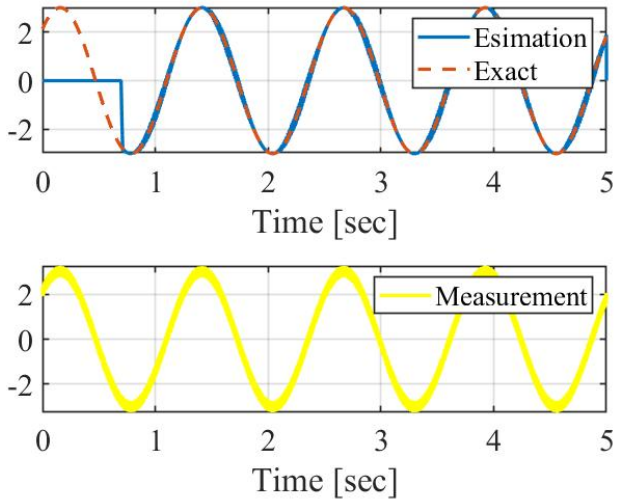

Figure 2.5: Reconstructed signal based on the biased signal $y_{m1}(t)$

The observer's performance remains accurate as the fast and finite convergence is still

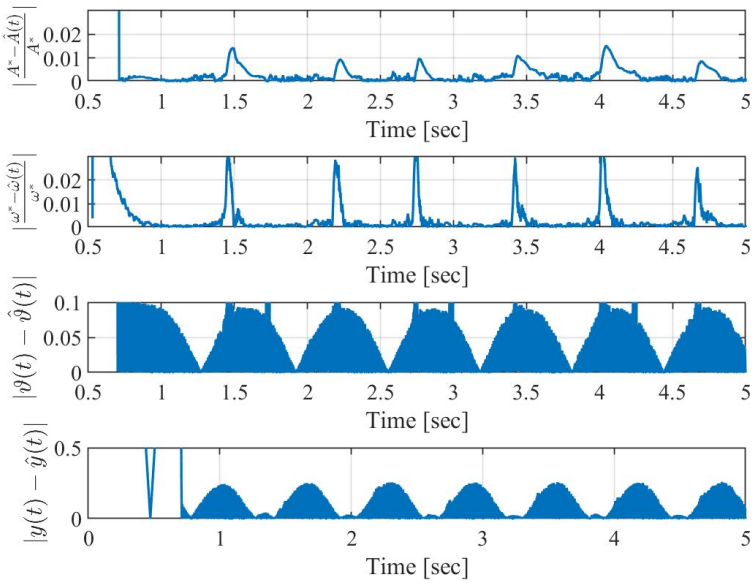

Figure 2.6: Estimation errors of $y_{m1}(t)$

established for amplitude, frequency and phase. From the reconstructed signal, it is noticeable that the method has no affect on the noise: it neither amplifies nor reduces it. Figure (2.6) shows that the errors magnitude have increased. As it became about 3% for amplitude and frequency and about 5% and 7% for the phase and the signal's reconstruction respectively.

2.4.2 Varying amplitude and constant frequency:

Noise-free scenario

Let us now consider the following signal : $y_2(t) = A(t)\sin(5t + \frac{\pi}{4})$, where the amplitude $A(t)$ is time dependant such that:

$$A(t) = \begin{cases} 10 & \forall\, t < 2, \\ 12 & \forall\, 2 \leqslant t < 5, \\ 6 & \text{otherwise.} \end{cases} \tag{2.35}$$

With this exemple, we aim at testing the proposed observer with the tuning parameters as suggested in [51]. Figure (2.7) shows that the estimation's inaccuracy is proportionnaly dependant on the variation value. It is noticeable that a 20% sudden rise of the amplitude

does not considerably affect the observer, whereas a sudden and considerable variation of the amplitude (until 50% of the initial value) will affect both frequency and amplitude estimations, as the convergence is not instantaneous and needs more time to stabilize, about $5s$ in this case. Which is considered relatively long. Figure (2.8) illustrate this phenomenon as it is noticeable that the relative error of both the amplitude and frequency suddenly rise to about 50% at $t = 5s$, when the amplitude drops. These errors only become negligeable at $t = 10s$.

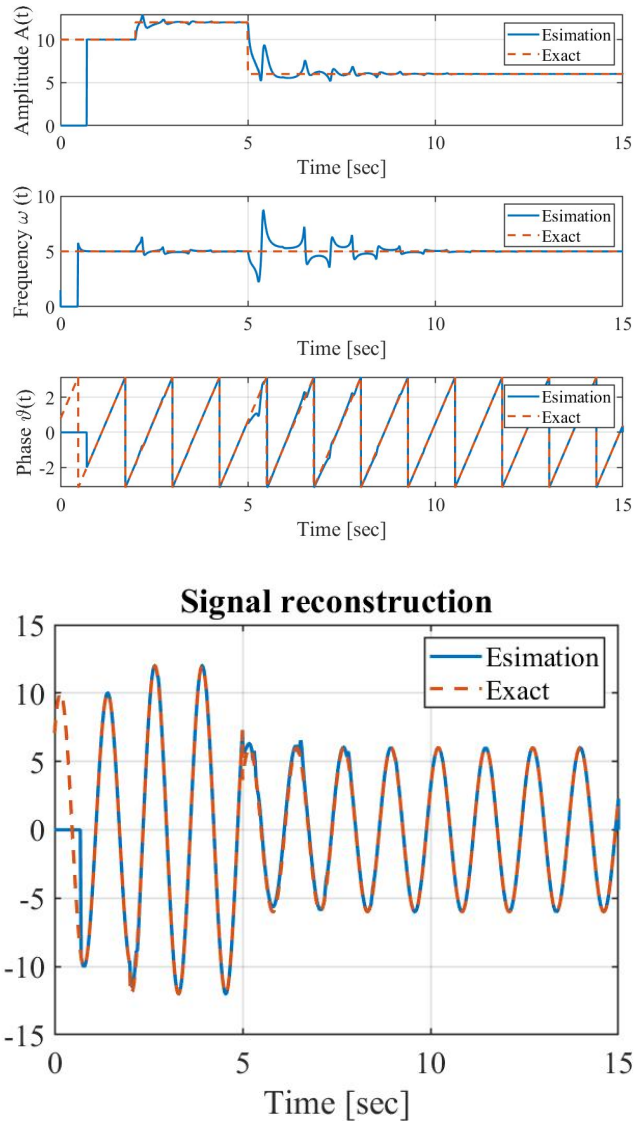

Figure 2.7: Amplitude, frequency, phase and signal estimation of the unbiased signal $y_2(t)$

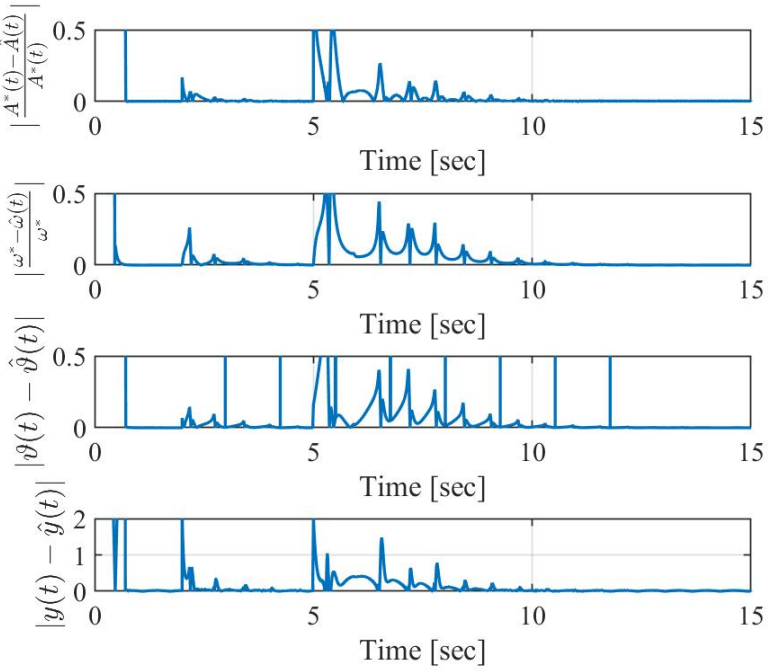

Figure 2.8: Esimation errors of $y_2(t)$

Noisy scenario

We consider the same previous signal $y_2(t)$ with an additive uniformly distributed noisy bias $d_2(t) \in [-1.5 \quad 1.5]$, such that: $y_{m2}(t) = y_2(t) + d_2(t)$. Keeping the observer's parameter the same, we estimate the amplitude, frequency and phase of the signal before reconstructing it as it is shown in figure (2.9). Compared to the unbiased signal, estimation of $y_{m2}(t)$ leads to noisy disturbed parameters. However, we need to keep in mind that the tuning parameters of the Volterra observer were kept relatively low as in the first example. We conjecture that increasing certain parameters can lead to better results. A conjecture we will explore more in the next and last example.

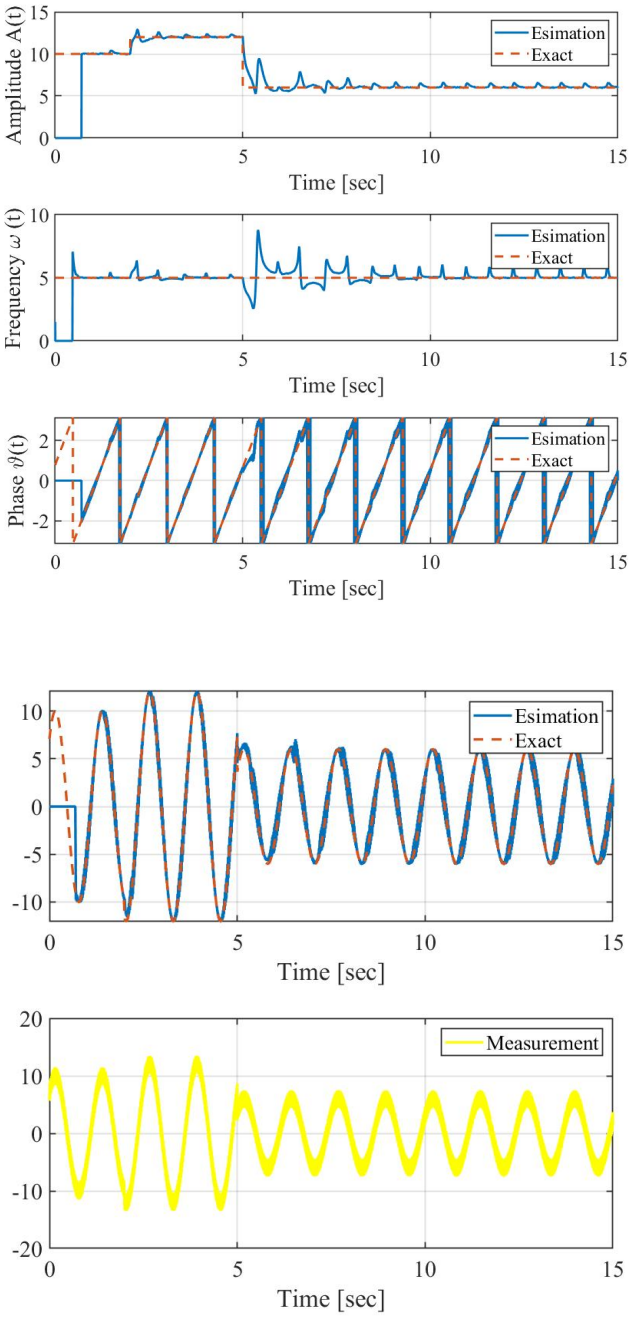

Figure 2.9: Amplitude, frequency, phase estimation and signal estimation of $y_{m2}(t)$

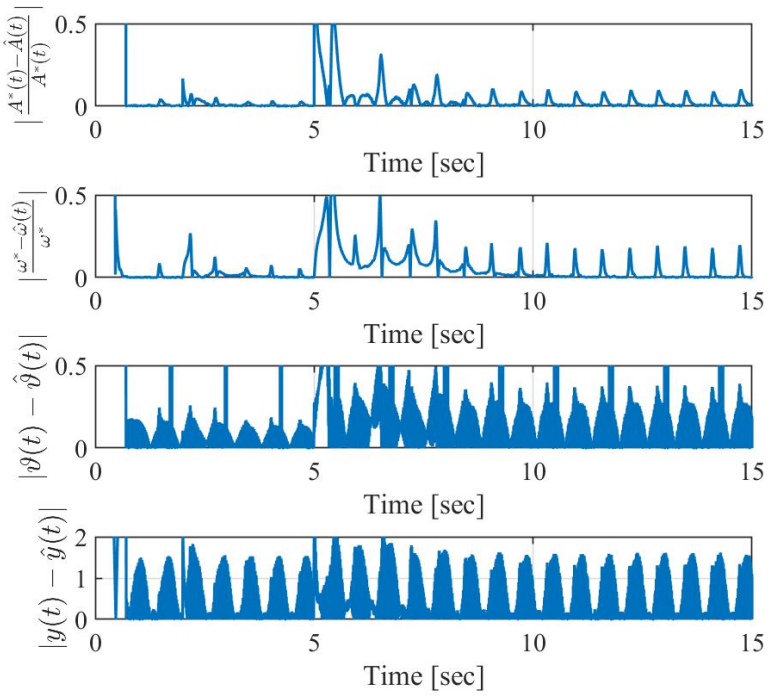

Figure 2.10: Estimation errors of $y_{m2}(t)$

2.4.3 Varying amplitude and frequency

Noise-free scenario:

Let us now consider the following signal biased: $y_3(t) = A_0(t) + A(t)\sin(2\pi f(t) + \frac{\pi}{3})$ where:

$$A(t) = \begin{cases} 10 & \forall\, t < 2, \\ 12 & \text{otherwise}, \end{cases} \quad A_0(t) = \begin{cases} 1 & \forall\, t < 2, \\ 0.8 & \text{otherwise}, \end{cases} \quad f(t) = \begin{cases} 20 & \forall\, t < 2, \\ 22 & \text{otherwise}. \end{cases} \tag{2.36}$$

In this particular example, the bias is not a randomized noise but a constant unknown. Both frequency and amplitude vary together. In order to estimate them, we replace the tuning parameters with higher ones as in [51].

Thus, the tuning parameters of the volterra kernel functions are $\bar{\omega} = 60$, $\omega = [50 \;\; 80 \;\; 100]$, $g = 30$, $g_a = 100$ and $\delta_\epsilon = 3\times10^{-4}$. We set the second order sliding mode observer with the gains: $L_1 = 2 \times 10^4$, $L_2 = 20$, $L_3 = 10^5$ and $L_4 = 50$. We keep the Euler discreditezation method with a sampling time of $T_s = 10^{-4}$s.

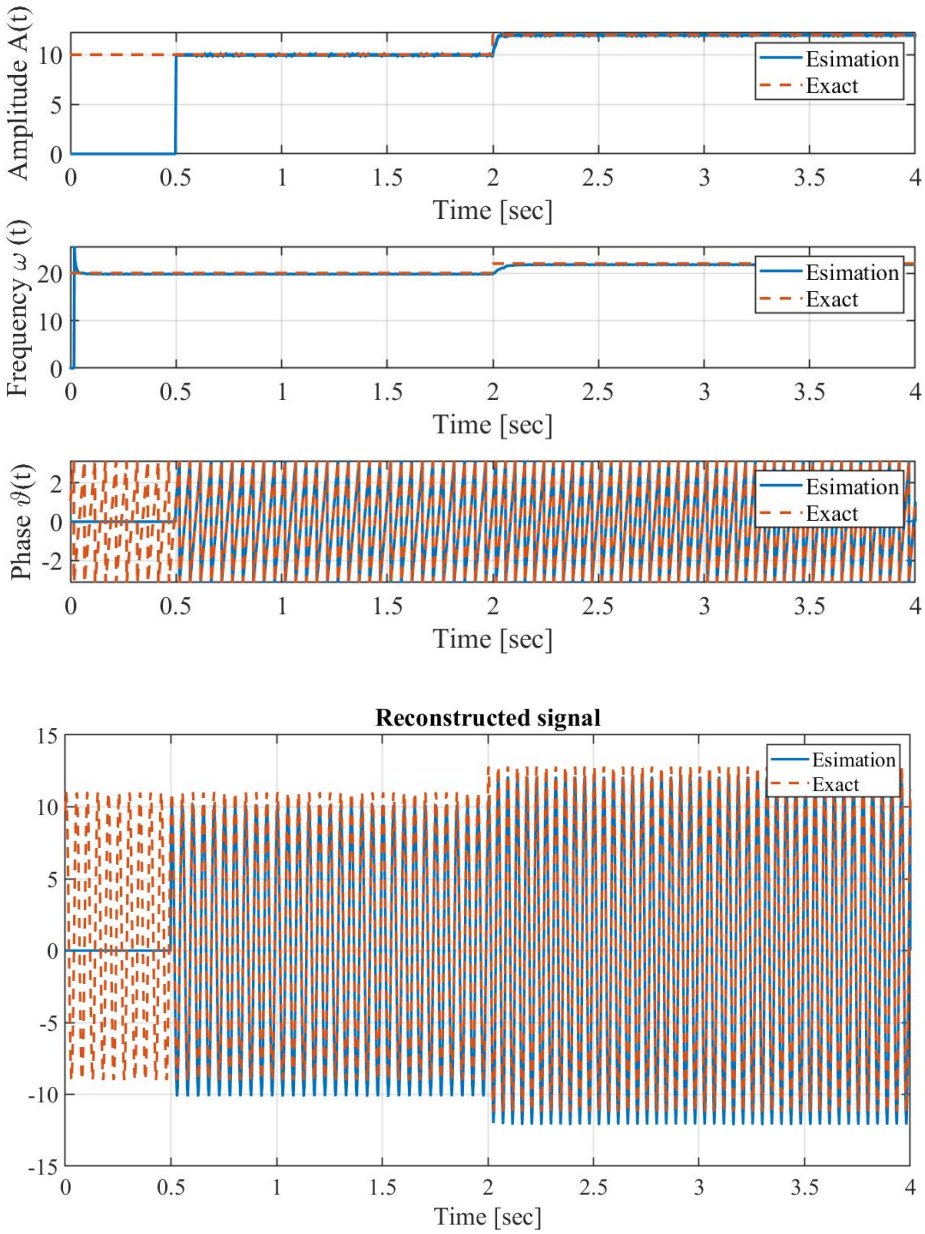

Figure 2.11: Amplitude, frequency, phase estimation and reconstructed signal of the unbiased signal $y_3(t)$

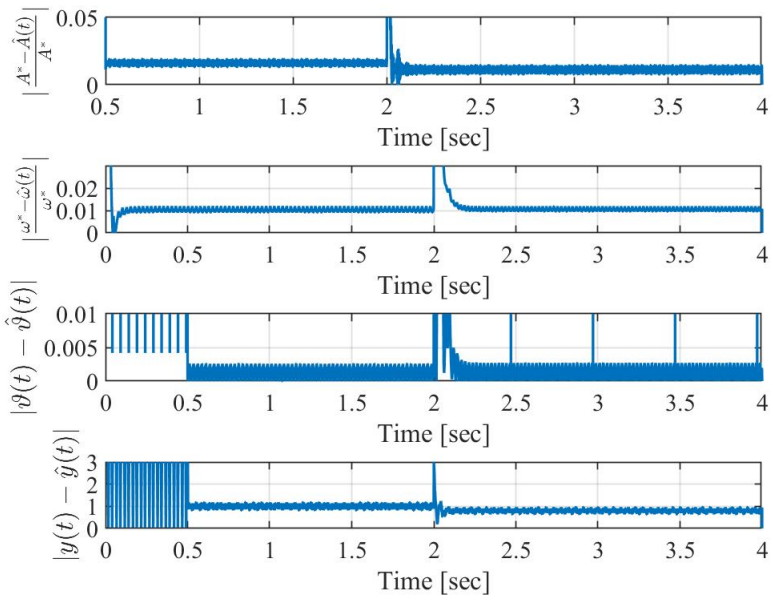

Figure 2.12: Estimation errors of $y_3(t)$

Figure (2.11) shows that a sudden change of the amplitude and frequency references does not always imply a peak phenomenon as we have previously seen. With the adequate parameters the convergence takes a relatively short time (about $0.1s$) and it is achieved smoothly. We can however notice that the reconstructed signal is shifted from the true $y_3(t)$ because the estimation does not take into account the bias $A_0(t)$ and simply ignores it. This is also apparent in (2.12) where the absolute error of the signal's estimation evolves around 1 when $t < 2s$and around 0.8 when $t > 2s$. These values represent the bias $A_0(t)$.

Noisy scenario:

Let us now consider the previous signal with another bias that is randomized, such that $y_{m3}(t) = y_3(t) + d_3(t)$, where $d_3(t) \in [-1.5 \;\; 1.5]$. As it is apparent in both figures (2.13) and (2.14) this additional disturbance affects the estimation in a moderate way as the amplitude and frequency's estimations errors both remain within the same magnitude as in the noise-free scenario. However. since this observer does not reduce the noise, both curves are clearly less smooth. This is especially apparent in the reconstructed signal's absolute error graph that is noisy.

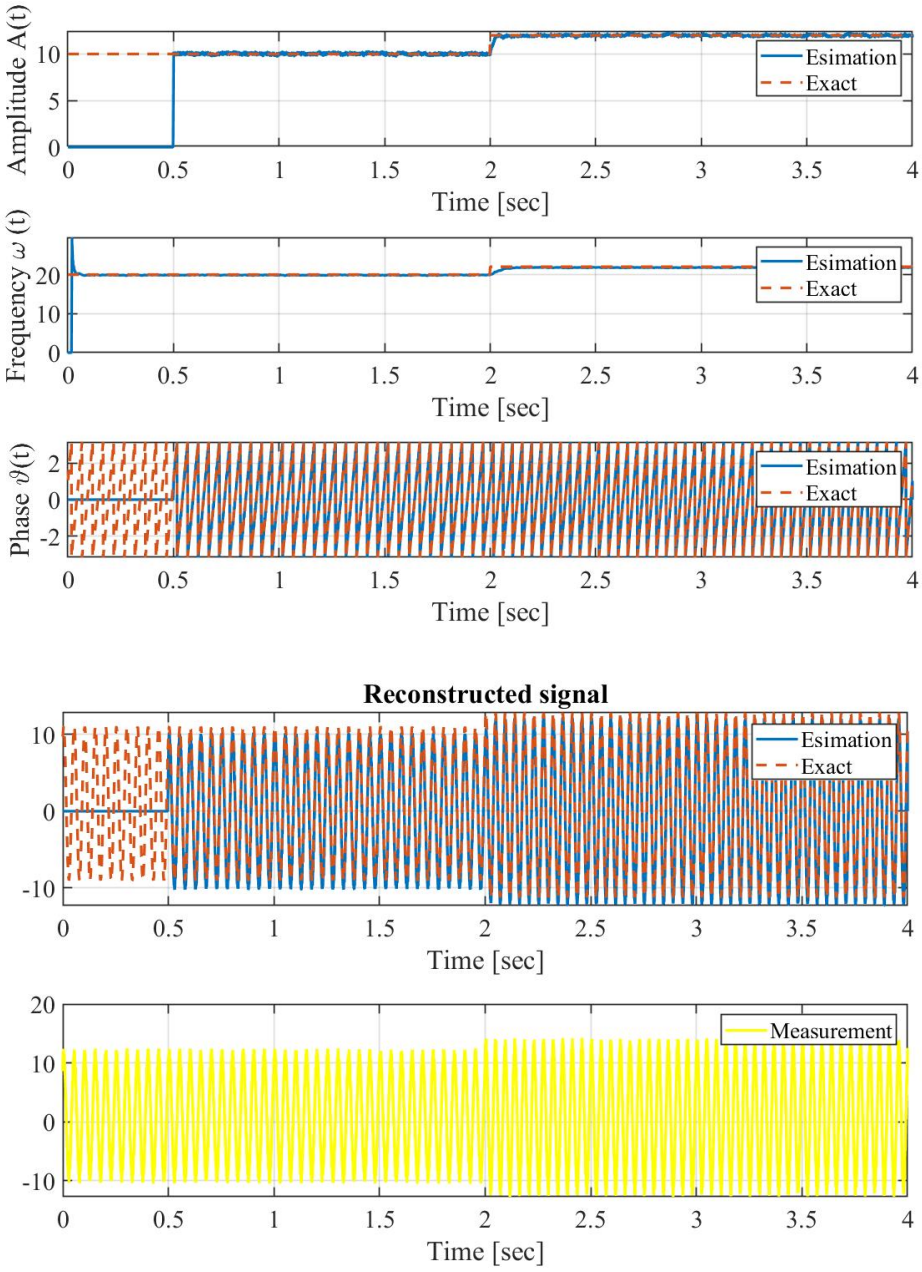

Figure 2.13: Amplitude, frequency, phase and signal estimation of the biased signal $y_{m3}(t)$

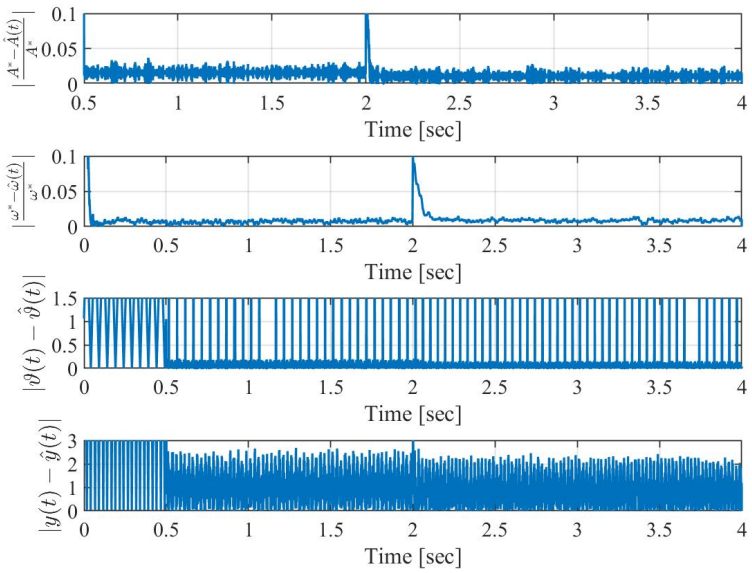

Figure 2.14: Estimation errors of $y_{m3}(t)$

2.5 Conclusion

The work in [51] focuses on the AFP problem and construct an observer to estimate the parameters of a sinusoidal signal. This work can be devided into several steps in order to understand the idea behind it where first step is to find a linear dynamic system that can generate the sinusoidal signal of interest. The authors, then, propose to transform the system into the Volterra space with a carefully chosen kernel function. The estimation of the states of the linear dynamic system is quite simple because of the properties of the Volterra operator. These properties are put such that the parameters to be estimated remain the same after the transformation to the Volterra space. This means that a reverse transformation is not needed to obtain the desired parameters, which considerably reduces the numerical issues of the method. At last, the authors introduce an adaptive law based on a second order sliding mode to estimate the signal's frequency, amplitude and the phase is subsequently deducted. The numerical simulations confirm the robustness of the observer when adequate tuning parameters can be found.

Chapter 3

The Volterra differentiator

3.1 Introduction

In this chapter we will introduce a novel approach to estimate the N first derivatives of a known signal based on the Volterra integral. This approach was first presented in [35] where it is essentially developed around bivariate kernel functions of the Fourier type (i.e: exponential). The authors discuss both the noise-free and noisy scenarios and conclude that the proposed method is only effective in the noise-free case because they observe a noise amplification that gets worse with differential degree increase.

Throughout this chapter, we will first conjecture an explanation of this phenomenon by observing the behavior of the chosen bivariate kernel function. Then, we will contribute by constructing a novel bivariate kernel function based on the Jacobi monovariate modulating function (see [20]) and adapt the Volterra integral to it. We will study the effect of this change on both the noise-free and noisy scenarios via a sensitive analysis and discuss the results of the numerical simulations.

3.2 Exponential bivariate non-asymptotical kernel functions

As we have seen in the previous chapter, the entire Volterra approach relies on the kernel functions family chosen to transform the signal into the Volterra space. The most used one is the exponential bivariate functions family (see [52], [50], [12], [35], [34] and [51]). The exponential bivariate non-asymptotical kernel functions were constructed similarly to the monovariate Fourier modulating functions (see chapter 5 and [20]) taking into consideration several conditions of the convergence of the approach.

Let us now explore the following exponential kernel family:

$$K_h(t,\tau) = e^{-\omega_h(t-\tau)}(1-e^{-\bar{\omega}\tau})^N, \quad \forall (t,\tau) \in \mathbb{R}_+^{\nvDash}, \tag{3.1}$$

where $h = \{1,\ 2, \cdots, N\}$, $\bar{\omega} \in \mathbb{R}_+$ and $\omega_h \in \mathbb{R}_+$.

Exploiting Newton's binomial, (3.1) can be written as follows:

$$K_h(t,\tau) = e^{-\omega_h t} \sum_{q=0}^{N} (-1)^q \binom{N}{q} e^{(\omega_h - q\bar{\omega})\tau}, \tag{3.2}$$

thus, the kernel's derivative with respect to the second argument is denoted:

$$K_h^{(i)}(t,\tau) = e^{-\omega_h t} \sum_{q=0}^{N} (-1)^q \binom{N}{q} (\omega_h - q\bar{\omega})^i e^{(\omega_h - q\bar{\omega})\tau}. \tag{3.3}$$

It is important to know that in the Volterra observation approach, the second argument τ is only used as a tool to satisfy the theoritical conditions. In practice, the design of the observer requires only the monovariate functions $K_h(t,t)$ and $K_h^{(i)}(t,t)$, which are obtained as follows when replacing $\tau = t$:

$$\begin{aligned} K_h(t,t) &= (1 - e^{-\bar{w}\tau})^N, \\ K_h^{(i)}(t,t) &= \sum_{q=0}^{N} (-1)^q \binom{N}{q} (\omega_h - q\bar{\omega})^i e^{-q\bar{\omega}t}. \end{aligned} \tag{3.4}$$

Notice that in a single exponential kernel family, the function does not depend on ω_h, i.e: $K_h(t,t) = K_k(t,t) = K(t,t)$, $\forall h, k = \{0, 1, ..., N\}$.

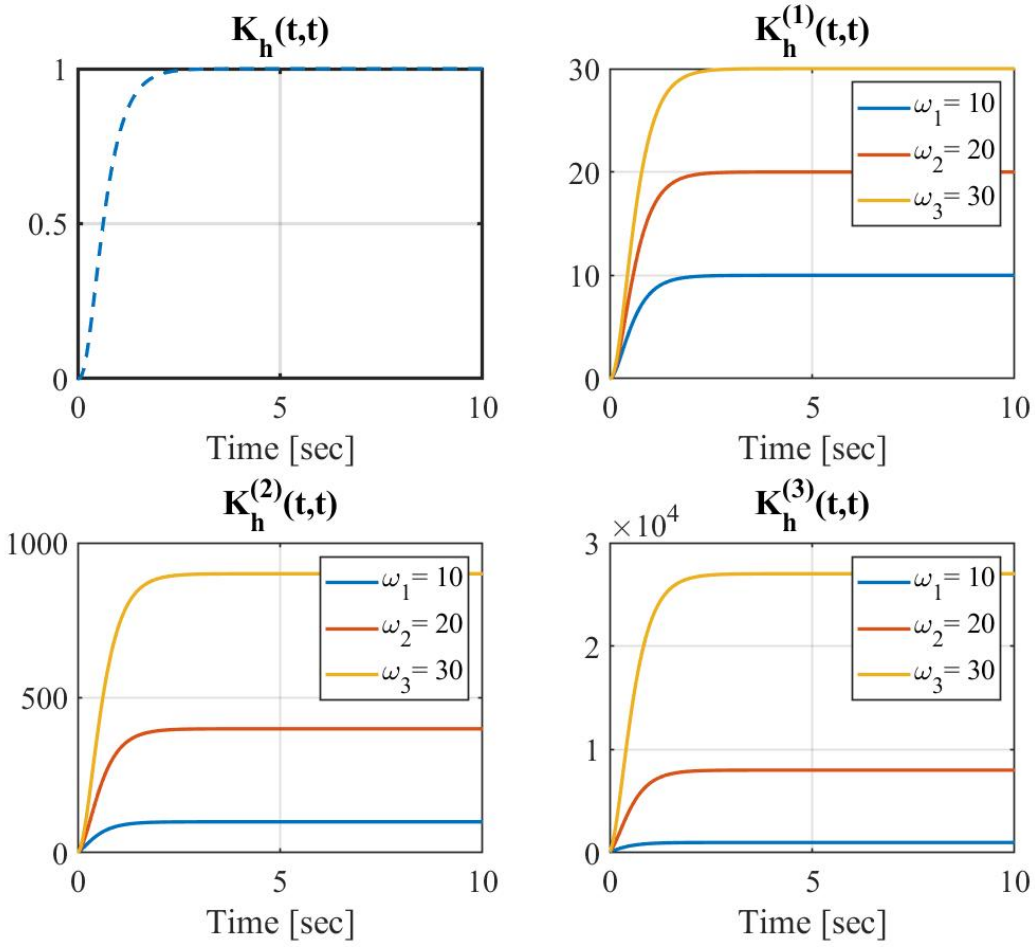

Figure 3.1: Exponential bivariate non-asymptotical kernel functions and their three derivatives behaviour for $\omega = [10, 20, 30]$

Figure (3.1) shows the shape of an exponential kernel family with $\bar{\omega} = 2.5$. We can notice that after a certain t_0, the kernel and its derivative can encompass the whole signal. This means that this type of kernel function does not need to be localized and adapted to each signal, which generalizes the approach. We can also notice that the function and its derivatives do not share the same magnitude, and this difference increases with increasing the value of w_h.

3.3 Polynomial bivariate non-asymptotical kernel function

The main idea behind this contribution is to exploit the polynomial shape of the Jacobi monovariate modulating function (see Chapter 5 and [20]) in order to construct a novel bivariate non-asymptotival kernel functions family with the adequate conditions for the Volterra estimation approach.

Taking into consideration all theoritical conditions, we propose the following bivariate non-asymptotic kernel functions family:

$$K_h(t,\tau) = (T-t)^{\bar{\omega}}\tau^{\omega_h},\ \forall (t,\tau) \in \mathbb{R}_+^{\not\varepsilon}, \tag{3.5}$$

where $\omega_h \in \mathbb{R}_+$ are the forgetting factors such that $\omega_h \geqslant N$, $\forall h = \{0,1,2,\cdots,N\}$ and $\bar{\omega} \in \mathbb{R}_+$. T is a positive constant that represents the time boundary, i.e. $t < T$.

The ith derivative with respect to the second argument is given by:

$$K_h^{(i)}(t,\tau) = \omega_h^i (T-t)^{\bar{\omega}}\tau^{\omega_h - i}, \tag{3.6}$$

thus for $\tau = t$ we have:,

$$K_h^{(i)}(t,t) = \omega_h^i (T-t)^{\bar{\omega}}t^{\omega_h - i}, \tag{3.7}$$

$\forall i \in \{0,1,\cdots,N-1\}$.

We compute some examples of these novel polynomial bivariate kernel functions and their three first derivatives to observe their evolution for $T = 20s$, $\bar{\omega} = 5$, with a sampling time $T_s = 10^{-4}$ in figure (3.2), where we can notice that the magnitude of the functions depends on the value of w_h instead of the degree of the derivatives. This is the first difference with the exponential kernel functions family. In this case, increasing ω_h increases the kernel's magnitude, so one must be careful when using different kernels in a computational method because some functions can be neglected relatively to others and this may cause numerical problems.

The second difference is the general shape of these functions as the polynomial kernel

functions do not capture all the information present in the signal in the same way. Notice, for example, how the peak of each curve moves to the left of the plot when the derivative's order increases. This particularity can be used in order to increase the robustness of the method in presence of disturbances by localizing the peak in the useful information region, filtering then all disturbances.

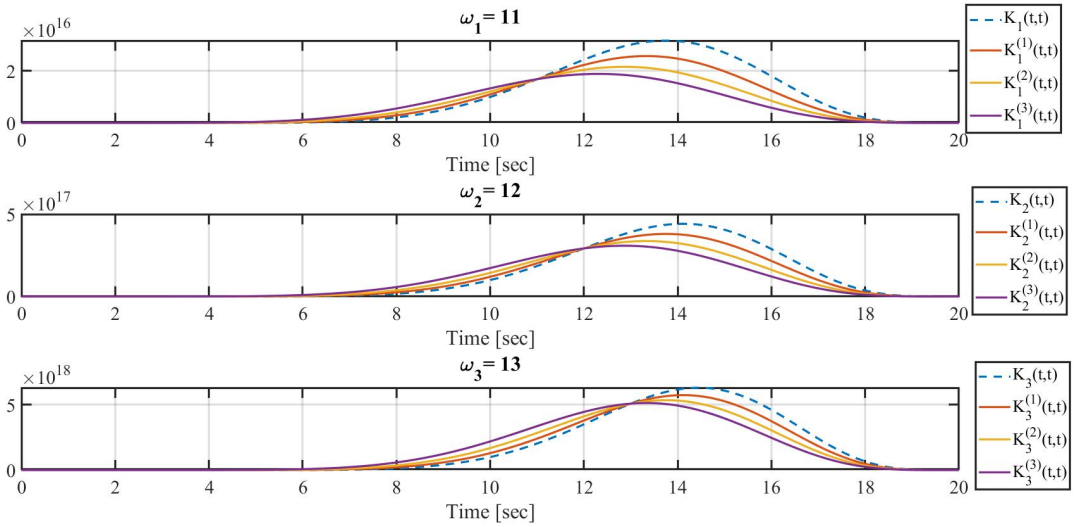

Figure 3.2: Polynomial bivariate non-asymptotical kernel function and its three derivatives behaviour for $\omega = [11, 12, 13]$

3.4 Normalization

Both types of the previous kernel functions can reach very high values, which is numerically challenging to compute. In order to avoid this problem, we propose to normalize the kernel functions $K_h(t,t)$ in order to keep them in a computable range.

Normalizing a function means dividing it by a known constant. This constant can be either the maximum of the function or its energy.

Consider a family of kernel functions $K_h(t,t)$, its normalized form is:

$$K_{h,norm}(t,t) = \mu K_h(t,t) \tag{3.8}$$

where $\mu = max(K_h(t,t))$ or $\mu = \int_0^\infty |K_h(t)|^2 dt$.

Both types of normalization can be applied, depending on the signal.

3.5 Volterra differentiator's construction

3.5.1 State observer

The idea behind this approach is to construct a linear time invarient dynamic system where the state vector is composed of the signal's derivatives and the output is the signal. Thus, let us consider the Taylor series expansion of $y(t)$ at $t = 0$:

$$y(t) = \sum_{i=0}^{\infty} \frac{y^{(i)}(0)}{i!} t^i. \tag{3.9}$$

The truncated approximation of the Taylor expansion is:

$$y_N(t) = y_N(0) + y_N^{(1)}(0)t + \frac{y_N^{(2)}(0)}{2!}t^2 + \cdots + \frac{y_N^{(N-1)}(0)}{(N-1)!}t^{N-1}, \tag{3.10}$$

where we assume $y_N^{(N)}(t) = 0$.

Thus, the signal $y_N(t)$ is generated by the following linear time invarient system:

$$\begin{aligned} \dot{x}(t) &= Ax(t), \\ y(t) &= cx(t), \ \ t \in \mathbb{R}_+, \end{aligned} \tag{3.11}$$

where

$$\begin{aligned} A &= \begin{bmatrix} 0 & 1 & 0 & \cdots & 0 \\ 0 & 0 & 1 & \ddots & \vdots \\ \vdots & \vdots & \ddots & \ddots & 0 \\ 0 & 0 & \cdots & 0 & 1 \\ 0 & 0 & \cdots & 0 & 0 \end{bmatrix} \in \mathbb{R}^{N \times N}, \\ c &= \begin{bmatrix} 1 & 0 & \cdots 0 \end{bmatrix} \in \mathbb{R}^N, \end{aligned} \tag{3.12}$$

with the state vector $x(t) = \begin{bmatrix} y_N(t), y_N^{(1)}(t), \cdots, y_N^{(i)}(t), y_N^{(N-1)}(t) \end{bmatrix}^T$.

The system (3.11) is obviously completely observable. The $(N-1)$ first derivatives derivatives of $y(t)$ can be estimated by replacing $y_N(t)$ by $y(t)$.

The observer proposed is the Luenberger's original form, which is a direct copy of the system as shown bellow:

$$\begin{aligned} \dot{\hat{x}}(t) &= A\hat{x}(t), \\ \hat{y}(t) &= c\hat{x}(t),\ t \in \mathbb{R}_+. \end{aligned} \tag{3.13}$$

The couple (A, c) being completely observable, we can proceed to the next steps.

3.5.2 Volterra estimator

Introduction to the Volterra estimation technique

The idea behind the Volterra estimator is to map the output signal $y(t)$ and its derivatives into a transformation space introduced by the Volterra integral. And just like with the modulating function methods (see Chapter 5), there exists a class of kernel functions that will make the initial conditions on the signal and its derivatives vanish.
The ith derivative of $y(t)$ induced by the Volterra operator is given below using (2.5):

$$\begin{aligned} [V_{K_h} y^{(i)}](t) = &\sum_{j=0}^{i-1} (-1)^{i-j-1} y^{(j)}(t) K_h^{(i-j-1)}(t,t) + \sum_{j=0}^{i-1} (-1)^{i-j} y^{(j)}(0) K_h^{(i-j-1)}(t,0) \\ &+ (-1)^i [V_{K_h^{(i)}} y](t), \quad i \in \{1, \cdots, N-1\}. \end{aligned} \tag{3.14}$$

Exploiting the non-asymptotic property of the kernel function (2.6) we obtain:

$$[V_{K_h} y^{(i)}](t) = \sum_{j=0}^{i-1} (-1)^{i-j-1} y^{(j)}(t) K_h^{(i-j-1)}(t,t) + (-1)^i [V_{K_h^{(i)}} y](t). \tag{3.15}$$

For $i = N$ and recalling the assumption that $y_N(t) = 0\ \forall t \in \mathbb{R}_+$:

$$[V_{K_h} y^{(N)}](t) = y^{(N-1)}(t) K_h(t,t), \tag{3.16}$$

which according to (3.14) is equivalent to:

$$\begin{aligned}(-1)^{(N-1)}[V_{K_h^{(N)}}y](t) &= \sum_{j=0}^{N-1}(-1)^{N-j-1}y^{(j)}(t)K_h^{(N-j-1)}(t,t)\\ &= \sum_{j=0}^{N-1}(-1)^{N-j-1}K_h^{(N-j-1)}(t,t)\hat{x}_j(t).\end{aligned} \tag{3.17}$$

Thus, the derivatives estimation problem is transformed into the following algebraic system:

$$v(t) = \Gamma(t)\hat{x}(t), \tag{3.18}$$

where

$$v(t) = (-1)^{N-1}\begin{bmatrix}[V_{K_0^{(N)}}y](t) & [V_{K_1^{(N)}}y](t) & \cdots & [V_{K_{N-1}^{(N)}}y](t)\end{bmatrix}^T,$$

and

$$\Gamma(t) = \begin{bmatrix}(-1)^{N-1}K_0^{(N-1)}(t,t) & (-1)^{N-2}K_0^{(N-2)}(t,t) & \cdots & K_0(t,t)\\ (-1)^{N-1}K_1^{(N-1)}(t,t) & (-1)^{N-2}K_1^{(N-2)}(t,t) & \cdots & K_1(t,t)\\ \vdots & \vdots & \vdots & \vdots\\ (-1)^{N-1}K_{N-1}^{(N-1)}(t,t) & (-1)^{N-2}K_{N-1}^{(N-2)}(t,t) & \cdots & K_{N-1}(t,t)\end{bmatrix}.$$

The transformation matrix $\Gamma(t)$ is not data sensitive, it depends only on the kernel function and its derivatives. Since, the kernel function here is considered a degree of freedom, it is constructed in order for this matrix to be invertible $\forall t > 0$. Once this condition is satisfied, the inverse transformation can be made in order to estimate $\hat{x}(t)$ as follows:

$$\hat{x}(t) = \Gamma^{-1}(t)v(t),\ \forall t > 0, \tag{3.19}$$

where $v(t)$ is estimated by a linear time varient dynamic system that we will define next.

Estimating the derivatives in the Volterra space

The goal now is to estimate the image of the derivatives estimations transformed into the Volterra space i.e $v(t)$.

Let us consider the definition of the Volterra transformation of the signal $y(t)$ induced by

$K_h^{(N)}(t,\tau)$, recalling (2.4):

$$[V_{K_h^{(N)}}y](t) = \int_0^t K_h^{(N)}(t,\tau)y(\tau)d\tau,\ t \in \mathbb{R}_+.$$

Consider $\xi_h(t) \triangleq [V_{K_h^{(N)}}y](t)$. Applying the Leibniz integral rule (2.3) to differentiate the previous integral with respect to the time variable, we obtain:

$$\dot{\xi}_h(t) = K_h^{(N)}y(t) + \int_0^t \frac{\partial}{\partial t}K_h(t,\tau)y(\tau)d\tau.$$

Then, the bivariate non-asymptotic kernel functions must be chosen such that the following condition is satisfied:

$$\int_0^t \frac{\partial}{\partial t}K_h(t,\tau)y(\tau)d\tau = g_h(t)\xi_h(t),\ g_h(t) < 0,\ \forall t \geqslant 0. \tag{3.20}$$

For $\xi(t) = \begin{bmatrix}\xi_0(t) & \xi_1(t) & \cdots & \xi_{N-1}(t)\end{bmatrix}^T$ we obtain the following LTV dynamic system:

$$\begin{aligned}\dot{\xi}(t) &= G(t)\xi(t) + E(t)y(t),\\ \xi(0) &= 0,\end{aligned} \tag{3.21}$$

where $G(t) = diag(g_h(t)) \in \mathbb{R}^{\mathbb{N}\times\mathbb{N}}$ and $E(t) = \begin{bmatrix}K_0^{(N)}(t,t) & \cdots & K_{N-1}^{(N)}(t,t)\end{bmatrix}^T$.
The satisfaction of the (3.20) implies that the matrix $G(t)$ is hurwitz $t \geqslant 0$. Therefore, the LTV system (3.21) is stable and converges. Since $v(t) = (-1)^{N-1}\xi(t)$, it is now possible to estimate it.

3.5.3 Exponential kernel function

In [35], the authors exploited the exponential bivariate non-asymptotical kernel functions as defined in (3.1) for this differentiator. The observer is design such that:

$$\hat{x}(t) = \Gamma_1^{-1}(t) v_1(t), \tag{3.22}$$

where:

$$\Gamma_1(t) = \begin{bmatrix} (-1)^{N-1} \sum_{q=0}^{N} (-1)^q \binom{N}{q} (\omega_0 - q\bar{\omega})^{N-1} e^{-q\bar{\omega}t} & \cdots & (1 - e^{-\bar{\omega}\tau})^N \\ (-1)^{N-1} \sum_{q=0}^{N} (-1)^q \binom{N}{q} (\omega_1 - q\bar{\omega})^{N-1} e^{-q\bar{\omega}t} & \cdots & (1 - e^{-\bar{\omega}\tau}) \\ \vdots & \vdots & \vdots \\ (-1)^{N-1} \sum_{q=0}^{N} (-1)^q \binom{N}{q} (\omega_{N-1} - q\bar{\omega})^{N-1} e^{-q\bar{\omega}t} & \cdots & (1 - e^{-\bar{\omega}\tau})^N \end{bmatrix}, \tag{3.23}$$

and $v_1(t) = (-1)^{N-1}\xi_1(t)$ and $\xi_1(t)$ is estimated using:

$$\begin{aligned} \dot{\xi}_1(t) &= G_1(t)\xi_1(t) + E_1(t)y(t), \\ \xi_1(0) &= 0, \end{aligned} \tag{3.24}$$

where :

$$G_1(t) = \begin{bmatrix} -\omega_0 & 0 & \cdots & 0 \\ 0 & -\omega_1 & \ddots & \vdots \\ \vdots & \ddots & \ddots & 0 \\ 0 & \cdots & 0 & -\omega_{N-1} \end{bmatrix}, \quad E_1(t) = \begin{bmatrix} \sum_{q=0}^{N} (-1)^q \binom{N}{q} (\omega_0 - q\bar{\omega})^N e^{-q\bar{\omega}t} \\ \sum_{q=0}^{N} (-1)^q \binom{N}{q} (\omega_1 - q\bar{\omega})^N e^{-q\bar{\omega}t} \\ \vdots \\ \sum_{q=0}^{N} (-1)^q \binom{N}{q} (\omega_{N-1} - q\bar{\omega})^N e^{-q\bar{\omega}t} \end{bmatrix}. \tag{3.25}$$

$\Gamma_1(t)$ is invertible for different values $w_h > 0$, $\forall t > 0$. [35]

Moreover, $G_1(t)$ is clearly hurwitz and the LTV (3.24) converges.

3.5.4 Polynomial kernel function

We propose to recreate the precedent differentiator with the novel polynomial bivariate non-asymptotical kernel functions family as it is defined in (3.5). The observer is designed such that:

$$\hat{x}(t) = \Gamma_2^{-1}(t) v_2(t), \tag{3.26}$$

where:

$$\Gamma_2(t) = (T-t)^{\bar{\omega}} \begin{bmatrix} (-1)^{N-1}\omega_0^{N-1} t^{\omega_0 - N - 1} & (-1)^{N-2}\omega_0^{N-2} t^{\omega_0 - N - 2} & \cdots & t^{\omega_0} \\ (-1)^{N-1}\omega_1^{N-1} t^{\omega_1 - N - 1} & (-1)^{N-2}\omega_1^{N-2} t^{\omega_1 - N - 2} & \cdots & t^{\omega_1} \\ \vdots & \vdots & \vdots & \vdots \\ (-1)^{N-1}\omega_{N-1}^{N-1} t^{\omega_{N-1} - N - 1} & (-1)^{N-2}\omega_{N-1}^{N-2} t^{\omega_{N-1} - N - 2} & \cdots & t^{\omega_{N-1}} \end{bmatrix}. \tag{3.27}$$

and $v_2(t) = (-1)^{N-1}\xi_2(t)$ and $\xi_2(t)$ is estimated using:

$$\begin{aligned} \dot{\xi}_2(t) &= G_2(t)\xi_1(t) + E_2(t)y(t), \\ \xi_2(0) &= 0, \end{aligned} \tag{3.28}$$

where :

$$G_2(t) = \begin{bmatrix} -\frac{\bar{\omega}}{T-t} & 0 & \cdots & 0 \\ 0 & -\frac{\bar{\omega}}{T-t} & \ddots & \vdots \\ \vdots & \ddots & \ddots & 0 \\ 0 & \cdots & 0 & -\frac{\bar{\omega}}{T-t} \end{bmatrix}, \quad E_2(t) = \begin{bmatrix} \omega_0^N (T-t)^{\bar{\omega}} t^{\omega_0 - N} \\ \omega_1^N (T-t)^{\bar{\omega}} t^{\omega_1 - N} \\ \vdots \\ \omega_{N-1}^N (T-t)^{\bar{\omega}} t^{\omega_0 - N + 1} \end{bmatrix}. \tag{3.29}$$

Similarly, $\Gamma_2(t)$'s rows and lines are obviously linearly independent $\forall t > 0$ which means that $\Gamma_2(t)$ is invertible. $G_2(t)$ is hurwitz and the LTV (3.28) converges $\forall t < T$.

3.6 Numerical simulations

In this section we will perform a sensitive analysis of the differentiator using both of the previous methods in order to point out the numerical problems that one can encounter and to highlight the effect of the tuning parameters. For all of the simulations above, we use Euler's discretization with a sampling time of $T_s = 10^{-3}s$. We also use the following absolute error definition $\epsilon_x = |x(t) - \hat{x}(t)|$.

3.6.1 Sensitive analysis using exponential kernel functions

First derivative estimation (N=2)

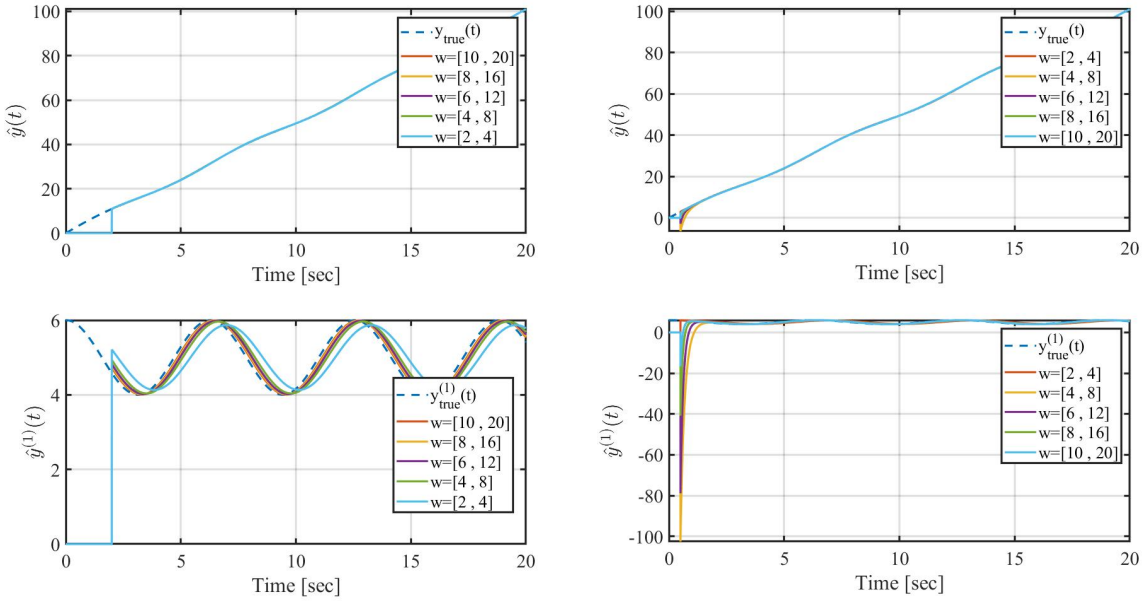

Figure 3.3: Activation time effect on the peaking phenomenon

In this first example we consider the following unbiased signal: $y_1(t) = 5t + \sin(t)$, and propose to estimate it and its first derivative for $\bar{\omega} = 2.5$ and different pairs of ω_h. We have previously stated that for $\Gamma_1(t)$ to be invertible the time variable t had to be strictly positive i.e: $t \geqslant \delta_\epsilon$, $\delta_\epsilon \in \mathbb{R}_+^*$. We call this δ_ϵ the activation time.

Theoretically, any value of δ_ϵ should be acceptable. However, small value of the activation time imply high values of $\Gamma_1^{-1}(t)$ which results in a peaking phenomenon. This

phenomenon is illustrated in figure (3.3) where we have put $\delta_\epsilon = 0.5s$ on the right estimation instead of $\delta_\epsilon = 2s$ as in the left estimation. Indeed, the difference between both estimations is very important as a high peak can induce several issues in practice. To our knowledge, there is still no systematic way in the literature to choose the activation time. Therefore, we consider it as another tuning parameter that we pick according to the signal measurement, the pair of w_h, and the forgetting factor $\bar{\omega}$ as all these factors play a role in the phenomenon. The left side of figure (3.3) shows that the signal's estimate is easily reached for all pairs of ω_h. On the other hand, the first derivative estimation is best for $\omega = [10,\ \ 20]$. In figure (3.4) we consider the previous signal biased with an additive disturbance $d_1(t)$ normally distributed in $[-3,\ 3]$. The signal is accurately estimated whereas the derivatives estimations are noisy. Notice that the higher the values of ω_h, the higher the noise is.

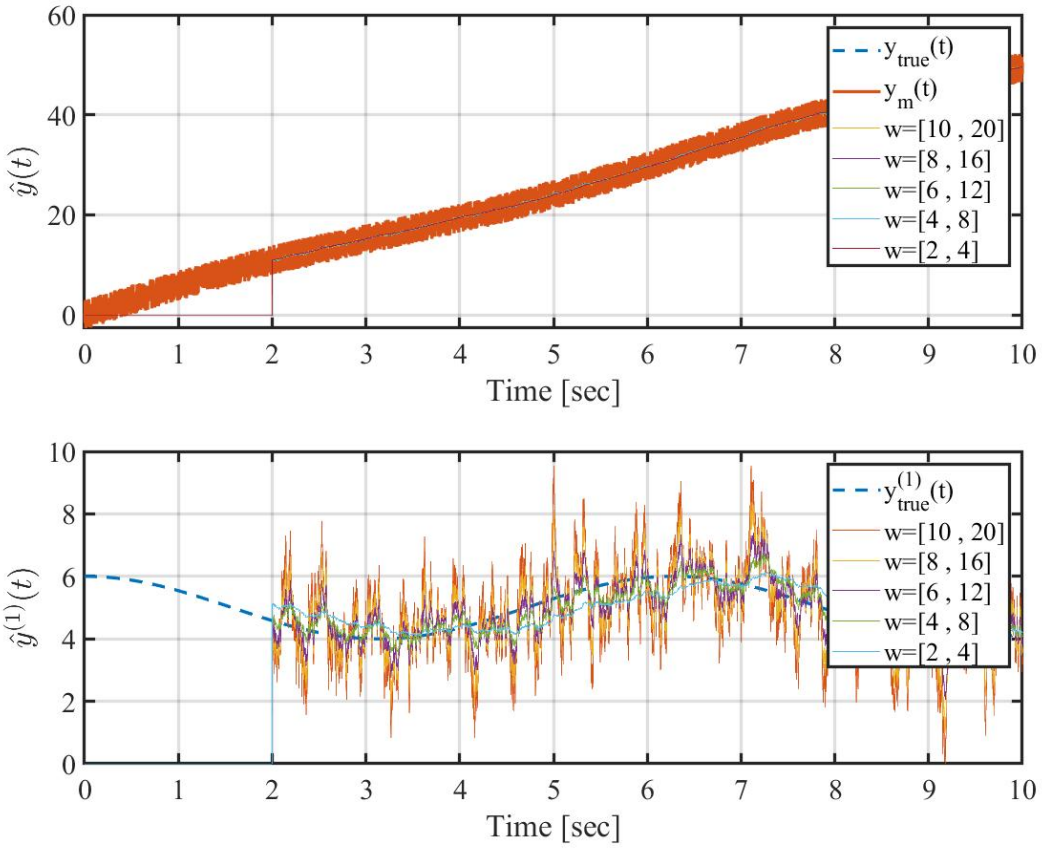

Figure 3.4: First derivative estimation based on noisy measurement with exponential kernel ($N = 2$)

Second derivative estimation $(N = 3)$

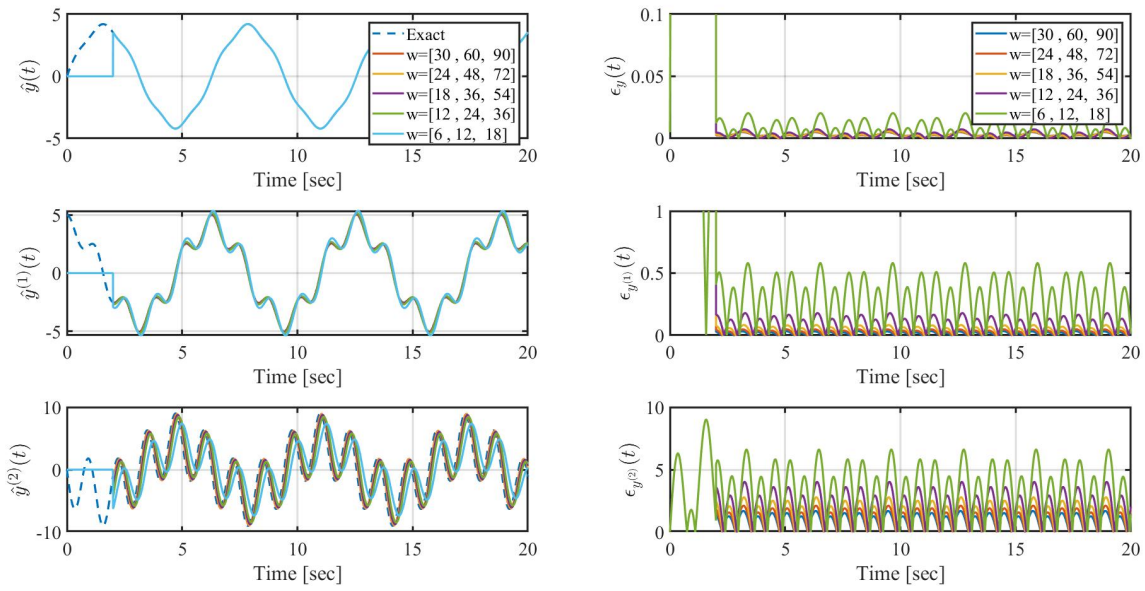

Figure 3.5: Second derivative estimation with exponential kernel $(N = 3)$

Let us now consider the following signal: $y_2(t) = 4\sin(t) + 0.5\sin(5t)$, and propose to estimate it and its first two derivatives using the exponential kernel, with $\bar{\omega} = 2.5$, varying the triplet ω_h.

Figure (3.5) shows the estimations and their absolute errors. We can arrive o the same conclusions as in [35] where it is stated that increasing the values of w_h increases the estimation accuracy of the algorithm. In our example, we can see that the *worst* triplet is $[6,\ 12\ , 18]$ and the *best* one is $[30,\ 60\ , 90]$. The second conclusion is that the higher the degree of the derivation is, the less accurate the estimation is. Indeed, this appears in the change of the magnitude's absolute error (10^{-1} for the signal, 10^{0} for the first derivative and 10^{1} for the second). Therefore, high degrees of derivation require high values of ω_h.

In figure (3.6), we have added to the signal $y_2(t)$ an additive noise $d_2(t)$ normally distributed in $[-0.25,\ 0.25]$. The figure shows that the noise is amplified in the derivatives estimations, as they completely loose their previous accuracy. The magnitudes of the estimation's error becomes 10^{1} and 10^{2} for the first and second derivatives respectively. We also notice that higher values of the triplet of ω_h amplify the noise most.

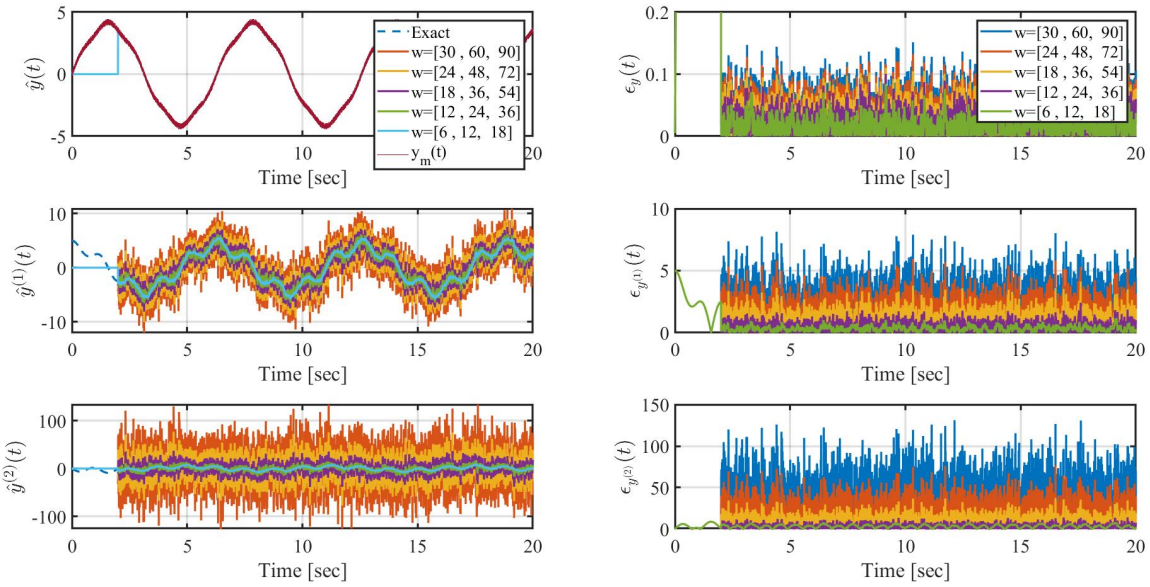

Figure 3.6: Second derivative estimation based on noisy measurement with exponential kernel ($N = 3$)

Third derivative estimation (N=4)

In figure (3.7), we propose to estimate the previous signal's $y_2(t)$ three first derivatives with different quadruplets of ω_h in order to further confirm the previous results. This figure illustrates the gradual loss of accuracy with the increase of the degree's derivative estimation. Notice that the quadruplet $w = [25,\ 50,\ 75,\ 100]$ gives the best results. Figure (3.8) illustrate the noisy scenario where the magnitude of the third derivative's absolute error is of 10^4, which makes the estimation completely useless as it is considered as noise only.

We can conjecture that this amplification is due to the shape of the exponential kernel function, as the kernel's final gain gets higher when ω_h increases. In the noise-free scenario, this increase helps the estimation as it makes it more accurate but in the noisy scenario, it amplifies the noise and risks to make the estimation useless. In order to deal with this problem, we can normalize the exponential kernel function or simply change its type. The first proposition is ill advised as it leads to numerical problems and we will explore the second option in the next subsection.

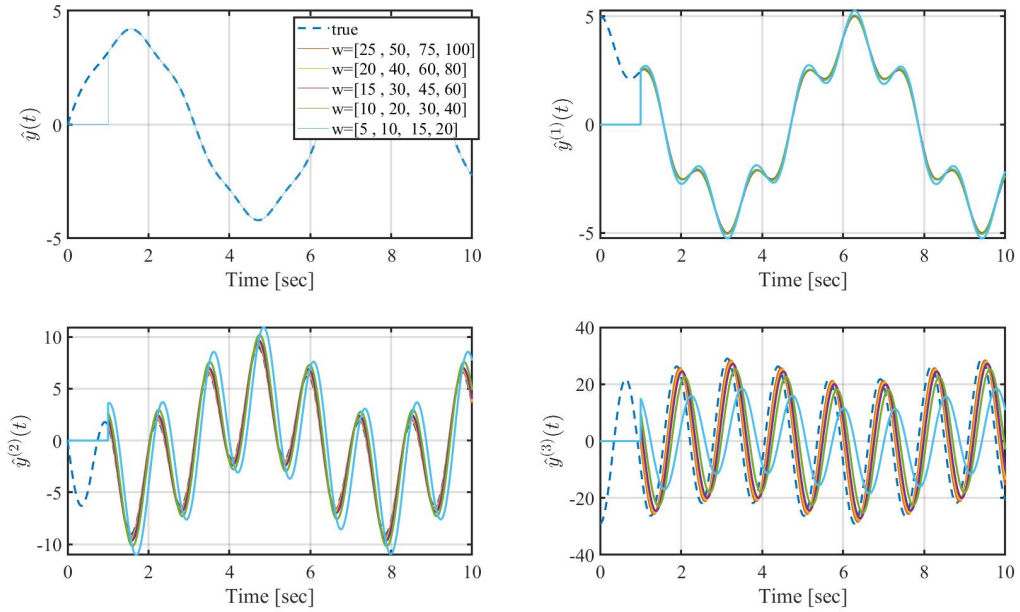

Figure 3.7: Third derivative estimation with exponential kernel ($N = 4$)

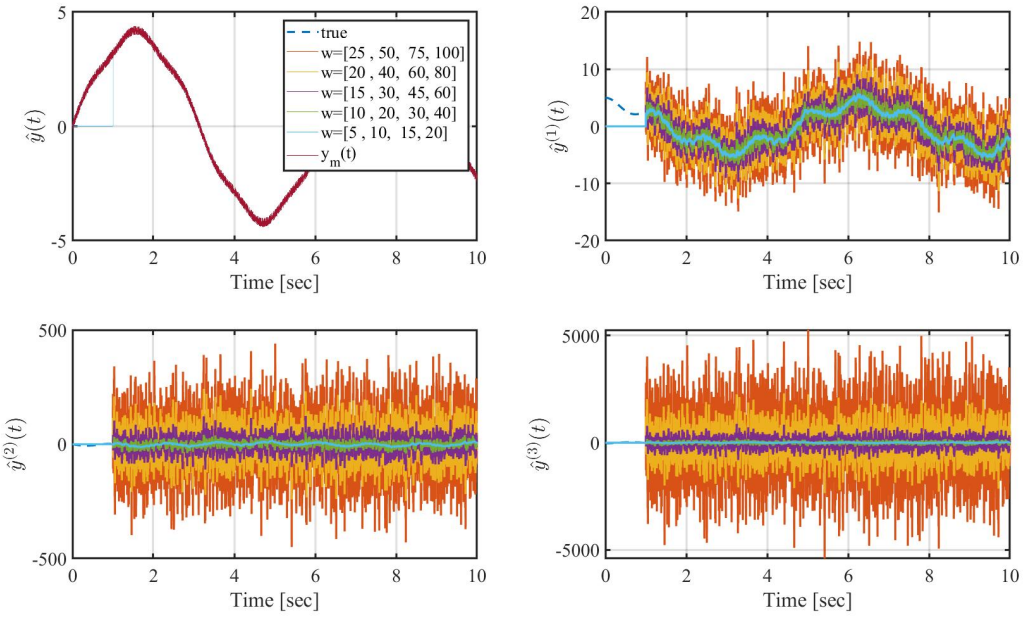

Figure 3.8: Third derivative estimation based on noisy measurement with exponential kernel ($N = 4$)

3.6.2 Sensitive analysis using the polynomial kernel function

First derivative estimation (N=2):

We consider the following signal $y_3(t) = 4\cos(2t) + 1$, and estimate its first derivative using the Volterra differentiator with bivariate polynomial kernel function family that has the following parameters: $\delta_\epsilon = 1s$, $T = 150s$ $\bar{\omega} = 5$, and vary pairs of ω_h in figure (3.9). It is worth to mention that $\bar{\omega}$ is also an important tuning parameter that has been chosen to such a value after several computations.

Our main goal was to find a pattern between the kernel's parameters ω_h in order to choose them adequately but such a pattern could not be found in practice. Indeed, the shape of the polynomial kernel transforms the problem of the tuning parameters choice into a localization problem, i.e: the polynomial kernel functions must be localized such that they do not annul the useful information. Which is a more difficult task then when dealing with an exponential kernel where increasing the forgetting factors increases the gains which amplify the whole signal and consequently results in better estimations.

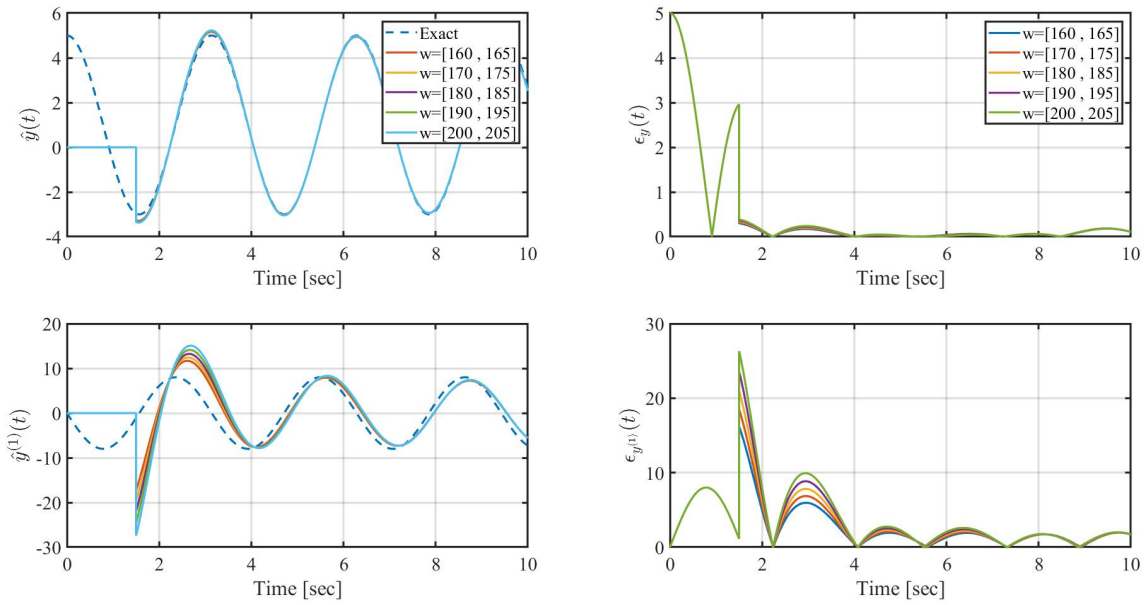

Figure 3.9: First derivative estimation with the polynomial kernel ($N = 2$)

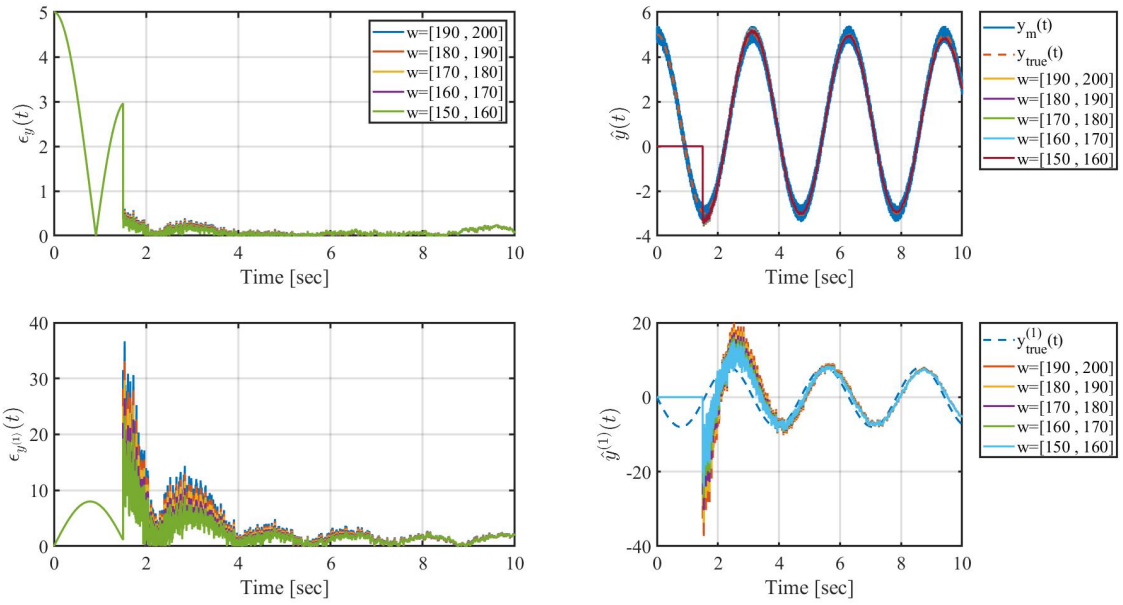

Figure 3.10: First derivative estimation with the polynomial kernel based on noisy measurements ($N = 2$)

In this particular case, for example, we can see that the error is minimal for low values of the ω_h but this difference is only apparent up to a certain time t_0. This can be explained by numerical issues related to the conditioning of $\Gamma_2(t)$, which can be settled by imposing a bigger activation time δ_ϵ. Indeed, the activation time depends on the norm of ω: the higher the norm of the vector is, the higher the peak phenomenon is, which imposes a relatively high activation time δ_ϵ.

Let us also mention that when the values ω_h increase into a certain magnitude (up to 230 for this example), a numerical problem appears: the conditioning of the matrix $\Gamma_2(t)$ as defined in (3.27). High degrees of the polynomial kernel family make this matrix ill-conditioned and its computation, unreliable. This particular numerical problem restrain the range of the values of ω_h that can be chosen since it becomes numerically impossible to compute the estimation up to certain ω_h.

Figure (3.10) shows the noisy scenario where the signal $y_3(t)$ is disturbed by an additive noise $d_3(t)$ that is normally distributed in $[-0.4, 0.4]$. We notice that the noise of the derivative estimation is amplified when using high values of ω_h. This amplification fades away with time and is important for any $t < t_0$ where the value of t_0 depends on the

parameters. Thus, the activation time should be around this t_0, which confirms that the higher the values of ω_h, the higher the activation time should be.

Second derivative estimation (N=3):

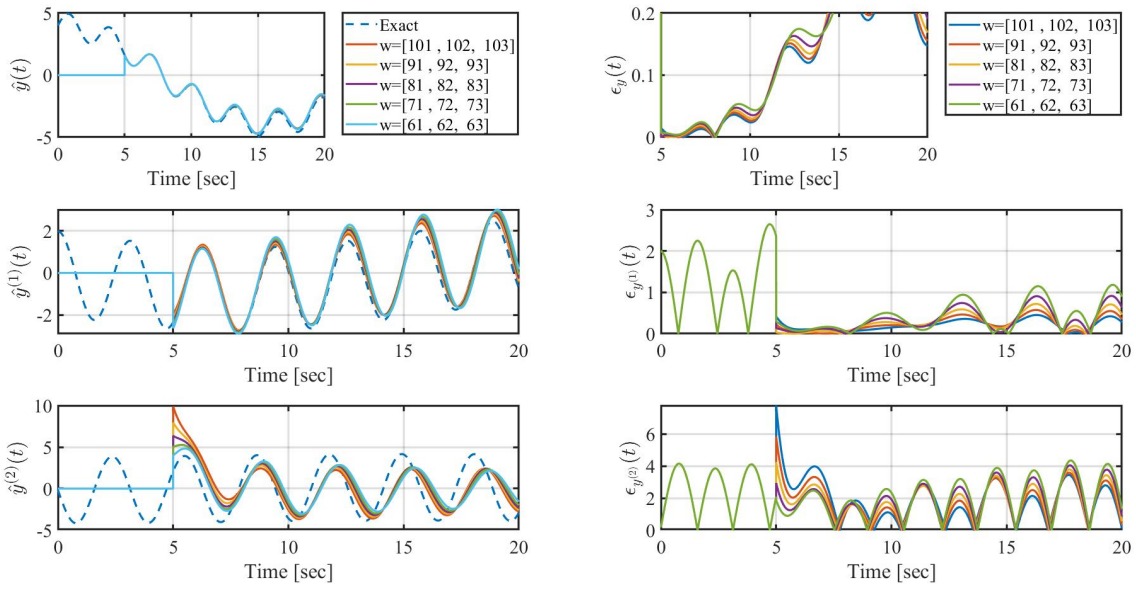

Figure 3.11: Second derivative estimation with the polynomial kernel based ($N = 3$)

We, now, estimate the signal : $y_4(t) = 4\cos(0.2t) + \sin(2t)$, and its two first derivatives with the following parameters of the polynomial kernel function : $T = 240s$, $\bar{\omega} = 5$ and $\delta_\epsilon = 5s$, varying ω_h, in figure (3.11).

This example clearly shows the limitations of this approach. Indeed, we can notice a peaking phenomenon in the second derivative estimation and this peak gets higher with high values of ω_h. Until $t = 8s$, it is noticeable that high values of ω_h induce a bigger error. But for $t \geqslant 8s$, this gets reversed and the absolute estimation error induced by smaller ω_h is the highest. We can also notice that for this example, the absolute error range increases with the degree of the derivative and the derivative estimation error is quite important due to the inadequate set of tuning parameters.

We then considered the noisy scenario, where the signal $y_4(t)$ is disturbed by an additive noise normally distributed in $[-0.5, 0.5]$. The results are shown in figure (3.12). We can notice that, on the contrary of the exponential kernel case, the noise is not amplified

but damped with time. This is due to the shape of the polynomial kernel function that enables it to have the same magnitude as its derivatives, which is not the case for the exponential kernel function.

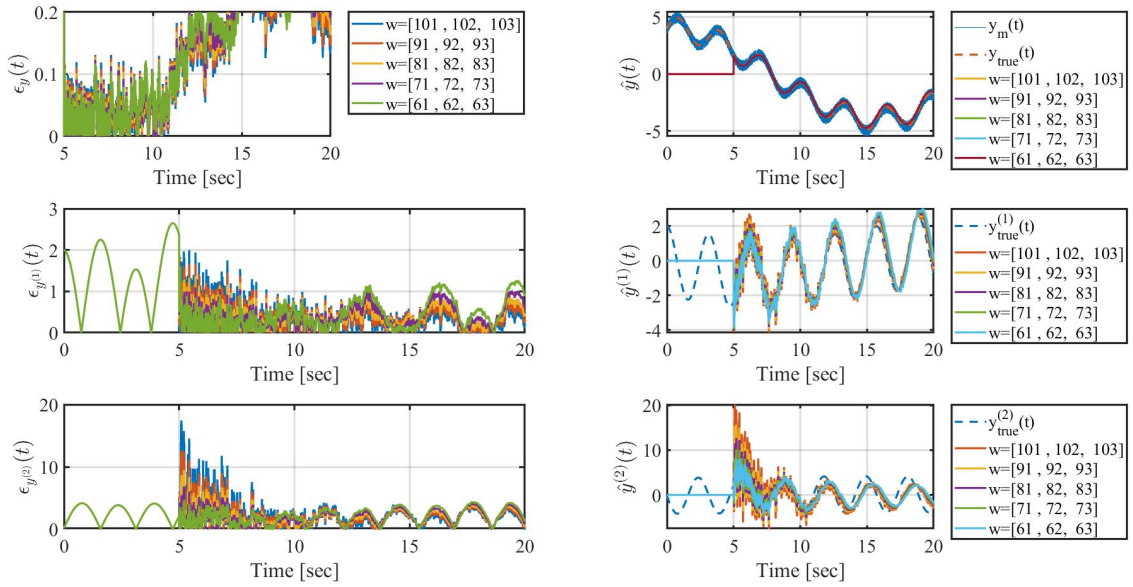

Figure 3.12: Second derivative estimation with the polynomial kernel based on noisy measurements ($N = 3$)

Third derivative estimation (N=4):

Figures (3.13) and (3.14) show a comparison between the estimation of the first four derivatives of the signal $y_4(t)$ first with the exponential kernel function with the following parameters: $\bar{\omega} = 2.5$, $\omega = [20, 40, 60, 80]$. Second, with the polynomial one where $\omega = 5$, $\omega = [41, 42, 43, 44]$ and $T = 240s$. With $\delta_\epsilon = 5s$.

In figure (3.13) the measurements are not biased by any noise. In this case we can see that the exponential kernel function gives more reliable results than the polynomial kernel and is therefor more efficient for each estimate.

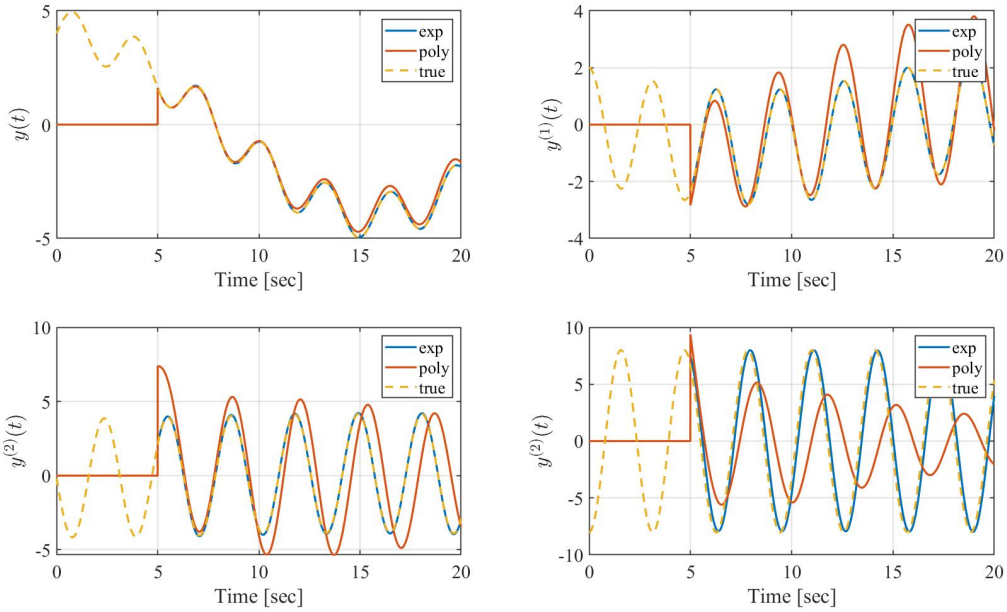

Figure 3.13: Comparing both kernels for third derivative estimation in the noise-free scenario ($N = 4$)

In the noisy scenario, it is important to mention that the original measurements are only biased by a relatively small noise $d_4(t)$ that is normally distributed in $[-0.2, 0.2]$.

Figure (3.14) shows how the exponential kernel function amplify this noise for all the derivatives estimation and this amplification gets more important when the differential degree rises. The polynomial kernel function, on the other hand, does not amplify the noise and behaves similarly as in the noise-free scenario. This difference when adding a disturbance can be explained by the shape of both of these kernels.

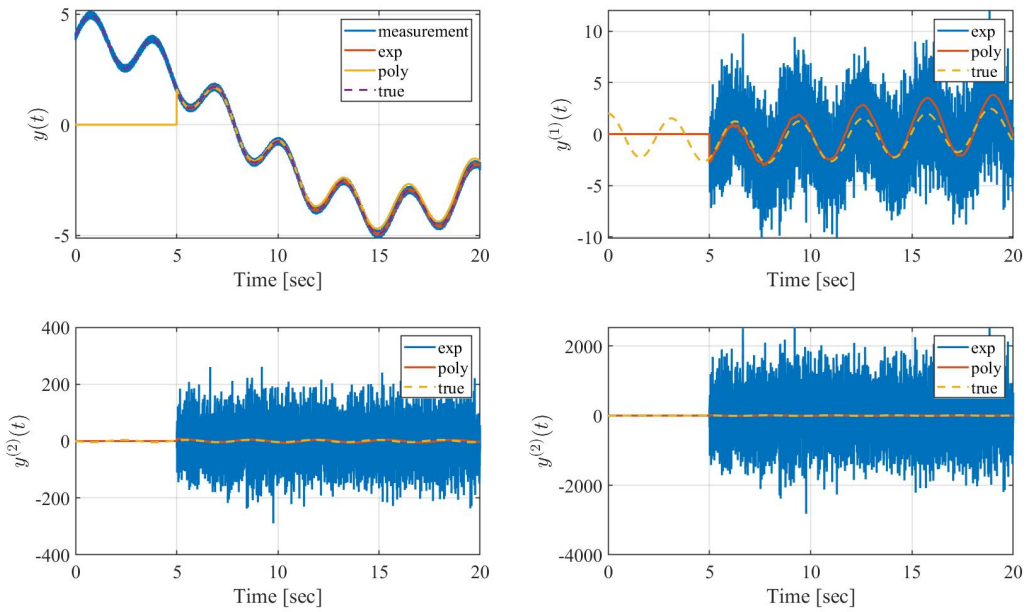

Figure 3.14: Comparing both kernels for third derivative estimation based on noisy measurements ($N = 4$)

3.7 Conclusion

In this chapter, we have confirmed that the exponential kernel functions family should be used in the Volterra differentiator only in the noise-free scenario where it gives fast convergence with accurate estimations [33]. A clear pattern between its parameters was found: the higher the parameters are, the better the accuracy is. This is especially important when high derivatives degrees come in hand where the estimation can loose its precision.The main problem with this method is that it lacks robustness. Indeed, in the noisy scenario, a relatively small additive noise is amplified in the derivatives estimations and makes the results useless.

In order to overcome this problem, we proposed a novel bivariate kernel functions family that is polynomial and constructed the Volterra differentiator around it. The polynomial kernel functions shapes prevents it to amplify the noise, which shows good potential in increasing the method's robustness.

However. this type of kernel comes with two main problems. The first one being the lack of a clear pattern when choosing the tuning parameters that compose the kernel. These

parameters are crucial for the estimation accuracy highly relies on them. Therefore, future work should focus on finding a method to choose them. One idea, for example, is to use a metaheuristic optimization algorithm to obtain ω_h and $\bar{\omega}$ with a criteria that minimizes the estimation error. The second problem is purely numerical and revolves around the transformation matrix $\Gamma_2(t)$ that is often ill-posed which induces errors in its inverse computation, resulting in unreliable results. One approach to overcome this issue is to over-saturate the transformation by adding more kernel functions to the estimation, transforming $\Gamma_2(t)$ into an $m \times n$ matrix and solving the estimation problem by using a least square algorithm, thus killing the invertibility problem. Another one is to investigate the properties of $\Gamma_2(t)$ and its invertibility in general, extract constrains for its well conditioning and impose those conditions on the kernel function.

Chapter 4

Modulating functions based method

4.1 Introduction

The modulating functions based method has a long history in the literature, with the a first appearance in 1957 [59], where the author, inspired by Laplace and Fourier transformations, proposed to use an integral transformation based on a weight function that he called *method function*, in order to identify high-order nonlinear dynamic systems. Since then, many have proven an interest in the concept and the method has seen many variations [56]. Today, the modulating functions based method (MFBM) is mainly used to estimate the parameters of PDEs ([2] and [3]) and fractional order PDEs ([29], [37], [5] and [6]) because the method offers the elimination of the initial conditions. Indeed, the definition of modulating functions (MF) revolves around the annihilation of the function and its derivatives on the borders, in order to cancel initial conditions on the signals' derivatives. This has lead to the construction of different types of modulating functions, the most common ones being Fourier (exponential), Jacobi (polynomial), sinusoidal MF, Hartley MF [20]. However, there are no systematic method for choosing a particular modulating function over another, because theoretically any function that satisfies those conditions should give acceptable results.

In this chapter, we propose to verify this last assertion by introducing a novel type of modulating functions that satisfies the conditions on the borders and is randomized in between. This work aspires to a better understanding of the importance of the modulating functions structure by also relaxing the differentiability and continuity conditions. We focus on estimating the parameters of simple ODEs by MFBM to illustrate the idea.

4.2 Principle of the modulating functions based method

Before explaining the principle of modulating functions based method, we first need to define what a modulating function is and then introduce the most important tool that makes this estimation method possible: *the generalized integration by parts.*

Definition 1 (modulating function) [56] A function $\phi \in \mathcal{C}^i([a,b])$, defined over $[a,b]$, is called a modulating function of order i with $i \in \mathbb{N}^*$ if:

$$\phi^{(j)}(a) = \phi^{(j)}(b) = 0, \ \forall j = \{0, 1, ..., i-1\}. \tag{4.1}$$

Lemma 1 (Generalized integration by parts) [4] Let $f \in \mathcal{C}^l(\mathbb{R})$ and $g \in \mathcal{C}^m(\mathbb{R})$, where $l, m \in \mathbb{N}^*$ with $m \leqslant l$. Then, for any interval $[a, b] \subset \mathbb{R}$, we have:

$$\int_a^b g(t) f^{(l)}(t) dt = (-1)^m \int_a^b g^{(m)}(t) f^{(l-m)}(t) dt + \sum_{k=0}^{m-1} (-1)^k \left[g^{(k)}(t) f^{(l-1-k)}(t) \right]_{t=a}^{t=b}. \tag{4.2}$$

The proof of this lemma is rather simple for it can be obtained by an enumerative inductive reasoning with successive integration by parts.

The principle of the modulating function based method relies on the combination of the *Lemma 1* with *Definition 1* .

Suppose we have a system that requires $y^{(i)}(t)$, the ith order derivative of observation variable $y(t)$. With an nth order modulating function $\phi(t)$ defined on the interval [0, T], with $n \geqslant i$, we can reduce the observation variable's derivative order by exploiting the modulating functions characteristics and the generalized integration by parts lemma as follows:

$$\int_0^T \phi(t) y^{(i)}(t) dt = (-1)^i \int_0^T \phi^{(i)}(t) y(t) dt. \tag{4.3}$$

The modulating function $\phi(t)$ being a degree of freedom, its ith derivative can be computed.

Advantages of the modulating functions based method: The MFBM addresses some a recurrent problems in estimation and therefore presents considerable advantages as it:

1. shifts the derivatives from the signal to the modulating functions, which are analytically known,

2. transforms the problem into a simple linear algebraic system that can be solved either by an inverse transformation (for square systems) or least square (for any rectangular system),

3. does not require the system's initial conditions, as the method gets rid off them thanks to the modulating functions properties at the borders,

4. is considered robust to external disturbances induced on the measurements as the integration dampens the noise.

4.3 Generalization of the modulating functions based method

4.3.1 Constant parameters estimation

Let us consider the following differential equation: [17]

$$\sum_{i=0}^{n} a_i \frac{d^i y(t)}{dt^i} = \sum_{i=0}^{m} b_i \frac{d^i u(t)}{dt^i}, \quad n \geqslant m, \tag{4.4}$$

where $y(t)$ is the output, $u(t)$ the input and a_i, b_i are the unknown system parameters to be estimated that are constant in $\mathbb{R}$. Without loss of generality, we assume $a_0 = 1$.

Step 1: multiply (4.4) by a modulating function $\phi_h(t) \in \mathcal{C}^{m+n+1}([0,\, T])$:

$$\sum_{i=0}^{n} a_i \phi_h(\tau) \frac{d^i y(\tau)}{d\tau^i} d\tau = \sum_{i=0}^{m} b_i \phi_h(\tau) \frac{d^t u(\tau)}{d\tau^i} d\tau. \tag{4.5}$$

Step 2: integrate (4.5) over the interval $[0,\, T]$:

$$\sum_{i=0}^{n} a_i \int_0^T \phi_h(\tau) \frac{d^i y(\tau)}{d\tau^i} d\tau = \sum_{i=0}^{m} b_i \int_0^T \phi_h(\tau) \frac{d^t u(\tau)}{d\tau^i} d\tau. \tag{4.6}$$

Step 3: using the the generalized integration by parts lemma (4.2), equation (4.6) becomes:

$$\sum_{i=0}^{n} (-1)^i a_i \int_0^T \frac{d^i \phi_h(\tau)}{d\tau^i} y(\tau) d\tau = \sum_{i=0}^{m} (-1)^i b_i \int_0^T \frac{d^i \phi_h(\tau)}{d\tau^i} u(\tau) d\tau. \tag{4.7}$$

We now define the following signals:

$$\tilde{y}_h^{(i)}(T) = (-1)^i \int_0^T \frac{d^i \phi_h(\tau)}{d\tau^i} y(\tau) d\tau, \quad \tilde{u}_h^{(i)}(T) = (-1)^i \int_0^T \frac{d^i \phi_h(\tau)}{d\tau^i} u(\tau) d\tau. \tag{4.8}$$

Assuming both input and output signals are known, $\tilde{y}_h^{(i)}(T)$ and $\tilde{u}_h^{(i)}(T)$ can be computed using numerical integration methods such as the trapezoidal, simpson $\frac{1}{3}$, simpson $\frac{3}{8}$... etc.

Step 4: rearranging (4.7) and using (4.8), we obtain:

$$\sum_{i=0}^{m} b_i \tilde{u}_h^{(i)}(T) - \sum_{i=1}^{n} a_i \tilde{y}_h^{(i)}(T) = \tilde{y}_h(T). \tag{4.9}$$

For $h = \{0, \cdots, K\}$ where $K \geqslant m + n + 1$, we can construct the following algebraic system:

$$A(T)\hat{\theta} = B(t), \tag{4.10}$$

where:

$$A(T) = \begin{bmatrix} \tilde{u}_0(T) & \cdots & \tilde{u}_0^{(m)}(T) & -\tilde{y}_0^{(1)}(T) & \cdots & \tilde{y}_0^{(n)}(T) \\ \tilde{u}_1(T) & \cdots & \tilde{u}_1^{(m)}(T) & -\tilde{y}_1^{(1)}(T) & \cdots & -\tilde{y}_1^{(n)}(T) \\ \vdots & \cdots & \vdots & \vdots & \cdots & \vdots \\ \tilde{u}_K(T) & \cdots & \tilde{u}_K^{(m)}(T) & -\tilde{y}_K^{(1)}(T) & \cdots & -\tilde{y}_K^{(n)}(T) \end{bmatrix} \in \mathbb{R}^{(K+1)\times(m+n+1)}, \tag{4.11}$$

and

$$B(T) = \begin{bmatrix} \tilde{y}_0(T) \\ \tilde{y}_1(T) \\ \vdots \\ \tilde{y}_K(T) \end{bmatrix} \in \mathbb{R}^{K+1}, \quad \hat{\theta} = \begin{bmatrix} \hat{b}_0 \\ \vdots \\ \hat{b}_m \\ \hat{a}_1 \\ \vdots \\ \hat{a}_n \end{bmatrix} \in \mathbb{R}^{m+n+1}. \tag{4.12}$$

Notice that when $K = m + n$, the algebraic system (4.10) becomes square. We then, choose the modulating functions such that $A(T)$ has linearly independent rows and the parameters can be estimated as follows:

$$\hat{\theta} = A^{-1}(T)B(T). \tag{4.13}$$

However, in practice we generally choose $K > m + n$. In this case, we solve (4.10) using

least square and we have:

$$\hat{\theta} = (A(T)^\top A(T))^{-1} A(T)^\top B(T). \tag{4.14}$$

4.3.2 Time-varying parameters estimation

The modulating function based method is also used for the time varying parameters scenario where the varying parameters are projected in a known basis. We will, then, need to estimate the coefficients of the chosen basis which transforms the problem and brings it back into a constant parameter estimation.

Let us go back, for example, to the differential equation (4.4) and consider that the parameters $a_i(t)$ are time varying. We do the projection of $a_i(t)$ in the space that is spanned by a set of known basis functions $\{\beta_j(t)\}_{j=1}^{V}$, as follows:

$$a_i(t) = \sum_{j=1}^{V} \xi_{j,i} \beta_{j,i}(t), \tag{4.15}$$

where the coefficients $\{\xi_j\}_{i=1}^{V}, V \in \mathbb{N}^*$ are the unknown parameters projections that need to be estimated. We just need to replace a_i by (4.15) in (4.4) and repeat the same steps as previously to obtain the algebraic system.

4.4 Existing types of modulating functions

Any differentiable monovariate function satisfying the condition (4.1) is a modulating function and can theoritically be used to identify a parameter. Therefore, there exists numerous types of modulating functions in the literature. In this section we will only recall some examples.

4.4.1 Sinusoidal modulating functions

The sinusoidal modulating function is the first modulating function ever constructed in [59] where it was presented as a *method function*.

$$\phi_h(t) = \sin^h(\frac{\pi}{T}t), \quad \forall t \in [0,\, T], \tag{4.16}$$

where $T \in \mathbb{R}_+^*$ and $h \in \mathbb{N}^*$, $\phi_h \in \mathcal{C}^n([0, T])$, $n \geqslant h$.

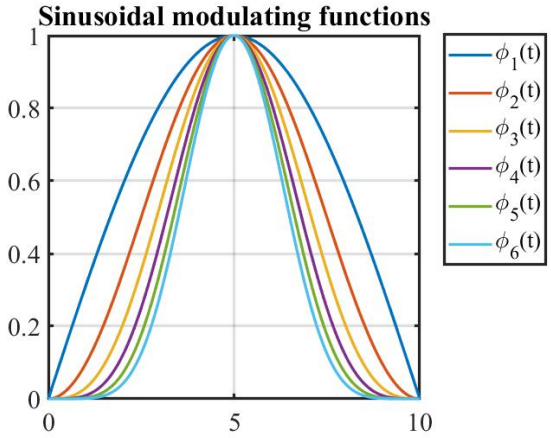

Figure 4.1: Sinusoidal modulating functions for $n = 6$

4.4.2 Hartley modulating functions

This type of modulating functions was introduced in [47] in order to identify a class of nonlinear continuous-time system. It is defined as follows:

$$\phi_h(t) = \sum_{j=0}^{n} (-1)^j \binom{n}{j} \operatorname{cas}\left((n+h-j)\frac{2\pi}{T}t\right), \quad \forall t \in [0, T], \tag{4.17}$$

where $\operatorname{cas}(x) = \cos(x) + \sin(x)$, $T \in \mathbb{R}_+^*$, $h \in \mathbb{N}^*$, $\phi_h \in \mathcal{C}^n([0, T])$, and $n \geqslant h$.

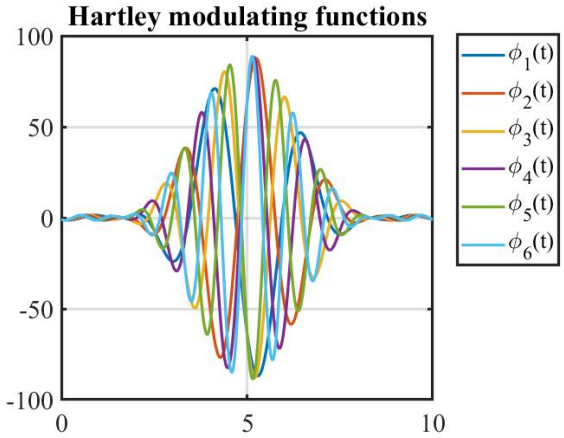

Figure 4.2: Hartley modulating functions for $n = 6$

4.4.3 Fourier modulating functions

This type of functions is presented in [48] where the periodicity of the exponential function $e^{jx} = \cos(x) + j\sin(x)$ is exploited in order to construct the following modulating functions: [20]

$$\phi_h(t) = e^{-j\alpha h}(e^{-j\frac{2\pi}{T}t} - 1)^K, \quad \forall t \in [0, T], \tag{4.18}$$

where α is a tuning parameter, $T \in \mathbb{R}_+^*$, $h \in \mathbb{N}^*$, $\phi_h \in \mathcal{C}^n([0, T])$, and $n \geqslant h$.

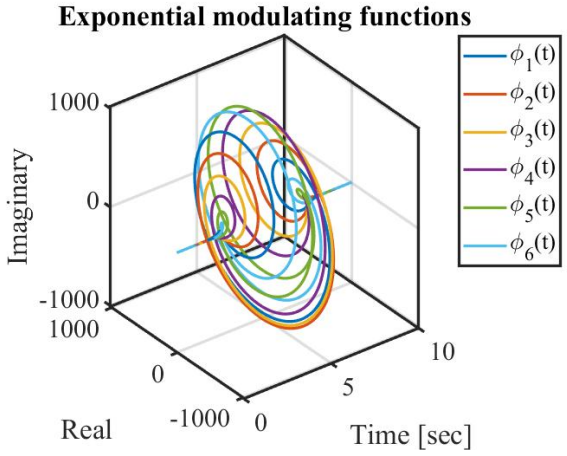

Figure 4.3: Fourier modulating functions for $\alpha = 1$, $K = 10$, and $n = 6$

4.4.4 Jacobi modulating functions

This type of modulating functions is a combination of Jacobi polynomial functions that vanish at the borders. [20] They are defined as follows:

$$\phi_h(t) = t^{h_1}(T - t)^{h_2}, \quad \forall t \in [0, T], \tag{4.19}$$

$T \in \mathbb{R}_+^*$, $h \in \mathbb{N}^*$, $\phi_h \in \mathcal{C}^n([0, T])$, $n \geqslant h$ and $h_1, h_2 \geqslant n$.

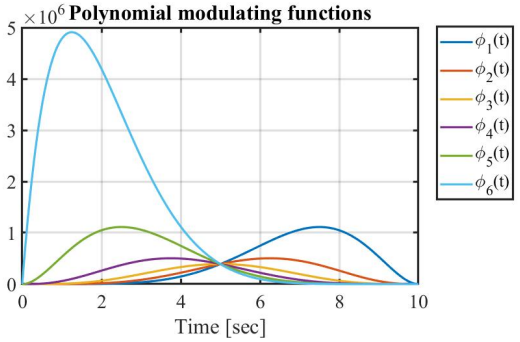

Figure 4.4: Jacobi modulating functions for $n = 6$

Notice how the magnitude of this type of functions can rise to very high values that can cause numerical problems in practice. In order to overcome these latter, we *normalize* these functions as in (3.8) by dividing each one by its energy.

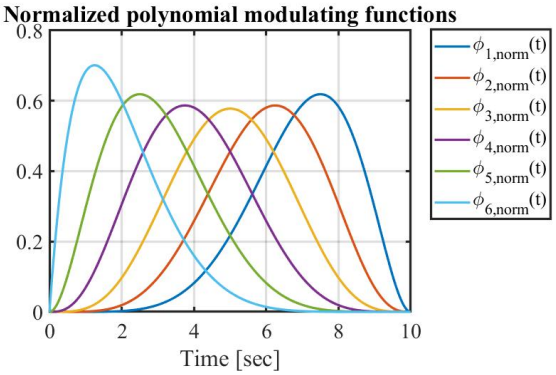

Figure 4.5: Normalized Jacobi modulating functions for $n = 6$

4.5 Randomized pseudo modulating functions

In this section, we will relax the differentiability condition of the modulating functions and propose novel pseudo-modulating functions that only satisfy the conditions on the border. This work's aim is to analyze the behavior of the method numerically when location and differentiability are ignored. Numerical simulations will be presented in the next chapter.

4.5.1 Uniformly distributed random pseudo modulating functions

$$\phi_i(t) = \begin{cases} random([\alpha, \beta]) & \text{if } 0 < t < T, \\ 0 & \text{otherwise,} \end{cases} \tag{4.20}$$

where $\alpha < \beta$ are real values, $i = \{1, ..., N\}$, and random is a function that generates random values uniformly distributed around $[\alpha, \beta]$.

Theoretically, this function is not continuous and therefore not differentiable on $[0,\ T]$ as it is illustrated in figure (4.5.1). Therefore, we will not use it to shift the derivatives.

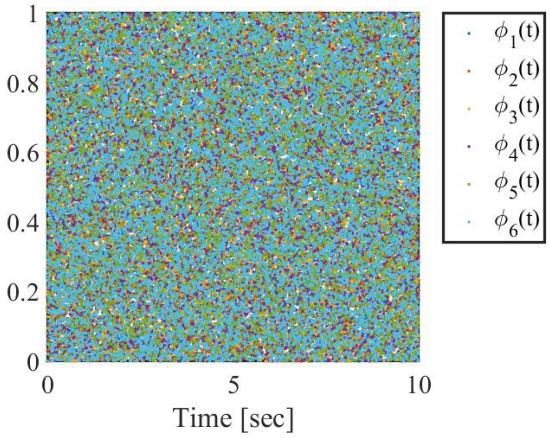

Figure 4.6: Uniformly distributed random modulating functions

4.5.2 Normally distributed random pseudo modulating functions

$$\phi_i(t) = \begin{cases} \frac{1}{\sigma\sqrt{2\,\pi}}\,\mathrm{e}^{-\frac{(t-\mu)^2}{2\sigma^2}} & \text{if } 0 < t < T, \\ 0 & \text{otherwise,} \end{cases} \tag{4.21}$$

where σ and μ are the standard deviation and the mean and are randomly chosen in [0 1] and [0 T].

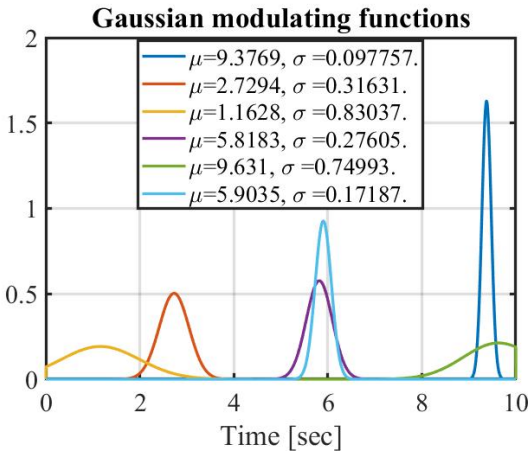

Figure 4.7: Normally distributed random modulating functions

4.6 Numerical simulations

In this section, we will consider the simple case of a homogeneous linear differential equation of the first order:

$$y^{(1)}(t) + ay(t) = 0, \ t \in [0, T], \tag{4.22}$$

where a is real constant that represents the missing parameter to be estimated.

We construct the algebraic system using the modulating functions method and implement the randomized modulating functions in both the noise-free and noisy cases. In order to make a fair comparison between the approaches, we will consider the absolute error $\epsilon_a = |\hat{a} - a|$.

In order to test the randomized pseudo-modulating functions, we will assume that we have measurements of both the signal and its derivatives.

4.6.1 Noise-free scenario

Let us consider the following solution to (4.22) :

$$y(t) = 2e^{-10t}, \ \forall t \in [0 \ T], \tag{4.23}$$

so the parameter to be identified is $a = 10$.

In figures (4.8) and (4.9), we have estimated the parameter a using two different types of random modulating functions and the absolute errors of both methods. The simulation were computed for different numbers of modulating functions (from 1 to 30) and for a sampling time $Ts = 10^{-4}s$. The pseudo-random modulating functions effectiveness are compared to the standard Jacobi modulating functions.

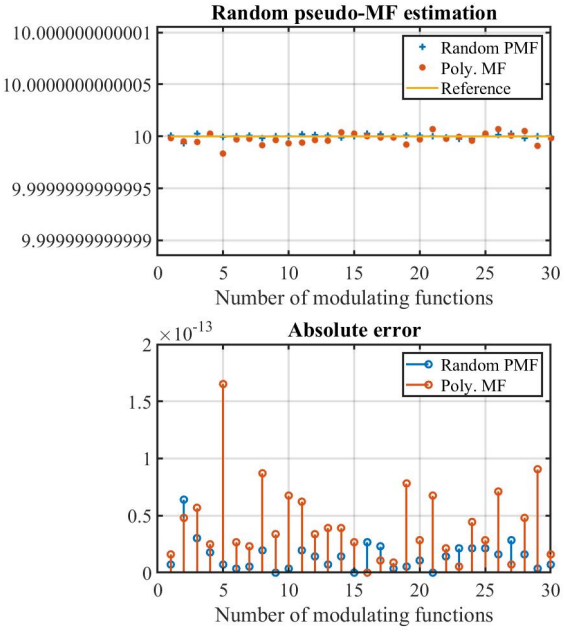

Figure 4.8: Estimating a with uniformly distributed pseudo-modulating functions

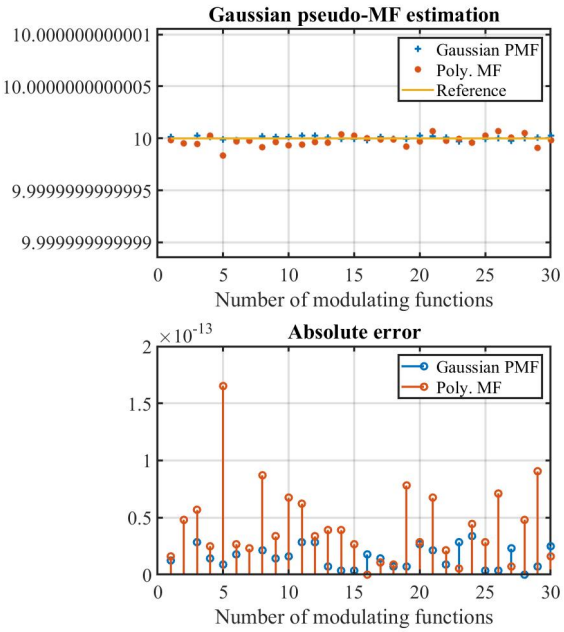

Figure 4.9: Estimating a with normally distributed pseudo-modulating functions

Both pseudo-modulating functions and standard Jacobi polynomial modulating functions give similar results as their error's range is the same, about 10^{-13}. However, and in a general view, we notice that the randomized pseudo-modulating functions give better results than the standard polynomial Jacobi functions. This can be explained by the fact that the randomized pseudo-modulating functions can encompass more important information since they are mode distributed in space.

The figures also show that increasing the number of the pseudo-modulating functions of the method has no effect on the results, as the variations we notice are due to the randomized aspect of the method. Indeed, the simplicity of this example exempt it from numerical irregularities. Therefore, it is advised to stick to the minimal number of pseudo-modulating functions in order to ease the computations.

4.6.2 Noisy scenario

Let us now consider the previous signal in (4.23) with an additive uniformly distributed noise in $[-0,05\ \ 0,05]$ as it is shown in figure (4.10). Figures (4.11) and (4.12) show the constant parameter estimation using the two random pseudo-modulating functions effectiveness compared to the classical Jacobi modulating function.

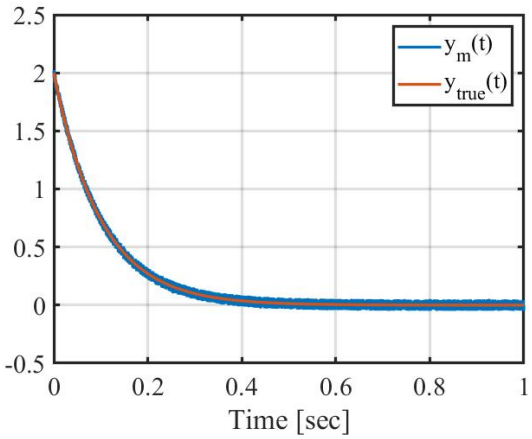

Figure 4.10: Measured signal in the noisy scenario

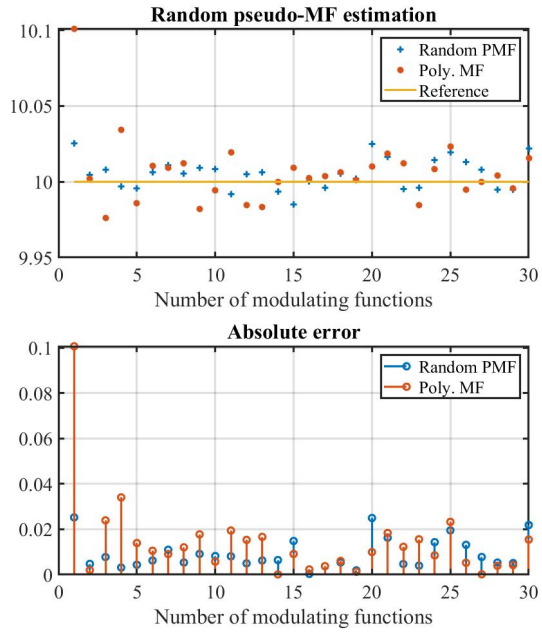

Figure 4.11: Parameter estimation in the noisy scenario with uniformly distributed pseudo-MFs

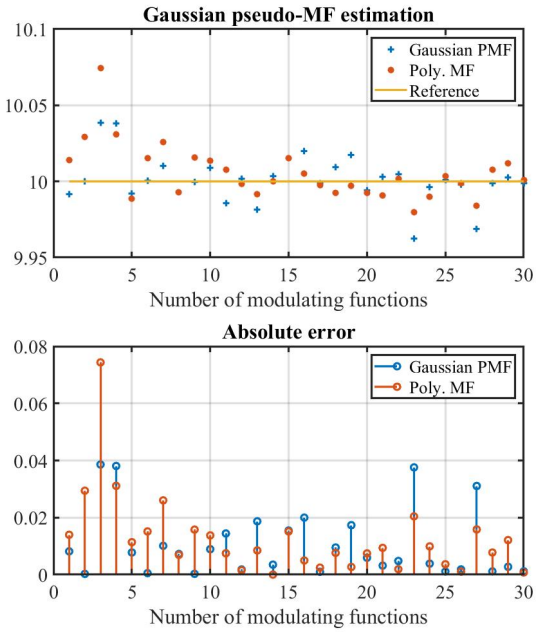

Figure 4.12: Parameter estimation in the noisy scenario with normally distributed pseudo-MFs

In the noisy scenario, the estimation's absolute error rises to a range of 10^{-1} for all types of modulating functions considered. The pseudo-modulating functions accuracies are still similar, but not necessarily better than the standard Jacobi modulating functions, depending on the number of modulating functions used. However, for $N = 1$, $N = 2$ and $N = 3$ both pseudo-modulating functions give better results than Jacobi as their errors do not surpass 4%, while the Jacobi MF has an 8% for $N = 3$.

We can also notice that, like in the noise-free case, increasing the number of modulating functions do not necessarily give better results. Therefore, sticking to a low number of modulating functions is still preferable.

The accuracy of this estimation is due to the integration of the measurements along with the modulating function as the integration is known for dampening the noise.

4.7 Conclusion

The modulating functions based method is an integral estimation approach that leads to a time invariant estimation through a constructed algebraic system. The general algorithm

is well known and used but one of the main problems with this method is the choice of the modulating functions family itself. Indeed, when systems get complicated, the existing types of modulating functions may fail to give proper results even though they obey to all theoretical conditions.

In this chapter, we suggested to verify these theoretical conditions importance by keeping the annihilation of the functions on the borders and relaxing the differentiability condition. We proposed a novel type of modulating functions that only vanish at the borders and are randomized in between. We have applied these pseudo-modulating functions on a simple ODE using two types of randomization: uniform and normal and compared both results. We can conclude that the pseudo-modulating function based method works both in the noise-free and noisy scenarios. The number of pseudo-modulating functions used is irrelevant for simple estimations and the method's accuracy depends only on the continuous aspect of the pseudo-modulating functions and their projection in space.

Chapter 5

Estimation of the arterial blood flow and the Windkessel parameter

5.1 Introduction

In this chapter, we will illustrate the importance of finite time estimation methods by applying the modulating functions based method on a real life problem that is crucial in both physiology and bio-engineering: the estimation of the arterial blood flow through the arterial network. Generally, the tools to estimate the blood flow are too invasive and ill advised, and the non-invasive ones are considered to be, either too complex, heavy to compute or expensive. Which is why the authors in [4], suggested an alternative to these methods by using a simple 0-D mathematical model of the arterial network: the two-element Windkessel . They also proposed to estimate the parameters of this model using modulating functions. Our goal throughout this work is to exploit this particular example in order to illustrate the advantages and limitations of the modulating functions method. In order to do so, we will briefly explain the basics of the cardiac cycle, go through the two-element Windkessel model and explain the steps to construct the algebraic system to estimate the parameters of interest. At last, we will provide a sensitive analysis for this estimation problem through numerical simulations and discuss the results.

5.2 Aortic blood flow and the Windkessel effect

5.2.1 Cardiac cycle phases

The aorta is the largest artery in the human body. It starts at the heart's left ventricle and extends to the abdomen in smaller branches that are called *arteries*. Figure (5.1) can be also found here. The cardiac cycle goes through 2 main phases : [11]

1. **The ventricular diastole:** it occurs after the relaxation of the ventricle where the the oxygenated blood is pushed into the atria. During this phase, the blood pressure is at its lowest and it is known as *diastolic pressure*.

2. **The systole:** it follows directly the diastole, where the ventricles ejects the blood out through the aorta. During this phase, the blood pressure reaches its maximum value and it is known as *systolic pressure*.

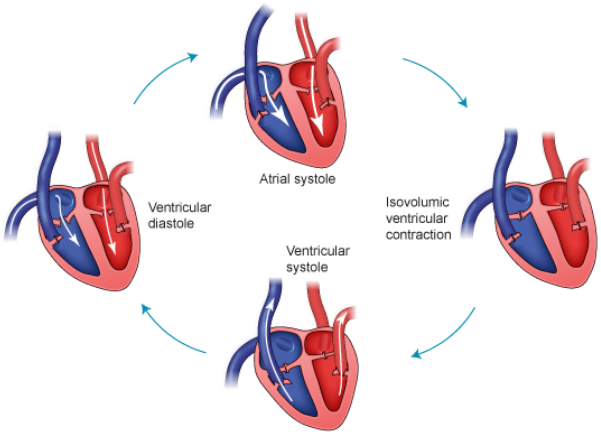

Figure 5.1: Cardiac cycle [11]

5.2.2 The two-element Windkessel model description

The Windkessel model was introduced in the 19th century by the physiologist Otto Frank, where he first described the mechanics of the heart with a hydraulic analogy. In this analogy, the heart is a water pump and the abdomen a chamber. He also suggested another analogy, that we will use later on to represent this phenomenon: the electrical circuits analogy.

In the electric analogy, the Windkessel model considers the following:

1. the electrical voltage represents the arterial blood pressure,
2. the current represents the blood flow,
3. the cables represent the arteries,
4. Arterial Compliance and Peripheral Resistance are modeled as a capacitor and a resistor, respectively [11].
5. the cardiac cycle starts at systole,
6. the period of the systole T_s is $\frac{2}{5}$th of the period of the cardiac cycle T_c.

Figure (5.2) illustrates the analogy where $Q_a(t)$ is the input arterial blood flow, $P_a(t)$ the blood pressure, R_p the peripheral resistance and C the arterial compliance. [4]

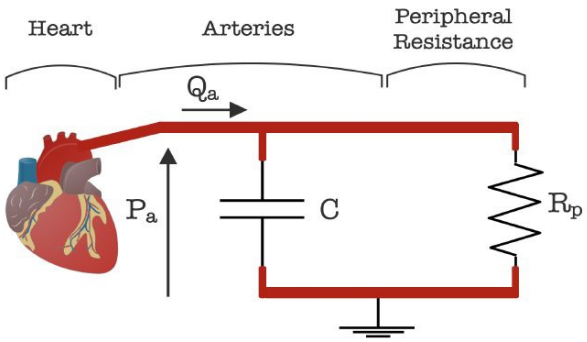

Figure 5.2: Electric equivalence of the hearts mechanisms [4]

Proposition: The Windkessel two elements model can be described by the following differential equation:

$$F_{in}(t) = \tau \frac{dP_a(t)}{dt} + P_a(t), \tag{5.1}$$

where we want to estimate $F_{in}(t) = R_p Q_a$ and $\tau = R_p C$. We suppose that the pressure $P_a(t)$ is known. The steps to obtain this equation can be found in [4].

5.3 Solving the estimation problem using modulating functions

In this section, we will explain the steps to construct the algebraic system for solving the estimation problem in system (5.1).

First, we need to project the time varying parameters to be estimated in known basis functions $\{\beta_i(t)\}_{i=1}^{V}$:

$$F_{in}(t) = \sum_{i=1}^{V} \xi_i \beta_i(t), \tag{5.2}$$

where $\{\xi_i\}_{i=1}^{V}$ are the projection of the blood flow in the space and the unknown coefficients to be estimated.

Replacing (5.2) in (5.1), we obtain the ODE:

$$\sum_{i=1}^{V} \xi_i \beta_i(t) = \tau \frac{dP_a(t)}{dt} + P_a(t). \tag{5.3}$$

Next, we multiply this last equation by a set of N modulating function family $\phi_h(t)$ and integrate over a time interval $[0,\, T]$:

$$\sum_{i=1}^{V} \xi_i \int_0^T \phi_h(t)\beta_i(t)dt = \tau \int_0^T \phi_h(t)\frac{dP_a(t)}{dt}dt + \int_0^T \phi_h(t)P_a(t)dt. \tag{5.4}$$

Now, we use the results of the generalized integration by parts lemma (4.2) to shift the blood pressure derivative to the modulating function and use the vanishing property at the borders to obtain:

$$\sum_{i=1}^{V} \xi_i \int_0^T \phi_h(t)\beta_i(t)dt + \tau \int_0^T P_a(t)\frac{d\phi_h(t)}{dt}dt = \int_0^T \phi_h(t)P_a(t)dt. \tag{5.5}$$

At last, we construct the linear system for multiple modulating functions:

$$A\theta = b, \tag{5.6}$$

where

$$\mathrm{A}=\begin{bmatrix} \int_0^T \phi_1(t)\beta_1(t)dt & \int_0^T \phi_1(t)\beta_2(t)dt & \cdots & \int_0^T \phi_1(t)\beta_V(t)dt & \int_0^T P_a(t)\frac{d\phi_1(t)}{dt}dt \\ \int_0^T \phi_2(t)\beta_1(t)dt & \int_0^T \phi_2(t)\beta_2(t)dt & \cdots & \int_0^T \phi_2(t)\beta_V(t)dt & \int_0^T P_a(t)\frac{d\phi_2(t)}{dt}dt \\ \vdots & \vdots & \cdots & \vdots & \vdots \\ \int_0^T \phi_N(t)\beta_1(t)dt & \int_0^T \phi_N(t)\beta_2(t)dt & \cdots & \int_0^T \phi_1(t)\beta_V(t)dt & \int_0^T P_a(t)\frac{d\phi_N(t)}{dt}dt \end{bmatrix} \in \mathrm{R}^{N\times(V+1)},$$

$$b = \begin{bmatrix} \int_0^T \phi_1(t)P_a(t)dt \\ \int_0^T \phi_2(t)P_a(t)dt \\ \vdots \\ \int_0^T \phi_N(t)P_a(t)dt \end{bmatrix} \in \mathbb{R}^N, \quad \theta = \begin{bmatrix} \xi_1 \\ xi_2 \\ \vdots \\ \xi_V \\ \tau \end{bmatrix} \in \mathbb{R}^{V+1}. \tag{5.7}$$

We solve this linear system using the least square method.

5.4 Analytical solutions of the 2-Element Windkessel model

In order to test the modulating functions method on system (5.1), we need to generate the input $P_a(t)$ and know the blood flow $F_{in}(t)$ and Windkessel parameter τ in advance for comparing the estimation results with the real parameters. We can do this either by using an existing data base (e.g. [64]) or by using the analytical solutions of the Windkessel model.

In this work, we propose to use both approaches. Therefore, we will now present the analytical solutions to generate these signals.

5.4.1 Blood flow analytical solution

As it is presented in [11], the blood flow in the aorta acts like a sinusoidal wave. Therefore, it can be modeled as follows:

$$Q_{a,anal}(t) = Q_{a,0} \sin\left(\pi * \frac{\mathrm{mod}\,(t, T_c)}{T_s}\right) \tag{5.8}$$

where T_c is the period of the cardiac cycle, T_s, the period of the systole, the function $mod(x_1, x_2)$ is the remainder of x_1 divided by x_2.

$Q_{in,0}$ is the maximum blood flow during the systole and according to [11] its value is of $424.1\,mL$.

5.4.2 Blood pressure analytical solution

Systolic phase

For simplification, we reduce equation (5.1) to:

$$\frac{dP_a(t)}{dt} + \frac{P_a(t)}{CR_p} = Q_a(t). \tag{5.9}$$

Equation (5.9) is an inhomogeneous equation of the first order, its solution is:

$$P_a(t) = c_1 e^{\frac{-t}{R_p C}} + \frac{-e^{\frac{t}{CR_p}} T_s Q_{a,0} R \left(C\pi R_p \cos\left(\frac{\pi t}{T_s}\right) - T_s \sin\left(\frac{\pi t}{T_s}\right)\right)}{T_s^2 + C^2\pi^2 R_p^2}, \tag{5.10}$$

with

$$c_1 = P_{ss} + \frac{Q_{a,0} T_s R_p [C\pi R_p]}{T_s^2 + C^2 * \pi^2 * R_p^2}, \tag{5.11}$$

where P_{ss} is the blood pressure at the start of the systolic cycle.

Further details can be found in [11].

Diastolic phase

In the diastolic phase, equation (5.9) becomes the following homogeneous first order differential equation:

$$\frac{dP_a(t)}{dt} + \frac{P_a(t)}{CR_p} = 0. \tag{5.12}$$

The solution of this equation is trivial:

$$P_a(t) = P_{sd}\, \mathrm{e}^{-\frac{t}{R_p C}}, \tag{5.13}$$

where P_{sd} is the blood pressure at the beginning of the diastolic phase.

5.5 Numerical simulations

The main purpose of this application is to highlight the characteristics of the modulating functions based method. Therefore, we will first perform a sensitive analysis of the method on this particular system, varying the main features of the method that may alter the results: the nature of the modulating functions, the number of the modulating functions and number of basis functions. We will use the analytical Windkessel model to generate the needed data and then try the set of parameters obtained on real measurements from the data base in [64].

In all of the above, we will consider the estimation of the blood flow in one cardiac cycle only (i.e: one systole and one diastole).

In this section, we consider the following relative errors:

$$\begin{aligned} \epsilon_\xi &= \frac{\|F_{in}(t) - \sum_{i=1}^{V} \hat{\xi}_i \beta_i(t)\|}{\|F_{in}(t)\|} \times 100, \\ \epsilon_\tau &= |\frac{\tau - \hat{\tau}}{\tau}| \times 100. \end{aligned} \tag{5.14}$$

5.5.1 Estimation via analytically generated data

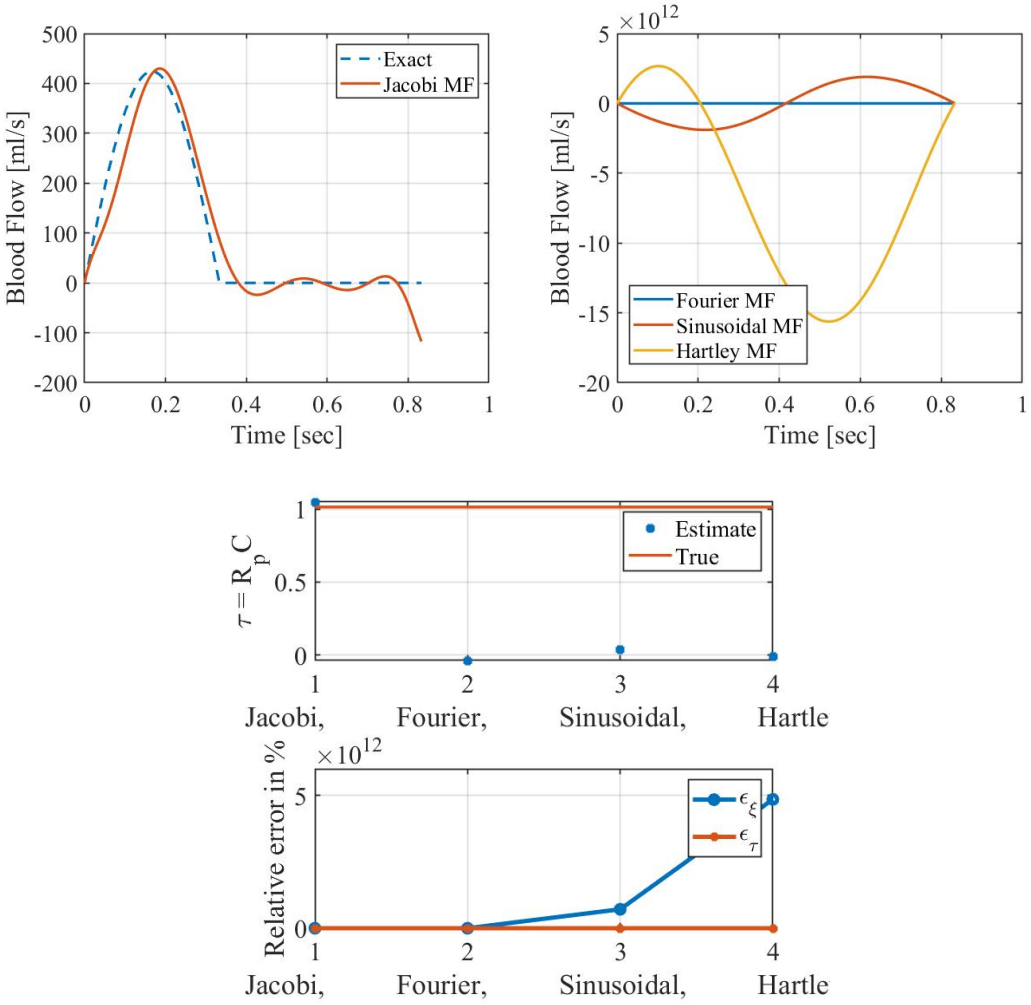

Figure 5.3: Performance of the estimation algorithm for different types of modulating functions

The first parameter that we need to settle is the nature of the modulating function.

Figure (5.3) illustrates the behavior of the algorithm for different types of modulating functions. We have computed this considering the standard Jacobi basis functions (see [19]), the number of basis: $V = 9$ and $N = 10$.

This figure shows that, from all of the considered types of modulating functions computed, only the Jacobi MF can be a candidate to solving this estimation, as all other modulating functions completely diverge. This divergence can be explained by the shapes of the modulating functions considered. Indeed, as we have previously seen in chapter 5, the Fourier, sinusoidal and Hartley modulating functions all peak at the middle of their time interval. Whereas in this case, the blood pressure peaks at the systole that happens in the first $\frac{2}{5}$th of the cardiac cycle. This means that only the Jacobi MF is designed such that it can encompass the input measurements.

5.5.2 Modulating functions number

In figure (5.4), we have computed the estimation algorithm for $V = 9$, using the Jacobi MF and varying the number of modulating functions. We notice, here, that both relative errors reach their minimum for $N = 11$, where $\epsilon_\xi \approx 20\%$ and $\epsilon_\tau \approx 2\%$. This preliminary result is promising enough for the estimation of the blood flow, especially considering the fact that this algorithm does not take more than $10s$ to compute.

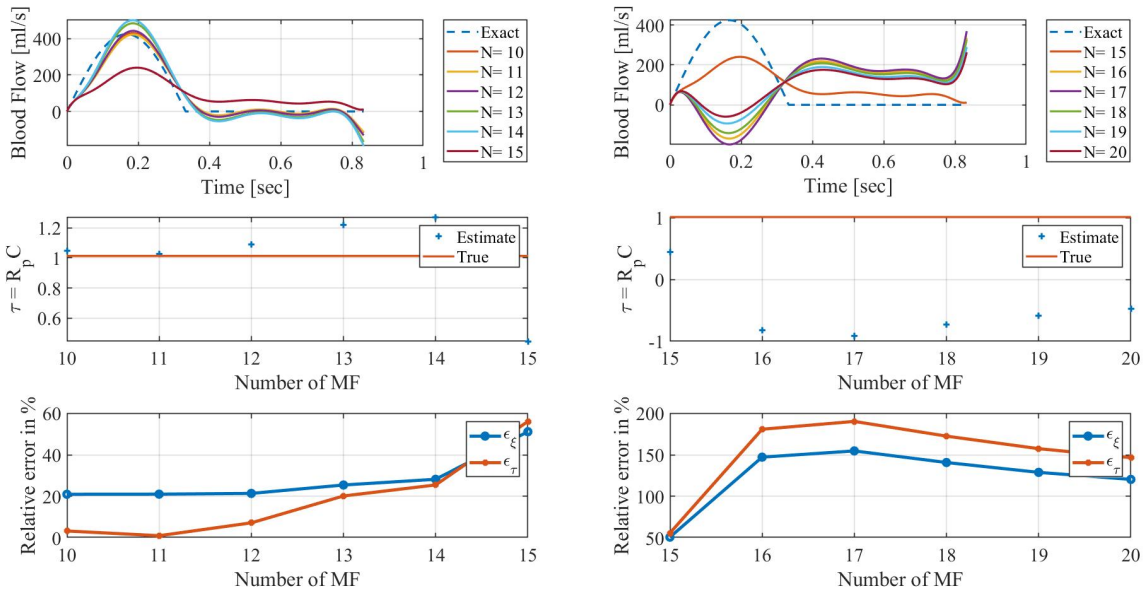

Figure 5.4: Performance of the estimation algorithm for different numbers of Jacobi MF

We also notice that the estimation algorithm starts diverging when N increases. This divergence can be explained by the ill-poisoning of the matrix A as defined in (5.3). Indeed, since this matrix is data-driven, it is very sensitive numerically and in this particular case, it is sensitive to the number of modulating functions. Throughout the numerical computing, we have noticed that the reciprocal conditioning number highly decreases to a range of 10^{-10} when $N > 14$, which makes the estimation results unreliable. Therefore we need to be very careful to this particular factor when computing this method as it can considerably alter the results.

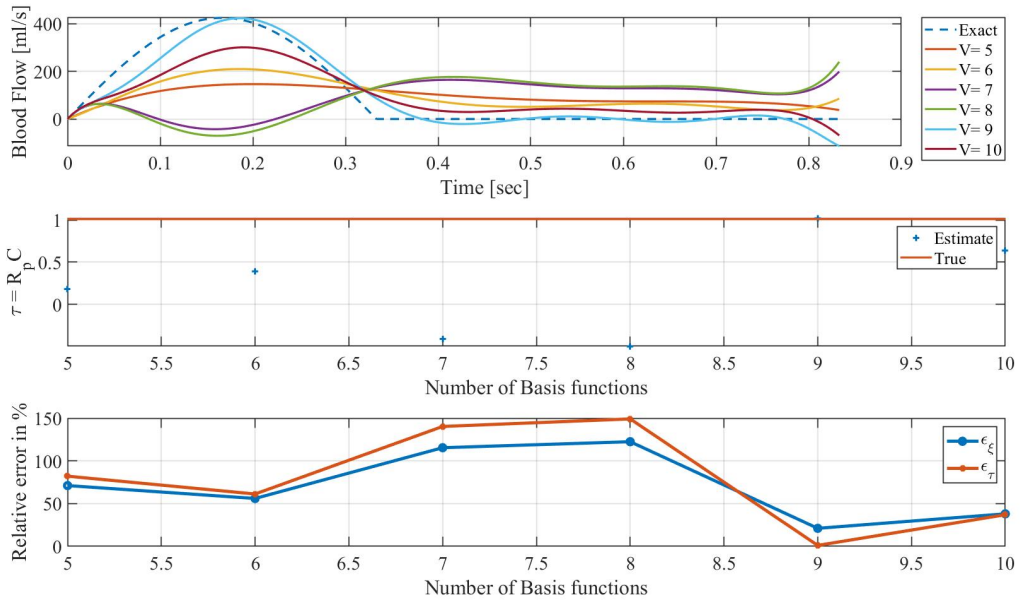

Figure 5.5: Performance of the estimation algorithm for different numbers of the Jacobi basis functions

Figure (5.5) confirms that the best number of basis functions for this estimation is 9. However, there does not seem to be any theoretical evidence to back this assertion up. Finally, we have set that the best set for this estimation algorithm is 11 Jacobi modulating functions with 9 Jacobi basis functions.

5.5.3 Estimation via a real data set

The database in [64] is an in-silico data set that reproduces the major hemodynamic signals such as the blood pressure and the blood flow as they are in-vivo. We select one virtual healthy subject from this database and use his blood pressure to estimate the arterial blood flow and the Windkessel parameter. Figure (5.6) shows the results that we get when using the MF estimation algorithm with $N = 11$, $V = 9$ with Jacobi modulating functions and standard Jacobi basis on this virtual subject. Clearly, this estimation is inaccurate and unsatisfactory as the relative error of the blood flow estimation is of 120%. This example illustrates perfectly the sensitiveness of this method as each system (each subject in this case), needs a novel set of parameters for the estimation algorithm to converge.

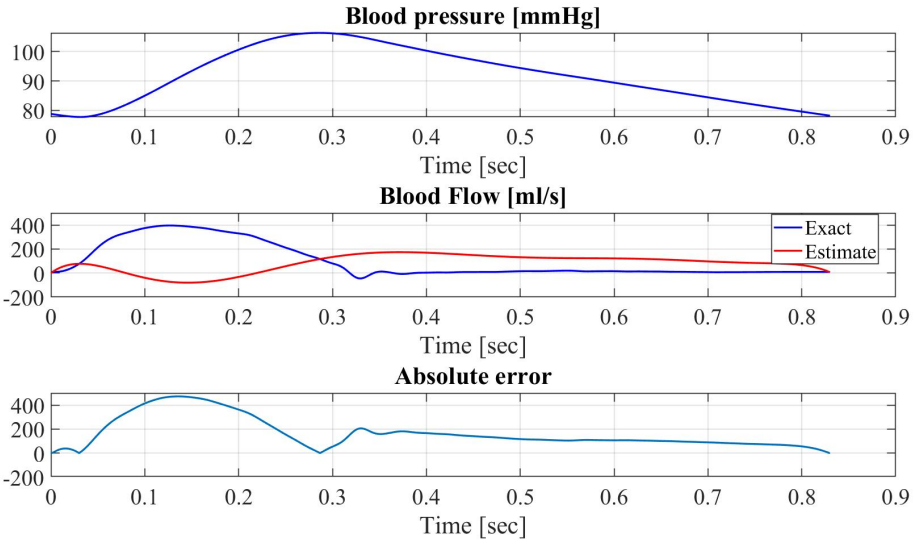

Figure 5.6: Blood flow estimation on a virtual subject with the MFBM parameters of the analytical model

We have run a set of simulations and found out that for this patient, the *best* parameter combination is : $V = 10$, $N = 12$ with Jacobi modulating functions and B-spline basis functions (see [25]). The results of the simulation are shown in figure (5.7), where the overall relative error degree of the blood flow estimation is about 34% which can be considered as a good preliminary result. However, the estimation does not encounter the real alteration and local variations of the real data. We also notice that the estimation

starts diverging at the end of the interval which increases the overall error.

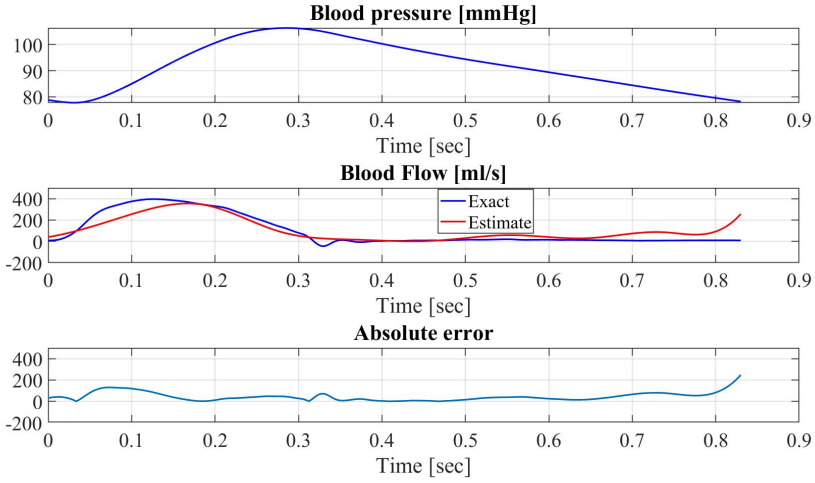

Figure 5.7: Blood flow estimation on a virtual subject with a novel set of the MFBM parameters

5.6 Conclusion

Estimating the arterial blood flow and the Windkessel parameter with the modulating functions based method is a very promising approach as it gives fast and finite convergence with relatively low computing requirements and represents one of the few non-invasive tools to do so [4]. However, this estimation algorithm still faces two main challenges: the data-sensitivity and numerical instability of the method. Indeed, we have seen that the set of modulating functions based method parameters that work on an analytically generated data does not necessarily work on a real subject. This means that the estimation method highly depends on the data, which may bring contradiction to the robustness claim. One idea to solve this problem, is to exploit the Windkessel analytical model of the blood flow by injecting it in the estimation algorithm. Estimating the blood flow will then imply estimating the Windkessel analytical parameters instead of the coefficients of the basis functions. Another way to improve the estimation results is to resort to the windowing approach for real time estimation with a moving horizon as it has been done in [3]. As for the numerical instability, future work should focus on using regularization methods to fix the ill-posedness that may occur [28].

General conclusion

Finite time convergence is an important concept in estimation theory that was widely investigated in the literature. Since the introduction of the concept, new observers such as the sliding mode [60], [63], [15] and supertwisting [18] were developed and old asymptotic observers were improved in order to give non-asymptotic convergence, e.g.: the high gain observer [10]. Throughout this work, we have investigated a novel kind of observation and estimation techniques: the integral based methods. The general idea behind this approach is to map the signal from a space to another via an integral transformation, estimate the signals or parameters in the new space and go back to the regular time domain via an inverse transformation if necessary.

The first approach that we have tackled is the Volterra technique [52],[50],[12],[33], as we have introduced it by reproducing the cascading observers to estimate the amplitude, frequency and phase of a biased sinusoidal signal [51]. This approach relies on transforming the biased sinusoidal signal into the Volterra space and remaining thereafter to estimate the parameters of interest using an adaptive second order sliding observer. We run a short sensitive analysis on the parameters of this observer and distinguished its robustness via the numerical simulations.

Next, and still using the Volterra approach, we investigated another problem: the Volterra differentiator. We first reproduced and explained the existing work in [35], that revolves around the existing exponential kernel functions family and we arrived to the same conclusions about the none effectiveness of this method in the noisy scenario. In order to overcome this issue, we conjectured an explanation of the phenomenon by addressing the shape of the exponential kernel functions family and suggested a novel family of kernel

functions: the polynomial kernel functions. We adapted the differentiator around this new kernel and run a set of numerical simulations to test its effectiveness. During which, we noticed difficulty in finding the right set of parameters for this novel kernel family. However, we have also noticed that this kernel family prevented the amplification of the noise and showed good potential in increasing the differentiator's robustness. Therefore, our future work will focus on finding a pattern for choosing these parameters. For example, a meta-heuristic algorithm for finding the optimal parameters with respect to a specific criteria would be a good candidate to over this issue in our future work.

After the Volterra approach, we introduced another integral transformation based technique that is very similar: the modulating functions based method [38],[37],[46],[5],[20]. This method's main idea revolves around the definition of modulating functions which are differentiable functions that vanish, with their derivatives, at the considered borders. Throughout our work, we suggested to verify these theoretical conditions importance by introducing a novel type of pseudo-modulating functions. These pseudo-MF relax the differentiability condition and keep the vanishing borders property, with a particularity: they are randomized in between. We have tried these pseudo-MF for a simple ODE parameter estimation and concluded the effectiveness of the estimation approach in both noise-free and noisy scenarios. As a future work, these pseudo-modulating functions should be tested on higher order systems in order to have a better understanding of their possible limitations.

At last, we have performed an application of these integral based estimation methods on a real estimation problem in the bio-engineering field: the estimation of the arterial blood flow. We reproduced the work done in [4] by considering the Windkessel 2-Element electric analogy in modeling one cardiac cycle and used the modulating functions based method to estimate the parameters of interest. This example illustrated perfectly the highlights and drawbacks of the MFBF as we have witnessed its fast and finite convergence but we have also seen that a small change in the input data requires a whole new set of the method's parameter in order to obtain a satisfactory convergence. One way of overcoming this issue might be rearranging the estimation algorithm by exploiting the

Windkessel analytical model [11]. Another way might be the moving horizon method that reduces the estimation window and theoretically results in better estimation accuracy [3]. We have also encountered numerical instability issues with most of the methods tested, as the ill-posedness of the problems induced by integral based methods is a major drawback that should be well investigated in future, by using regularization methods [28].

Bibliography

[1] Abeer, A., Liu, D.-Y., and Laleg-Kirati, T.-M. Theory and application of the modulating function method—i. review and theory of the method and theory of the spline-type modulating functions. *SIAM Journal on Scientific Computing 37*, 6 (2015), A2813–A2839.

[2] Asiri, S., and Laleg-Kirati, T.-M. Modulating functions-based method for parameters and source estimation in one-dimensional partial differential equations. *Inverse Problems in Science and Engineering 25*, 8 (2017), 1191–1215.

[3] Asiri, S. M., Elmetennani, S., and Laleg-Kirati, T.-M. Moving-horizon modulating functions-based algorithm for online source estimation in a first order hyperbolic pde. vol. 139, p. 061007.

[4] Bahloul, M. A., and Kirati, T.-M. L. Finite-time joint estimation of the arterial blood flow and the arterial windkessel parameters using modulating functions. In *IFAC* (2020).

[5] Belkhatir, Z., and Laleg-Kirati, T. Estimation of multiple point sources for linear fractional order systems using modulating functions. *IEEE Control Systems Letters 2*, 1 (2018), 7–12.

[6] Belkhatir, Z., and Laleg-Kirati, T. M. Parameters and fractional differentiation orders estimation for linear continuous-time non-commensurate fractional order systems. *Systems Control Letters 115* (2018), 26–33.

[7] Bernard, P. *Observer Design for Nonlinear Systems*. Springer, 2019.

[8] Bhat, S. P., and Bernstein, D. S. Lyapunov analysis of finite-time differential equations. In *Proceedings of 1995 American Control Conference - ACC'95* (1995), vol. 3, pp. 1831–1832 vol.3.

[9] Bhat, S. P., and Bernstein, D. S. Finite-time stability of continuous autonomous systems. *SIAM Journal on Control and Optimization 38*, 3 (2000), 751–766.

[10] Burlion, L., Ahmed-Ali, T., and Lamnabhi-Lagarrigue, F. Updating the gain of global finite-time high gain observers. In *2011 50th IEEE Conference on Decision and Control and European Control Conference* (2011), pp. 8145–8150.

[11] Catanho, M., Sinha, M., and Vijayan, V. Model of aortic blood flow using the windkessel e ect. In *Mathematical Methods in Bioengineering* (2012).

[12] Chen, B., Li, P., Pin, G., Fedele, G., and Parisini, T. Robust finite-time estimation of biased sinusoidal signals: A volterra operators approach. *Automatica 106* (2019), 1–7.

[13] Defoort, M., Djemai, M., Floquet, T., and Perruquetti, W. Robust finite time observer design for multicellular converters. *IEEE Transactions on Industrial Electronics 42*, 5 (2011), 1859–1868.

[14] Doan, T., Kalauch, A., and Siegmund, S. Exponential stability of linear time-invariant systemson time scales. *Nonlinear Dynamics and Systems Theory 9*, 1 (2008), 37–50.

[15] Drakunov, S., and Utkin, V. Sliding mode observers. tutorial. In *Proceedings of 1995 34th IEEE Conference on Decision and Control* (1995), vol. 4, pp. 3376–3378 vol.4.

[16] Engel, R., and Kreisselmeier, G. A continuous-time observer which converges in finite time. *IEEE Transactions on Automatic Control 47*, 7 (2002), 1202–1204.

[17] Fedele, G., and Coluccio, L. A recursive scheme for frequency estimation using the modulating functions method. *Applied Mathematics and Computation 216*, 5 (1972), 1393–1400.

[18] Floquet, T., and Barbot, J. P. Super twisting algorithm-based step-by-step sliding mode observers for nonlinear systems with unknown inputs. *IEEE Transactions on Automatic Control 38*, 10 (2007), 803–815.

[19] Guo, B.-Y., Shen, J., and Wang, L.-L. Generalized jacobi polynomials/functions and their applications. *Applied Numerical Mathematics 59*, 5 (2009), 1011–1028.

[20] Guo, Q. *Online identification and control of robots using algebraic differentiators*. Automatic. Ecole Centrale de Lille, 2015.

[21] Guo, Q., Perruquetti, W., and Gautier, M. On-line robot dynamic identification based on power model, modulating functions and causal jacobi estimator. In *2014 IEEE/ASME International Conference on Advanced Intelligent Mechatronics* (2014), pp. 494–499.

[22] Halmos, P. R. *A Hilbert space problem book*. Springer, 1991.

[23] Hammouri, H., Targui, B., and Armanet, F. High gain observer based on a triangular structure. *International Journal of Robust and Nonlinear Control 12*, 6 (2002), 497–518.

[24] Hammouri, H., Targui, B., and Armanet, F. Corrections to "a global high-gain finitetime observer". *IEEE Transactions on Automatic Control, Institute of Electrical and Electronics Engineers 62*, 1 (2017), 509 – 510.

[25] Haron, H., Rehman, A., Adi, D. I. S., Lim, S. P., and Saba, T. Parameterization method on b-spline curve. *Information and Modeling in Complexity 2012* (2012), 22.

[26] Haskara, I. Sliding mode control with sigmoid function for the motion tracking control of the piezo-actuated stages. *Electronics Letters 71*, 6 (1998), 1051–1067.

[27] Hazewinkel, M. *"Volterra equation*. Springer, 1991.

[28] Honerkamp, J., and Weese, J. Tikhonovs regularization method for ill-posed problems. *Continuum Mechanics and Thermodynamics 2* (1990), pages17–30.

[29] JANICZEK, T. Generalization of the modulating functions method into the fractional differential equations. *BULLETIN OF THE POLISH ACADEMY OF SCIENCES, TECHNICAL SCIENCES 58*, 4 (2010).

[30] Kalman, R. E. A new approach to linear filtering and prediction problems. *Journal of Basic Engineering 82*, 1 (1960), 35–45.

[31] Kalman, R. E., and Bucy, R. S. New results in linear filtering and prediction theory. *TRANS. ASME, SER. D, J. BASIC ENG* (1961), 109.

[32] Khalil, H. K. *Nonlinear Systems*. Prentice Hall, 1996.

[33] Li, P., Boem, F., Pin, G., and Parisini, T. Deadbeat simultaneous parameter-state estimation for linear continuous-time systems: a kernel-based approach. In *2018 European Control Conference (ECC)* (2018), pp. 2493–2498.

[34] Li, P., Boem, F., Pin, G., and Parisini, T. Kernel-based simultaneous parameter-state estimation for continuous-time systems. *IEEE Transactions on Automatic Control* (2019), 1–1.

[35] Li, P., Pin, G., Fedele, G., and Parisini, T. Non-asymptotic numerical differentiation: a kernel-based approach. *International Journal of Control 91*, 9 (2019), 2090–2099.

[36] Li, Y., Xia, X., and Shen, Y. A high-gain-based global finite-time nonlinear observer. In *2011 9th IEEE International Conference on Control and Automation (ICCA)* (2011), pp. 483–488.

[37] Liu, D., Laleg-Kirati, T., Gibaru, O., and Perruquetti, W. Identification of fractional order systems using modulating functions method. In *2013 American Control Conference* (2013), pp. 1679–1684.

[38] Liue, D., Laleg-Kirati, T., Perruquetti, W., and Gibaru, O. Non-asymptotic state estimation for a class of linear time-varying systems with unknown inputs. *IFAC Proceedings Volumes 47*, 3 (2014), 3732–3738.

[39] Luenberger, D. Observers for multivariable systems. *IEEE Transactions on Automatic Control 11*, 2 (1966), 190–197.

[40] Luenberger, D. An introduction to observers. *IEEE Transactions on Automatic Control 16*, 6 (1971), 596–602.

[41] LYAPUNOV, A. The general problem of the stability of motion. *International Journal of Control 55*, 3 (1992), 531–534.

[42] Menard, T., Moulay, E., and Perruquetti, W. A global high-gain finite-time observer. *IEEE Transactions on Automatic Control 55*, 6 (2010), 1500–1506.

[43] Menold, P. H., Findeisen, R., and Allgower, F. Finite time convergent observers for nonlinear systems. In *42nd IEEE International Conference on Decision and Control (IEEE Cat. No.03CH37475)* (2003), vol. 6, pp. 5673–5678 Vol.6.

[44] Michalska, H., and Mayne, D. Q. Moving horizon observers and observer-based control. *IEEE Transactions on Automatic Control 40*, 6 (1995), 995–1006.

[45] Ménard, T., Moulay, E., and Perruquetti, W. Global finite-time observers for non linear systems. In *Proceedings of the 48h IEEE Conference on Decision and Control (CDC) held jointly with 2009 28th Chinese Control Conference* (2009), pp. 6526–6531.

[46] N'Doye, I., Asiri, S., Aloufi, A., Asem Al-Awan, A., and Laleg-Kirati, T. Intelligent proportional–integral–derivative control-based modulating functions for laser beam pointing and stabilization. *IEEE Transactions on Control Systems Technology 28*, 3 (2020), 1001–1008.

[47] PATRA, A., AND UNBEHAUEN, H. Identification of a class of nonlinear continuous-time systems using hartley modulating functions. *International Journal of Control 62*, 6 (1995), 1431–1451.

[48] PEARSON, A. E., AND LEE, F. C. Efficient parameter identification for a class of bilinear differential systems. *Proceedings of 7th IF AC Symposium on Identification and System Parameter Estimation , University of York , U.K. (Pergamon) 18*, 5 (1985), 161–165.

[49] PERRUQUETTI, W., FLOQUET, T., AND MOULAY, E. Finite-time observers: Application to secure communication. *IEEE Transactions on Automatic Control 53*, 1 (2008), 356–360.

[50] PIN, G., CHEN, B., AND PARISINI, T. The modulation integral observer for linear continuous-time systems. In *2015 European Control Conference (ECC)* (2015), pp. 2932–2939.

[51] PIN, G., CHEN, B., AND PARISINI, T. Robust finite-time estimation of biased sinusoidal signals: A volterra operators approach. *Automatica 77* (2019), 120–132.

[52] PIN, G., LOVERA, M., ASSALONE, A., AND PARISINI, T. Kernel-based non-asymptotic state estimation for linear continuous-time systems. In *2013 American Control Conference* (2013), pp. 3123–3128.

[53] POLUBARINOVA-KOCHINA, P. Y. Modulating functions. *Translated from Izvestiya Akademii Nauk SSSR,*, 5 (1972), 152–153.

[54] POLYAKOV, A. Nonlinear feedback design for fixed-time stabilization of linear control systems. *IEEE Transactions on Automatic Control 57*, 8 (2012), 2106–2110.

[55] POLYAKOV, A. Discontinuous lyapunov functions for nonasymptotic stability analysis. *IFAC Proceedings Volumes 47*, 3 (2014), 5455–5460.

[56] Preisig, H., and Rippin, D. Theory and application of the modulating function method—i. review and theory of the method and theory of the spline-type modulating functions. *Computers Chemical Engineering 17*, 1 (1993), 1–16.

[57] Protter, Murray H.and Morrey, C. B. J. *Differentiation under the Integral Sign*. Springer, 1985.

[58] Shen, Y., and Xia, X. Semi-global finite-time observers for nonlinear systems. *Automatica 44*, 12 (2008), 3152–3156.

[59] Shinbrot, M. On the analysis of linear and nonlinear systems. *Trans. ASME 79* (1957), 547–552.

[60] Shtessel, Y., Edwards, C., Fridman, L., and Levant, A. *Sliding Mode Control and Observation*. Birkhauser, 2014.

[61] Sulaiman, M., Patakor, F. A., and Ibrahim, Z. *New Methodology for Chattering Suppression of Sliding Mode Control for Three-phase Induction Motor Drives*. Systems and control, 2014.

[62] Swikir, A., and Utkin, V. Chattering analysis of conventional and super twisting sliding mode control algorithm. In *2016 14th International Workshop on Variable Structure Systems (VSS)* (2016), pp. 98–102.

[63] Utkin, V. Variable structure systems with sliding modes. *IEEE Transactions on Automatic Control 22*, 2 (1977), 212–222.

[64] Willemet, M., Chowienczyk, P., and Alastruey, J. A database of virtual healthy subjects to assess the accuracy of foot-to-foot pulse wave velocities for estimation of aortic stiffness. *American Journal of Physiology-Heart and Circulatory Physiology 309*, 4 (2015), H663–H675.

[65] Xu, R., and Zhou, M. Sliding mode control with sigmoid function for the motion tracking control of the piezo-actuated stages. *Electronics Letters 53*, 2 (2017), 75–77.

[66] Yu, X., Li, P., and Zhang, Y. The design of fixed-time observer and finite-time fault-tolerant control for hypersonic gliding vehicles. *IEEE Transactions on Industrial Electronics 65*, 5 (2018), 4135–4144.